
THE UNIVERSITY *of* EDINBURGH

THE UNIVERSITY *of* EDINBURGH

School of Engineering

# SKELETON BOBSLEIGH MECHANICS:

# ATHLETE-SLED INTERACTION

Iain Roberts


A thesis submitted to the University of Edinburgh

For the degree of Doctor of Philosophy

February 2013

## DECLARATION

I declare that this thesis has been composed by myself and is all my own work except where otherwise stated.

Iain Roberts

July 2012

## ACKNOWLEDGEMENTS

So many have helped throughout this project and I thank you all. Firstly thank you to my supervisors, Dr Jane Blackford, Dr Tim Stratford and Dr Martin Gillie who made this project possible.

Thank you also to everybody who helped with the electronics and the workshop. I have lost count of how many times I needed alterations to my sleds and you always did a great job even when I was due on a plane in a matter of hours.

A special thank you to my family for all their support as I charged around the world, the early morning trips to the airport and the donated campervan which certainly kept the costs down in Europe. It would be good to go on a holiday now where the overnight temperature is a little warmer than -20° C.

My teammates have been fantastic, thank you especially Ben Sandford, Tionette Stoddard, Katharine Eustace for sliding on my equipment that I built over the years and thank you to all the support staff that have contributed through the New Zealand Academy of Sport, particularly Dr Angus Ross for the painful training, it was worth it. Thank you also to Dirk Matschenz, it was a roller coaster of a journey and I would not have been able to experience this amazing sport without your help.

Most importantly, thank you to my wife Jill. You have been patient throughout my skeleton obsession and I cannot thank you enough for all that you have done for me.

137.035 998 78 (91)

## ABSTRACT

Skeleton is one of the three Olympic sporting disciplines to be held in the manmade bobsleigh tracks. The sport of skeleton uses a one-man sled, on which the athlete travels headfirst down a mile long track reaching speeds of up to 147 km/h. As with many sports the engineering of the equipment is playing a greater role in the overall performance of the athlete. Although the sled alone cannot win medals a poor choice of equipment can be the difference between winning and losing. The primary focus of this research is on the trajectory and response of the sled frame and how these relate to athlete perception during a descent and overall performance. Sleds were instrumented with accelerometers and strain gauges that enabled the mechanical behaviour of the sled to be determined quantitatively. Qualitative data comprised of athlete training logs (mainly from the author), provided information about the feel and perception of the run. Tests were made on whole tracks, dedicated push-tracks and in the laboratory. In addition this PhD has touched on aerodynamics and runner-ice interaction.

The thesis is split into three main sections: (1) The initial push phase of a descent was investigated at the Torino Sliding Centre and Calgary Olympic Park with a sled instrumented with an accelerometer. Using a single axis in the forwards direction of the sled determined the sensitivity of the measuring and acquisition device along with the capabilities and quality of information gained. Through analysis it is possible to identify the dynamics that occur during a push start and how to interpret them in order to improve athlete performance during the push start. (2) A whole descent at the Koenigssee International Race Track was measured using a three axis accelerometer. The dynamics at specific track locations were examined in detail and linked with athlete perception. Comparison of multiple descents enables the sled trajectory to be quantified to determine the overall success of the resultant trajectory. This analysis shows there is scope for maximizing athletic performance in conjunction with quantitative

instrumentation of the equipment. (3) Complete descents at the Lake Placid Olympic Park were made on a sled instrumented with rosettes of strain gauges. The strain gauges were calibrated in the laboratory. Analysis of strain gauge data from the track showed the extent of deformation of the frame upon entering and exiting curves and while under the g-forces experienced, again this data is compared with athlete perception. Consideration is briefly given as to how these dynamic measurements can be used to evaluate current and future frame designs.

**TABLE OF CONTENTS**

## LIST OF FIGURES

## LIST OF TABLES

# 1 INTRODUCTION

# 2 FUNDAMENTALS OF SKELETON BOBSELIGH

# 3 THE PUSH START

# 4 TRAJECTORY ANALYSIS OF THE KOENIGSSEE INTERNATIONAL RACE TRACK

# 5 SLED DYNAMICS AT THE LAKE PLACID INTERNATIONAL RACE TRACK

# 6 GENERAL CONCLUSIONS

# 1 INTRODUCTION

## *1.1 The Sport of Skeleton Bobsleigh*

The winter sport of skeleton bobsleigh is held on man-made ice tracks. The tracks are used for all three disciplines of Bobsleigh, Skeleton and Luge. In skeleton athletes descend lying face-down and travel head-first upon a sled. The sport originated in the 1880s, but has received particular interest since it was reintroduced into the Winter Olympic Games in 2002. International Skeleton races typically consist of two combined descent times with the pinnacle events of the Winter Olympics and World Championships being held over four combined descent times. With each descent typically having a duration of a minute, total race times can be 4 minutes with first and second place potentially separated by 0.01 of a second.

Engineering processes and applications are continually applied in the world of sport in pursuit of maximising athlete performance. Skeleton bobsleigh is no exception. Increasing awareness of the sport has been accompanied by more rigorous attempts to increase athletes' chances of success.

Skeleton is a sport where having good equipment plays a vital role in the success of the athlete. This can easily be seen when considering the nature of the sport. The ice tracks are typically a mile in length consisting of straights and banked corners. The descent begins from standing. The sled, approximately shoulder width and shoulder to knee in length, is placed on the ice, the handles no higher than 0.2 m from the ice surface. The athlete bends forwards to grip the sled handle, (Fig 1.1) and accelerates the sled along the ice as fast as possible. Once a top speed is achieved they dive headfirst onto the sled

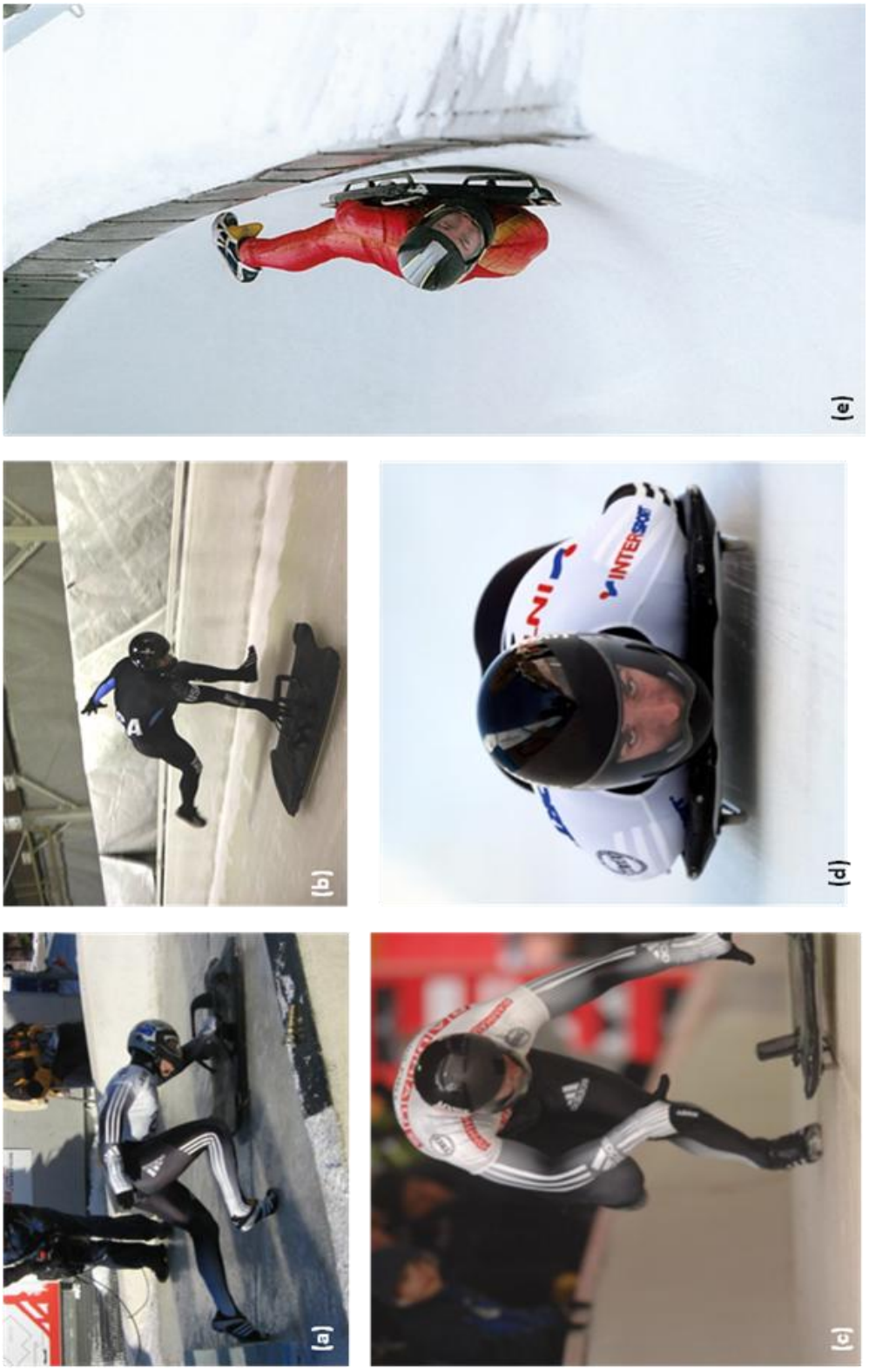


**Figure 1.1 – The skeleton athlete begins their descent by exploding off the starting block (a). Pushing the sled out in front they continue to accelerate until maximum velocity is achieved (b). At this point they dive headfirst onto the sled (c) and settle into race position (d) to steer the optimum path down the track (e)**

with a final surge of power to achieve maximum loading velocity. Quickly settling into a race position with hands by their sides the athlete steers the sled through the banked turns of the track to achieve the optimum trajectory for the fastest descent.

There are 14 tracks which regularly feature on the international racing calendar. Top speeds achieved ranging between 115 km/h and 147 km/h with up to 5 g of force lasting for no more than 2 s in the corners. Each of the 14 tracks have unique characteristics, furthermore the Federation International de Bobsleigh et de Tobogganing, FIBT, allows only 6 training runs before a race. It is therefore essential to identify the key areas of the track to generate velocity and have a thorough understanding not only of the track dynamics but how the sled will respond under the harsh conditions experienced during the descent.

## *1.2 The Skeleton Sled*

The skeleton sled comprises of three main elements, (Fig 1.2):

i) *Frame*: the frame of the skeleton sled is a steel construction, approximately shoulder width and shoulder to knee in length. In its most basic form, it is a rectangular steel frame with a centre saddle to support the athlete's body.

ii) *Bellypan*: mounted onto the underside of the frame is a smooth outer covering usually of fibreglass or carbon fibre composite which not only acts as an aerodynamic aid sealing the underside of the sled but also ensures the outer of the sled is smooth for athlete protection.

iii) *Runners*: securely fixed to the left and right side of the frame are two steel runners that pass through the bellypan at the mounting points and run beneath the

sled. They are the components in direct contact with the ice which enable the athlete to control the position of the sled.

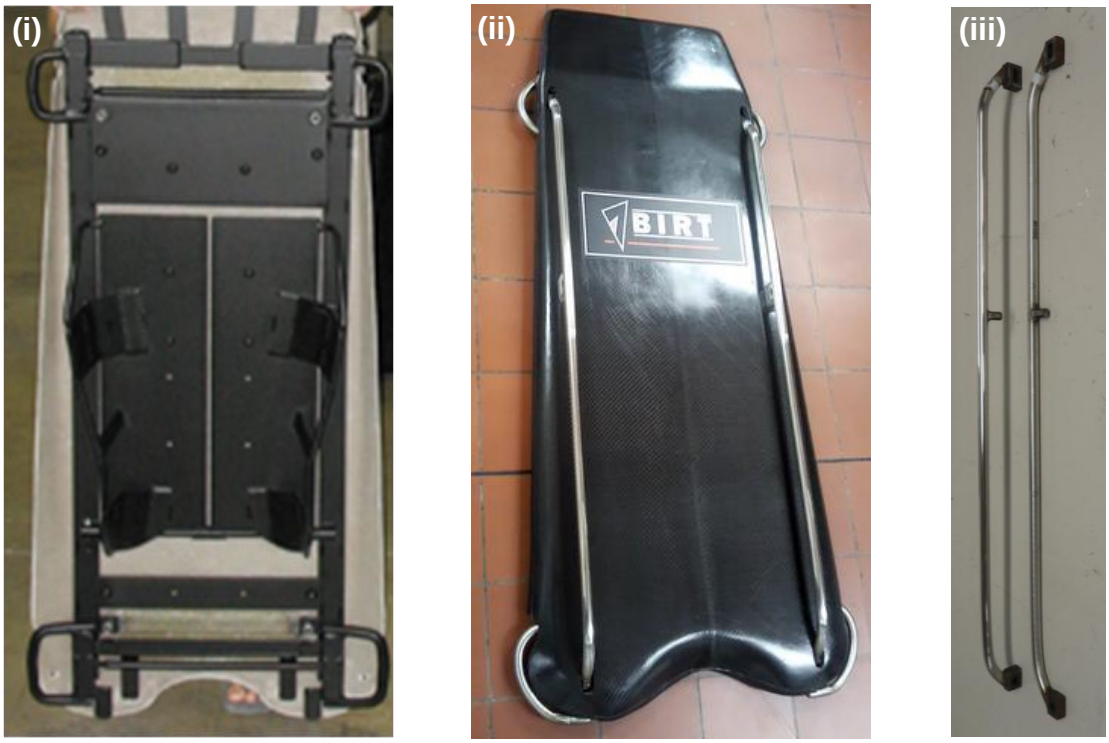


**Figure 1.2 – A skeleton sled comprises of three main elements. (i) Frame, (ii) bellypan and (iii) runners**

## *1.3 Factors Affecting Performance*

My personal involvement in the sport forms the initial motivation to this research project. I raced internationally between 2003 and 2010 with 57 international appearances, 7 podium placements, three World Championships and the 2010 Winter Olympic Games. To increase my chances of success I wanted to gain a thorough understanding of how best to target my training to become a better athlete and also set up my equipment to race as fast as possible.

First thoughts may indicate that engineering principles could be applied to aerodynamics and frictional contact with the ice as these present the main forms of drag. The FIBT has strict regulations on the overall dimensions and materials for construction in order to maintain safety within the sport. In doing so limits the possibilities for variation in the outer aerodynamic profile of the sled and the material choice for the steel runners. Regulations were changed in 2004 and since then only one type of steel can be used for the runners.

The race begins with an explosive push start and although it does not dictate the final race positions a competitive push start is required to be able to win the race. In 2009 / 2010 the athletes regularly in the top 20 of the men's World Cup had all achieved a podium position in their career and the spread of push start time was up to 9% that of the fastest starter in the field. Studying the accelerations that occur throughout the push start increases an understanding of the athlete's application of force and can aid in tailoring the strength and conditioning, and technique training accordingly. (A detailed study of the push start is given in Chapter 3).

Tracks typically in the region of a mile in length, after the push start it is crucial to control the sled's descent through the challenging turns. Tracking the sled's trajectory and comparing it to athlete perception of sled response and positioning during the run provides valuable insight into the intricacies of sled control. This highlights the importance of being aware of what the athlete is attempting to achieve and what actually occurs in the descent.

The frame of the sled has significant scope for it to be adapted to individual athlete requirements. The athlete steers the sled by flexing the frame along the diagonals creating an asymmetry in the contact patch between the runners and the ice. Small changes in the dimensions of the rectangular frame or the saddle placement / construction has significant impact on the subsequent movement and response of the sled. Firstly, by fully understanding the trajectory of the sled in detail at critical sections of the track can aid the athlete in improving their driving ability. Once there is a solid foundation in what the athlete is trying to achieve the sled can be optimised to allow the athlete to position the sled as best they can, generating as much velocity as possible.

The focus of this research project is on tracking the trajectory and response of the sled and examining how this correlates to athlete perception and performance. An outline of how this is investigated follows:

CHAPTER 2 introduces the fundamentals of the sport of skeleton. A review of relevant work to date and the restrictions set by the sporting governing body highlights potential research areas of interest. The current equipment and steering techniques are presented to aid in discussions later in the thesis.

CHAPTER 3 investigates the push start. Using a single axis accelerometer in the forwards direction enables phases of the push start to be identified. The results are beneficial to target athlete training.

CHAPTER 4 uses a tri-axial accelerometer over a whole descent of the Konigssee International race track in Germany. Investigating specific curves within the track show that subtle changes to the trajectory and the effectiveness of athlete performance can be determined.

CHAPTER 5 shows the application of strain gauges to the frame of a skeleton sled. The sled used had adjustable stiffness and was tested at the Lake Placid Olympic Sliding Complex in USA. The change in strain gauge output for the different stiffness settings is presented and discussed in terms of overall performance.

# 2 FUNDAMENTALS OF SKELETON BOBSLEIGH

In this chapter I will introduce the sport of skeleton in detail. The intensity of the racing calendar and how this directs the athlete's focus towards training techniques and equipment is presented. This is followed by a review of research published to date and relevant background knowledge to help identify areas where further research could benefit the athlete.

Then considering the restrictions posed by the FIBT, three applications of engineering techniques and the potential gains can be discussed:

i. Aerodynamics
ii. Frictional contact between the sled and the ice
iii. Frame response

Finally an overview of current equipment used by elite athletes and general control / steering techniques are introduced.

## *2.1 The International Racing Circuit*

The sport of skeleton has 4 international racing circuits, Americas Cup, Europa Cup, Intercontinental Cup and World Cup. Each circuit consists of 8 races, typically held between November and February. There are 14 tracks worldwide that regularly feature on the racing calendar with varying characteristics requiring a wide range of technical skill. It is imperative to have a thorough understanding of the track dynamics in order to drive the optimum path down the track and also have responsive equipment so that the sled can be positioned as efficiently as possible. The question of how responsive is difficult to answer as each track has unique geometry. This may present a desire for a sled that can be adjusted to best suit different tracks however the time between races is minimal, limiting additional practice or testing. The 6 official training runs prior to a race are usually 2 a day over three days, however there has also been 3 a day over 2 days

so it is essential to identify the key areas that enable a sled to be tailored to both the individual tracks geometry / characteristics but also the athletes preferred driving style in order to generate velocity or maintain it as efficiently as possible. Ultimately it is the athlete that must control the sled and so too many variables within the sled frame may perform better but cause the athlete to struggle to adjust to the altered setup within the training time available.

Without the track trajectory knowledge or suitable equipment, errors in driving performance can result in significant loss of speed, not necessarily where the track is at the fastest point, for example curves 3-4-5 at the Altenberg track form an Omega-shape. Failure to control the trajectory can cause the sled to flip over, (Fig 2.1).

**Figure 2.1 – Transition between curves 4 and 5 at Altenberg. If the athlete misses the timing to control the transition they can easily flip onto their backs. This athlete competes at the highest level and after the 6 official training runs successfully recorded the 9th fastest time in the World Cup.**

## 2.2 Previous Studies in Sliding Sports

A number of studies have been published relating to the family of sports held on bobsleigh tracks, some of which specifically relate to skeleton. In comparison to other fields of research there is relatively little published work on the sport of skeleton as it is a minority sport coupled with the competitive nature and the desire to gain the advantage over rival athletes. However, since being reintroduced to the Winter Olympic Games in 2002 there has been growing public awareness of the sport and with it insights into the academic research, which has also been picked up on by the media.

The predominant areas within all three of the sliding sports (bobsleigh, skeleton and luge) that have gained academic interest are the push start, aerodynamics and the interaction with the ice. The ability to accelerate as fast as possible from stationary at the start provides the advantage over other athletes. Minimising aerodynamic drag can help maintain any gains made through the push or driving ability. The interaction with the ice has two distinct areas of interest. Firstly is the mechanism of the sliding process to minimise frictional contact and secondly the ability to control the sled and turning dynamics during a descent.

The following is a summary of research published in these areas, along with relevant background work highlighting the motivation for additional research.

### 2.2.1 Athlete Physical Attributes and the Push Start

Each skeleton descent commences with the athlete pushing the sled in a bent over running position. The athlete who can generate the fastest push start has the advantage,

with the remainder of the field needing to outperform them through driving technique. It is a common rule of thumb in the sliding sport community that 0.01 s at the top of the track can accumulate a 0.03 s advantage at the finish, assuming no driving errors are made. This is purely through observation of trends and is more applicable at some tracks than others depending on how forgiving driving errors can be.

Brüggemann et al. (1997), Morlock and Zatsiorsky (1989) refer to a good push start in bobsleigh and luge being a prerequisite in order to achieve excellent overall performance. Brüggermann et al. (1997) highlighted that the final positions for the top 15 competitors in bobsleigh and luge at the Lillehammer Winter Olympics 1994 were determined through driving ability and not the push start alone. Zanoletti et al. (2006) presents a statistical correlation for push start and descent times in skeleton and confirms that the push start is also essential for a competitive overall performance in skeleton. Bobsleigh has more response than a skeleton sled due to the additional mass and steering mechanism and Brüggerman et al. (1997) shows a strong correlation between push start times and final descent times of 77%. Zanoletti et al. (2006) finds that elite athletes in skeleton have less correlation between push start times and final descent times, 23% for the men and 40% for women, highlighting how unforgiving driving errors are on a skeleton sled.

With such importance in generating speed through the push start, nations with a larger involvement in the sport conduct talent identification programmes to seek those with the most potential. BBSKA (2007), BCS (2007) and Bullock et al. (2009a) have extensive talent identification programmes in skeleton with physical requirements for the initial stages published online. They typically involve speed and power tests through standing high jumps, weight lifting exercises and sprinting as Sands et al. (2005) shows that elite

athletes are typically able to achieve 85 % of their upright sprint times over 30 m when in a skeleton pushing position.

Of particular interest to the skeleton push start is the work of Bullock et al. who has had numerous publications on aspects of the push start from a sports science and biomechanical perspective. Conducting an investigation into physical training techniques Bullock et al. (2009b) research athlete exposure to an acute bout of whole-body vibrations and the impact it may have on the skeleton start and 30m sprint performance. This is a training technique that has mixed results with Cochrane and Stannard (2005) showing positive results in plyometric performance, whilst Cormie et al. (2006) report no significant correlation between the exposure to vibration and explosive physical performance. The latter is also the conclusion of Bullock et al. (2009b) showing that it does not appear to have a positive effect on sprinting over distances relevant to skeleton.

Bullock et al. (2008) investigates the skeleton push start performance in detail. Using video footage they measure acceleration over 0-15 m and velocity at the 15 m, 45 m marks and conclude that the 15 m velocity is of greater importance in assessing the overall performance of the push start, additionally acknowledging that the results at 45m may be useful when considering each tracks unique characteristics.

Similarly, Sands et al. (2005) investigated the skeleton push start performance of the US national skeleton team and is in agreement with Bullock et al. (2008) on the importance of the 0-15 m split time although includes the 0-30 m time as a positive indicator of performance. This is perhaps due to those with a taller physical stature affecting ability

to accelerate from a standstill are still able to generate a high loading velocity by the 30m without sacrificing an irrecoverable time deficit in the earlier stages.

Whilst skeleton descents are timed to 0.01 s the sport of luge is timed to 0.001 s as the sleds are more responsive and so race times are more tightly grouped. Held in the same tracks as skeleton, luge is a very different sport beginning in a seated position with the athlete using their arms to propel themselves forwards down a steep tower start. With the smaller margins of time separating finish positions the luge athletes understand the advantage that can be gained in the start. Lembert et al. (2011) and Platzer et al. (2009) show the development of a measurement and feedback training tool to improve athlete arm strokes during a luge start. This involved simulating the start on a conveyor belt construction and monitoring performance with accelerometers fixed to the athlete's hand.

Studies discussed so far deal with athlete anthropometry and pushing, however the athlete must also descend the track. Larman et al. (2008) use the St Moritz skeleton World Championships 2007 to see if there is an "ideal" mass and height and although they state that it is difficult to identify an optimum body height and weight they do note a particular physique was shared by the men's and women's champions at that event. This is perhaps premature based on a single race as the following season it was an athlete with a very different physique that won the women's World Cup. The more extensive work of Bullock et al. (2009c, 2009d) use a far larger data set of skeleton races and athletes showing that different tracks have race outcomes that are largely unpredictable based on body shape. It is also peculiar that St Moritz be used for a general study, Larman et al. (2008) and Roche et al. (2008), as it exhibits characteristics unlike any other track on the racing circuit. It is the only natural track that is carved

each season from ice while other tracks have a permanent concrete structure for the track geometry and is refrigerated creating a relatively thin layer of ice on the surface. Not only is the track construction unique but the altitude and location tends to create a considerably cold, dry environment. When considering the complexities of the structure and mechanical behaviour of ice, Schulson (2002), with such a different ice formation and environmental factors it is no surprise that trends tend to differ at St Moritz. Through observation it is not uncommon for the St Moritz track to speed up as the day progresses, whilst other tracks can deteriorate rapidly with use and become slower.

### *2.2.2 Aerodynamic Studies in the Sliding Sports*

Alongside the work of Larman et al. (2008), Roche et al. (2008) also presents a study of skeleton at St Moritz. They develop an initial model of aerodynamic drag using a single degree of freedom in the sled's direction of motion. The study looks at variation in athlete height and weight and the associated pressure and skin friction as functions of speed. They note that flow separation cannot accurately be modelled in this manner but as the skin friction is a smaller contributing factor (approximately 20%) is a valid initial approach. The model agrees with final descent times but exhibits a large variation through the mid section of the track. Roche et al. suggest that this is due to unknowns in track geometry and timing eye locations, and also considers that ice friction variation due to athlete driving should be included in the model in future work. At this stage of an initial model it is perhaps a spurious result to agree with final descent times with significant unknowns and variation for the majority of the track.

Dabnichki et al. (2004) and Motallebi et al. (2004) present studies in the two man bobsleigh and the use of variable crew position as a factor in the aerodynamic drag. Initially motivated after the introduction of women's bobsleigh and potential safety

issues of ergonomic design. The female athletes were using the current men's sleds which were too large for the typical female athlete. Modifications required to aid in injury prevention during a descent sparked new interest in aerodynamic studies. Motallebi et al. (2004) used wind tunnel testing and found potential aerodynamic gain with a 9% reduction in coefficient of drag when varying two man bobsleigh crew position. There is less flexibility for manoeuvring skeleton athlete position to achieve similar aerodynamic gains, yet it is of my opinion that as little as 5% of the World Cup field makes full use of possibilities within the rules of saddle position and overall sled preparation.

Wind tunnel testing has large financial requirements. The basic test facilities have static floors which introduces error as the air flow over the stationary surface and test sled is not indicative of the sled travelling over a surface through static air. Even at the best facilities results that incorporate a rolling road in the set up can also suffer by failing to match the surface roughness of the ice itself, particularly the surface asperities of ice. CFD studies comparing variations in wind tunnel setups for testing skeleton, Hastings (2008), shows static floors to have a 7 % discrepancy over rolling roads and a further 2.5 % if the track geometry (walls) are not considered. Lewis (2006) presents a thorough investigation of two man bobsleigh aerodynamics using wind tunnel experiments and Computational Fluid Dynamics (CFD). The results provide recommendations on the front and rear cowling, crew position and aerodynamic drag around axles. A similar study for skeleton would have greater errors in the wind tunnel from the lower position of the athlete and sled within the turbulent boundary layer. Considering also the restrictions by the FIBT in the sport of skeleton, the external profile of the sled can have little variation. In addition the saddle mount for the athlete to lie in cannot be used to alter the athlete's body position for aerodynamic gain. While bobsleigh, being of significantly larger construction, can benefit from aerodynamic studies it is generally of

less interest to skeleton with more gains being made in overall performance by focusing on the athlete's ability to control the sled.

The scope for aerodynamic improvement has also been the source of controversy in the sport of skeleton. The women's Gold medallist at the 2010 Winter Olympics was the subject of protests after the first two heats on day one. Claims were made of illegal aerodynamic fairings on her helmet. Consistently achieving top 10 in the world prior to this with a standard helmet she was undoubtedly an athlete of exceptional ability. It is perhaps a shame that the success is also a historic indicator of the potential dangers of sports engineering and the sometimes "grey area" of the rules. Fortunate to avoid serious penalties considering a male athlete was disqualified for not removing covers from their runners 45 minutes prior to the start of the race, which is a requirement by all athletes to ensure the steel runners cool to similar temperatures by the time the race commences. This could easily have been remedied by forcing the athlete to "ice-box" the sled, a process of laying the runners on the ice before their descent for a period of time to cool the steel temperature negating any unfair heat advantage.

Hastings (2008) conducted an initial computational fluid dynamics study to investigate changes in aerodynamic drag with alterations to curvature of the skeleton athlete profile finding a potential 7 % improvement from spinal curvature. This is potentially useful for talent identification purposes to recruit future athletes into the sport. A CFD project was also carried out at Sheffield Hallam University using a laser scanned geometry of Kristan Bromley, a skeleton athlete more notably recognised for his work on ice friction in the sport of skeleton than aerodynamics.

### 2.2.3 Interaction with the Ice

#### 2.2.3.1 Mechanisms of Sliding on Ice

The research of Bromley (1999) is some of the most extensive to skeleton specific research to date. The primary focus of his PhD was on the frictional contact between the runners and the ice. He has had one of the most successful athletic careers in the history of the sport and in the 2003/04 season was overall World Cup winner, winning all but one of the World Cup races. Along with his brother, Richard Bromley, and Bromley Technologies they have researched all aspects of the sport and after the rule change in 2004 restricted the steel for the runners he continued to have success becoming World Champion in 2008.

Prior to the FIBT restricting the runners steel type to an austenitic stainless from a single source and branded with FIBT approval Bromley was not alone in the material research of steel and ice interaction in the sliding sports. Hainzlmaier et al. (2004), Hokkirigawa (2002), Hainzlmaier (2005) all researched the sliding of steel on ice and methods to reduce the frictional contact. Even after the rule change the interaction with the ice is still of interest due to the harshness and speed of the contact, Fauve et al. (2008), Penny et al. (2007). The kinetic friction of ice is a subject investigated intensively, many conducting tribology experiments using pin on disc and pendulum drum apparatus, Bowden and Hughes 1939, Evans et al. (1976), Oksanen and Keinonen (1982), Akkok et al. (1987), Marmo et al. (2005), Maeno and Arakawa (2003). These studies are useful in understanding the fundamentals of ice friction for the slower speeds, up to 10 m/s, and the relationship between the coefficient of ice friction with sliding speed, vertical loading and surface temperature. At velocities consistent with the sliding sports, 40 m/s,

the magnitude of levels recorded from pin on disc measurements become drowned by noise signals due to vibrations in the measurement apparatus.

Penny et al. (2007) investigates a theoretical approach to overcome the errors of high speed experiments by formulating a mathematical model of the kinetic friction of ice. Specifically for speed skating they account for contact area, ploughing force and shear stress between the blade and the ice surface. In comparison with investigations of the kinetic friction of ice, Colbeck et al. (1996), Houdijk et al. (2000), De Koning (2000) and in particular the experimental work of De Koning et al. (1992) shows promise for the mathematical model to calculate the coefficient of ice friction and is extrapolated to the higher sliding speeds relevant to skeleton for varying ice surface temperatures. Whilst uncertainty over ice surface hardness removes some accuracy from the model, Poirier et al. (2011) uses ice surface hardness measurements to adapt the model for improved accuracy.

The experimental techniques to investigate the kinetic friction of ice focus strongly on frictional heating, pressure melting, ploughing, thickness of the meltwater film, electrostatic charging, adhesion and shear forces. Colbeck et al. (1996) investigates the sliding temperatures of ice skates using direct measurements from a thermocouple protruding through the blade and upon comparison with thermodynamic theory determines frictional heating to be the dominant mechanism.

Continuing to use principles of heat transfer and theoretical models of Bejan (1989), Stiffler (1984), Penner (2000) a thermal response to sweeping in the sport of curling was developed by Marmo et al. (2006) and aided coaches and athletes improve their

sweeping technique and subsequent control of the curling stone through an improved understanding of the formation of the melt water film. It is interesting that Strausky and Krenn (1998) attempted to measure the thickness of the melt water film through a Fluorescent Spectroscopic study and determined it to be less than 50nm as this was the detection limit of the experimental setup.

#### *2.2.3.2 Ice Chipping and Turning Dynamics in the Sliding Sports*

Whilst applying research on the kinetic friction of ice to slower speed sports of curling and speed skating can aid athletes improve their performance, the speeds achieved in skeleton indicate that it is not only the interfacial water layer to slide on that is of interest but also the severity of the interaction with the ice surface.

As previously discussed a significant factor in the magnitude of errors during high speed experimental measurements is due to the vibrations that occur and the subsequent harsh interaction with the ice surface. It is ultimately this deformation to the ice that allows the skeleton athlete any control over the sled. Although the interaction between a sled and ice differs greatly from that of skis on snow, it can be envisaged similarly to skis carving, where the damage to the ice surface can be controlled by the athlete to create an asymmetric contact patch and turn the sled, discussed in Section 2.8. Investigations of turning and control while skiing and snowboarding, Sanders (2004), Nordt et al. (1999), Brennan (2003), Sahashi and Ichino (2001) apply ski edge angle to the theory and carving of snow. Tada and Hirano (1999) use ice cutting data to investigate skiing on icy hard snow. They derive empirical expressions for angled forces on the ice surface related to cutting depth and elastic deformation from which a numerical turning model simulating the turning ski is formed. Similarly, Heinzelmaier (2004) created an FE model to investigate how this deformation of the ice may occur in bobsleigh and for

plastic deformation concluded that in a 2 g corner a compression depth of 0.18 mm would form. Field measurements showed the bobsleigh left grooves up to 0.5 mm depth in a single run highlighting the need to include dynamic effects to the model. Fuave et al. (2008) use an experimental technique to test impact friction between steel and ice. Here with luge as the primary focus and in high radius corners where approximately 2 g is achieved finds the luge runner leaves grooves with depths 0.35 mm in the ice. This may seem high as the mass is far less than a bobsled with crew, however a luge runner has a sharper edge than a bobsleigh runner.

While the deformation of the ice surface is a necessity to control the sled, too much will slow it down. Braghin et al. (2011) created a multi-body model on bobsleigh to investigate weight distribution and inclination of the steering axis to reduce frictional contact without impairing sensitivity of steering and control of the sled. To validate the contact between the bobsleigh and the ice in the model they used two gyroscopic sensors and 16 strain gauges to experimentally determine the contact forces.

The work of Braghin et al. (2011) highlights the need to understand mechanical process within the equipment to optimise control and minimise frictional contact with the ice. Turning dynamics in bobsleigh, Hubbard et al. (1989) and in luge, Mössner et al. (2011) was simulated using weight, drag, friction and surface reaction forces. Experimental measurements with accelerometers were used to validate the simulation.

Accelerometers are widely used to improve the understanding of many complex motions in physical activity and improve training methods. Slawson et al. (2008), James et al. (2004), Ohgi et al. (2000) apply accelerometer output to improve swimming stroke

technique, Sato et al. (2009) uses accelerometers to study weightlifting technique, James et al (2004) also investigates rowing oar angle. Whilst these all use accelerometers to study dynamic motions for feedback on athlete performance Champoux et al. (2007) investigates bicycle structural dynamics using accelerometers with the aim of improving the ride and reducing fatigue in construction.

In summary, the significant gains in the push start show that additional research into the dynamic motion from stationary will be extremely beneficial. Much of the published work focuses on athlete anthropometry. The work of Lembert et al. (2011) utilises accelerometers in the luge start to improve technique. Although luge is a very different sport to skeleton a similar approach could also benefit skeleton athletes.

The push start is only one factor in overall performance. There appears to be little research in the specifics of the trajectory during a skeleton descent. Investigating full descents could also aid in modifying skeleton sleds for improved control and a reduction in the frictional contact with the ice.

## *2.3 Federation Internationale de Bobsleigh et de Tobogganing Rules and Regulations*

The Federation Internationale de Bobsleigh et de Tobogganing, FIBT, has strict rules and regulations governing the equipment and so must be considered in detail to determine how best to investigate the sport. The sled can only be accelerated by the pushing force of the athlete and gravity. There can be no steering or braking mechanisms other than the flex of the frame and also no sophisticated control devices,

including hydraulic, pneumatic or electrical. The sleds must be structurally robust in order to withstand forces that occur through repeated runs on a bob track.

The weight of the sled can vary. For men it is between 33 kg and 43 kg where the athlete and sled combined cannot exceed 115 kg. For women the sled can weigh 29 kg to 35 kg without exceeding a combined weight of 92 kg. The frame must be constructed of steel.

The two steel runners attached to the frame beneath the sled are constructed from 16mm diameter steel rods of steel type 1.4435 (an austenitic stainless steel), supplied and tested by the FIBT (2006). Both ends of the runners are curved and runner blocks welded to them to enable fixing to the sled frame, and must be done so without any form of suspension or damping mechanism. Midway along the runner an additional post is welded that runs freely in a guide on the frame to minimise lateral movement during a descent, (Fig 2.2).

There are no dimensional specifications for the runner blocks or posts. Treatment of the runners by coating / plating, hardening or heat treatment to attempt to improve their performance is forbidden. Hand polishing for general maintenance is allowed. The rear of the runner is cut with grooves. The only restrictions being that the depth of the groove does not exceed a distance of 2 mm from the surface of the ice and cannot cause excessive damage to the ice, (Fig 2.3).


**Figure 2.2 – Close up of the rear section of the runner showing the guide post to minimise lateral movement and the curved ends of the runner.**

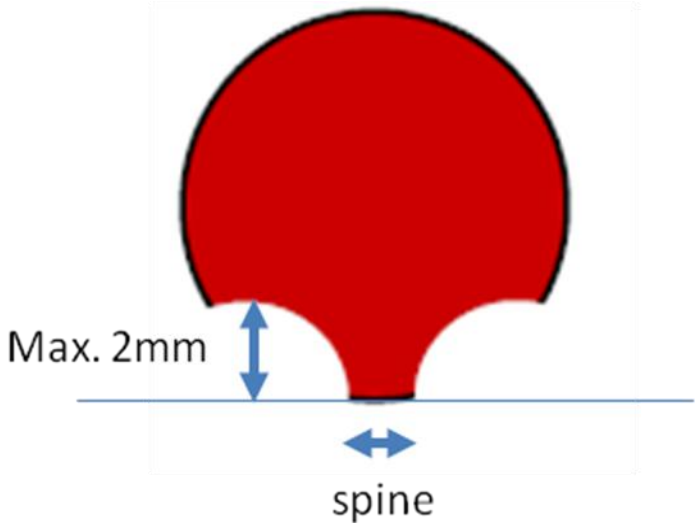


**Figure 2.3 - Cross section of a skeleton runner indicating the spine and maximum groove depth.**

Typically two grooves per runner creating a spine in the region of 1.2mm however there is no restriction on the number of grooves and there has been success on single groove runners where the angle of incidence at the edge of this single groove creates a spine

edge. The radius of the groove or distance between them can be varied for different ice-conditions, track dynamics or individual driving styles.

Where the runners are attached to the frame an adjustable tension is to be applied creating an arc / bow. This is referred to as the "*rock*" and can vary in magnitude with personal preference. Typically it is adjusted by tightening a bolt at one end of the runner. It is the grooves of the runner that enable the athlete to control the sled and will be discussed in detail in section 2.5.

The frame dimensions must fall within the following:

Length: 800 – 1200mm

Height: 80 – 200mm (including runners with bow)

Width: 340 – 380mm (measured from runner centre to runner centre)

Overall the frame is rectangular with further dimensional restrictions on the transverse and longitudinal bars, both being made from continuous pieces of steel with minimum cross sections 30 x 5mm and 25 x 3mm respectively, (Fig 2.4, FIBT (2012)).

Connecting corners of the frame must be welded or bolted (minimum two bolts per joint to prevent any rotation and thus removing possibility for advanced steering mechanisms). The transverse and longitudinal bars must be orientated in a common plane with a vertical tolerance limit of 2mm. The locations of the mounts to attach the runners must be within 80mm of the front transverse bar and 30mm of the rear and done

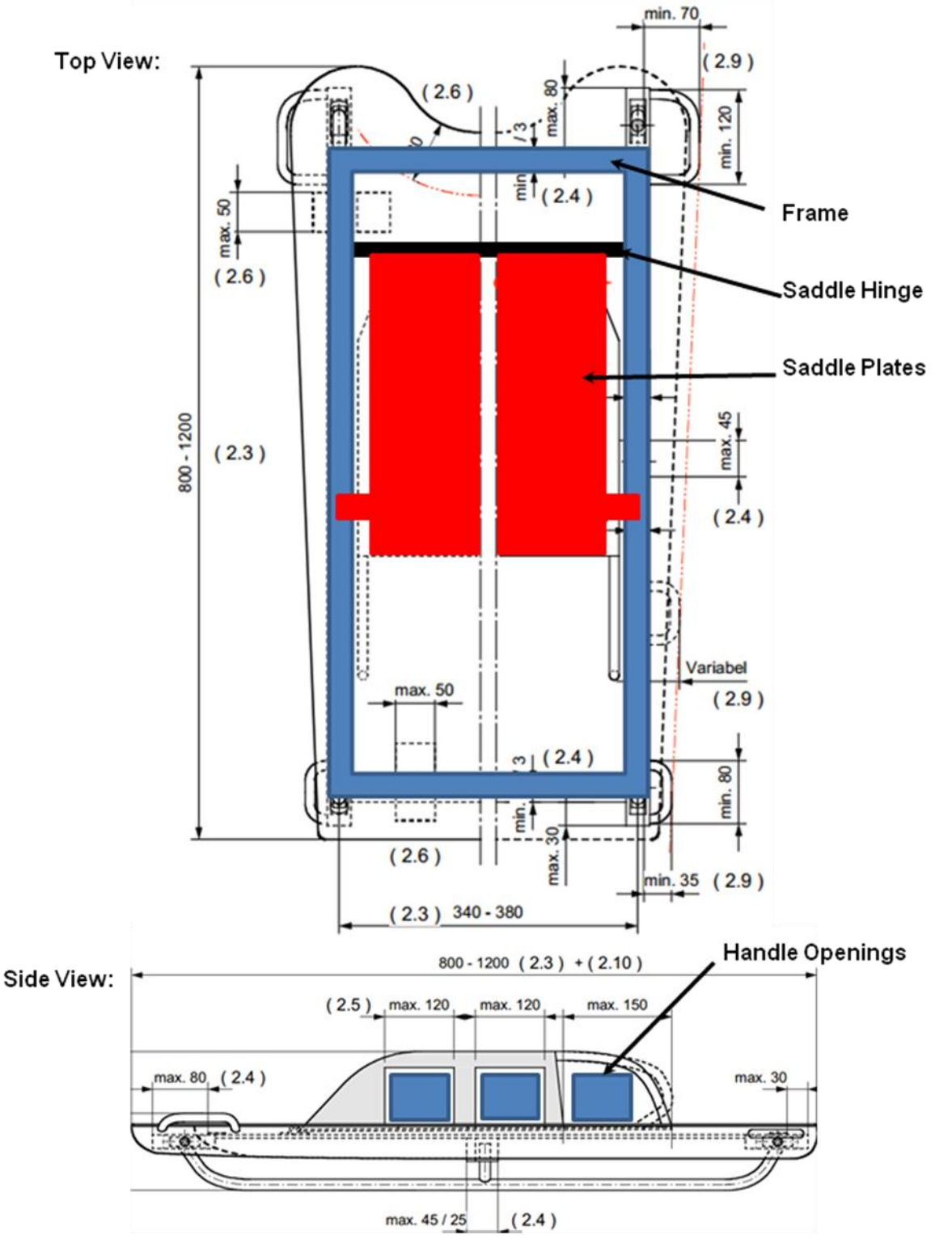


**Figure 2.4 - Schematic from FIBT Rules 2012. The frame, hinged saddle plates and handle openings are highlighted**

in a manor that creates a rigid connection to the frame. The lateral guide for the runner post is also limited in size, not exceeding 25 x 45mm (width and length). All additional components of the sled must be bolted or welded to the frame.

Within the frame a saddle of no more than two halves is mounted (Fig 2.4), typically in the form of steel plate. It is on these plates that handles are attached to enable the athlete to both push the sled at the start and subsequently aid them in maintaining position throughout the descent. The handles can have a maximum of three openings, two 120mm openings towards the front and the third being 150mm to the rear of the handle, (Fig 2.4).

When in race position these handles are situated between the athlete's body and arms so that the arms are outside the handles during the run. The saddle plates must not have any lateral movement or be higher than the remaining supporting surface of the sled removing the possibility of enhancing aerodynamics by altering the athlete's profile.

Bumpers to withstand impact during a descent must be made from round steel bar and mounted at the front and rear corners of the sleds, minimum length 120 mm and 80 mm respectively and at least 12 mm in diameter providing a minimum of 70 mm clearance at the front and 35 mm at the rear. The front bumper may also angle up to 15 mm above the top surface of the sled otherwise a lower positioning may catch the ice on the entry and exits of curves. The rear bumpers may be mounted forward of the rear corners, but no further than the rear of the saddle, providing the clearance complies with the linear plane formed from the front and rear corner clearance specifications.

A single piece bellypan is mounted on the underside of the frame. It must be convex throughout with a concavity tolerance of 3 mm over a 30 mm length in all directions, the exception being within 80 mm of the front edge. Multiple local protrusions are not allowed neither is laminating the frame into the bellypan. There can be 4 laminated strips of up to 50mm used to mount the bellypan. The bellypan must not exceed the height of the top surface of the sled. As little as 15 years ago this was constructed from steel plate, but has since been replaced with fibreglass and more recently carbon fibre.

The top surface is to be padded and must be levelled flat. Additional weight may be bolted or welded to the sled so that the athlete can match the weight restrictions set out in the rules and in a manner that optimises athlete control of the sled. However fairings, spoilers and aerodynamic elements are prohibited and there can be no energy absorbing materials used in the sled components or between them.

Even with these thorough rules there are numerous approaches for engineering applications to benefit the sport of skeleton. The important question is "*where can the significant gains be made*?" That is in considering experimental limitations and financial investment what application has the greatest scope for significantly improving the overall performance? Three key areas that can be optimised to reduce descent times are: aerodynamics, runner – ice interaction and frame response. These will be considered in detail in the following sections.

## *2.4 Aerodynamics*

With any high speed activity there is the significant drag factor of wind resistance. Considering the nature of the sport of skeleton it is apparent that the main source of

aerodynamic drag would be from the athlete themselves. Both as the predominant contributor to the frontal cross-section and the overall surface area profile causing skin friction and turbulent flow. Hastings (2008) formed a foundation CFD model to investigate and quantify the aerodynamic significance of potential variables and found the sled profile to be only 9% of the drag of the total system and therefore best to focus efforts on the athlete. It may be thought that this could be of interest if a talent identification process was to be undertaken to introduce potential athletes to the sport. It is interesting to note though that over the last decade there has been no single dominant body type in the sport of skeleton. It appears that each build has its own advantages and disadvantages with the overall success more dependent on the cumulative effect of athlete experience / ability and push start times. However general observation since 2004 shows a shift towards those with a build that bio mechanically pushes faster at the start forcing the remaining athletes at a disadvantage and must outperform through driving ability.

In order to quantify the influence of aerodynamic drag the flow regime needs to be determined. This is dependent on the density and dynamic viscosity of the air with the length and velocity of the sled / athlete system. The characterization of the flow regime is quantified by using this information to calculate the Reynolds number (Re) by:

$$Re = \frac{\rho v L}{\mu} \qquad \text{(Eq. 2.1)}$$

Where $\rho$ and $\mu$ are the density and dynamic viscosity of air being 1.22 kg/m$^3$ and 1.79x10$^{-5}$kg/m.s respectively, $v$ is the velocity and $L$ is the length of the athlete where $v$ = 35m/s and $L$ = 1.75m for this approximation resulting in Re = 4 x 10$^6$. A Reynolds number of this magnitude places the air flow in the turbulent regime. Using a similar approximation Hastings (2008) also constructed a basic energy model to investigate the

sensitivity of overall descent times to start velocity, frictional contact with the ice and aerodynamic drag. The outcome resulted in aerodynamic drag being less critical than start velocity and kinetic friction of ice, with the coefficient of kinetic friction having 6 times more influence.

There are aerodynamic gains to be made in terms of saddle / body position, helmet construction, speedsuit material and fit, and bellypan profile all of which would require extensive wind tunnel testing and computational analysis. The difficulties of repeatable measurements and accuracy of wind tunnel testing, due to the low position of the skeleton sled and athlete within the turbulent boundary layer, combined with the strict rules of the FIBT prohibiting any component / addition that may serve as an aerodynamic aid reduces the level of engineering interest in an aerodynamic study. It is interesting to note that prior to the 2006 Torino Olympic Games it was observed that two major competing nations in the sport, both with access to wind tunnel facilities, came to two very different conclusions in terms of the more aerodynamic speedsuit to use. A more beneficial aerodynamic study could be conducted on the track in long straight sections using a comparison between athletes and noting performance shifts with equipment alterations, combined with the athlete's sensation to turbulent reduction.

### *2.5 Runner Design, Set Up and Interaction with the Ice*

The other physical form of drag is that of the contact between the runners beneath the sled and the surface of the ice. Stiffler (1984) used the conservation of energy and thermodynamic principles to determine the coefficient of friction between a non-melting slider on a melting surface and the dependency on the velocity of the slider.

This is quantified as:

$$\mu = \frac{2k(T_m - T_0)}{\sigma\sqrt{\pi\alpha l_c U}} \qquad \text{(Eq. 2.2)}$$

Where $k$ is the thermal conductivity of the slider, (16 W/(m.K) for stainless steel), $T_m$ is the melting point of the substrate, $T_0$ the ambient temperature, $\alpha$ the thermal diffusivity of the slider, ( 3 x $10^{-6}$ $m^2$/s for stainless steel) and $U$ the velocity of the slider (35 m/s). The remaining variables are athlete specific with $\sigma$ denoting the load per unit area and $l_c$ the length of contact. Both of these values are dependent on the athlete and sled setup and for this approximation will be 1.2 MPa and 0.2 m respectively. These are conservative when considering the rounded profile of the runner and surface roughness of the track therefore producing an over estimate for the coefficient of friction, $\mu$ = 0.01. This is in agreement with the work of Bromley (1999) and consistent with frictional heating being the dominant mechanism for creation of a meltwater film on which the sled slides. However, this is for sliding with no external interaction from the athlete and only under the acceleration due to gravity. Steering dynamics results in a harsher interaction between the runners and the ice, Hubbard (1989), quantified an upper limit for the coefficient of friction measuring a bobsled lateral skid to be 7 times greater due to the damage / chipping of the ice surface. Furthermore with the g-force experienced in the corners being significantly greater, the FIBT restricting a limit of 5 g for no more than 2 seconds, the impact friction tests of Fauve (2008) reach a maximum coefficient of friction of 0.18 for luge. This is due to the increased penetration of the runner into the ice surface under such g-force. The athlete is attempting to achieve the optimum trajectory down the track and so it is of interest to optimize control without excessively increasing the coefficient of friction through steering dynamics or high g-force.

As previously stated the primary variable on runner fabrication is the specific geometry of the grooves, or "groove cut". With the FIBT restriction of using a single type austenitic stainless steel for the runners raises the question of, "*what is the optimum cut?*" The answer to this will be different for every athlete depending greatly on their physical characteristics; sleds of differing weights and variable bow in the runner itself. The ice conditions must also be considered, the athlete has the opportunity to change the runners for a suitable "groove cut" for the particular conditions. The rules of the FIBT allow scope to vary the dimensions of the runners to compensate for differing athlete builds, driving styles, sled setup and weather / ice conditions. However, the number of runners permitted a season is limited to 4 sets only and is strictly regulated, FIBT (2008).

It can be considered that the principle behind the grooves of the runners is to allow the athlete to *control* the sled down the track. Every steer essentially damages the ice surface in order to get the desired results. The runner will only damage the ice surface as much as the down force causes it to. The process itself is likely to be a combination of surface chipping and plastic deformation. The athlete must *determine a point of instability* by changing the runner cut and bow. In general too much control can indicate a high coefficient of friction with the ice and is slow, (Fig 2.5).

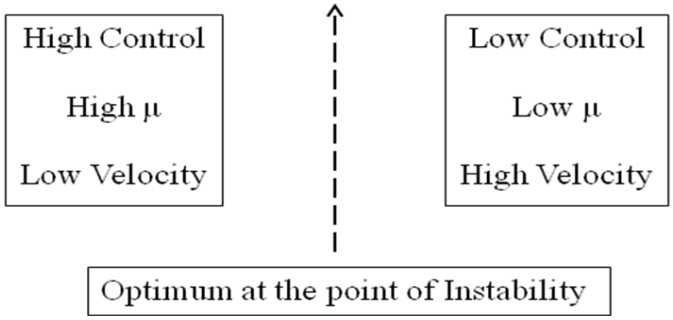


**Figure 2.5 - A skeleton runner provides control by damaging the ice surface. The athlete chooses a suitable runner by determining a point of instability where sufficient control is provided without sacrificing velocity.**

Athletes determine the optimum runner by altering the sharpness of the spine edge, groove geometry and reducing the contact patch by increasing the bow. Preferably in that order as altering the rock also adjusts tension in the frame therefore too large a shift in bow can cause unnecessary complications in frame response. As no physical alterations are allowed to the runners means that the material tests of Bromley (1999) cannot currently be applied.

Where Bromley (1999) is of interest is when considering the FIBT material is an austenitic stainless steel which exhibits work hardening. Therefore when an athlete polishes their runners for maintenance they can cause plastic deformation and in doing so a resistance to further deformation builds up and the surface hardens. This has caused concerns as to the variation in surface hardness of different sets of runners. Also polishing techniques to prepare the runners for races should not involve the use of additional lubricants as this can leave surface contaminants that may reduce the frictional contact.

There is another factor to consider, perhaps the most important and most overlooked in the skeleton community - the curved ends of the runners. The material is supplied by the FIBT in 1 – 1.2m lengths of round bar. The process itself of bending the bar to fit the runners must be undertaken with care to attempt to achieve as even a curve and as symmetric a pair of runners as possible. The runners are bent in a cold forming process so that the work hardening from the original processing is not lost and the runners remain strong enough for use. The radius of the curve at the endpoints of the runner, (Fig 2.2), plays an important role as it determines the rate of increase of curvature when tension is applied to the runner and therefore controls the contact patch with the ice. Athletes should be aware of this as changing runner manufacturers may therefore require

an alteration to the magnitude of curvature to achieve a comparable contact patch. It is generally overlooked that this tension is not only in the runner but also the frame of the sled and so the curve of the runner can have significant consequences on how the frame responds and therefore should not be ignored as a variable in the frame setup.

### *2.6 Frame Response*

Skeleton sleds have substantial weight with the majority contribution being from the steel frame. The construction must be able to withstand the forces exerted on the sled-athlete system during a descent. In a sport where the steering is achieved by athlete weight transference it follows that different athletes need different attributes from the sled to achieve optimum performance. The sport of skeleton does not currently recognize this fully. Many athletes make do with the equipment that is available to them, usually with crude alterations and additional weight lashed to the frame to achieve a static balanced position on the runners with complete disregard as to how this may affect the functionality of the rest of the components during a dynamic descent.

Two aspects are apparent from observing the sport of skeleton:

1) It favours the experienced

2) Some *messy* runs are still fast

The first is true for any activity, Gladwell (2008) postulate that for any activity 10 000 hours of practice are required to fulfil potential. Gladwell also highlight the importance of recovery between practice sessions. Many top athletes will agree that there are no real secrets to the best lines down a track and also have had the same steering approach

for many years, yet times continue to improve. The winner not being the athlete with a *perfect run* but is the athlete who recovers best when mistakes occur. A common view on why this occurs is to do with relaxation. Of course every athlete involved in the sport is willing to commit to tackling the tracks yet it is human nature to become tense in extreme situations. With no forms of suspension in a skeleton sled it seems apparent that high body tension would cause excessive vibrations through the sled frame and a constant chatter between runners and ice resulting in unnecessary damage to the surface and therefore slower times. A more relaxed athlete would absorb the motion of the frame and allow the sled to gather momentum more easily. This was highlighted in my own performance when I achieved a personal best in a race whilst suffering from the flu. I was alert enough to steer when required and video footage showed a far more relaxed position on the sled.

The second observation of fast runs with untidy lines suggests the overall frictional drag is still low. From personal experience there have been occasions where a descent felt to have large errors only to find at the bottom of the track that the time was comparable to a previous run with fewer errors. In these situations it perhaps highlights that the errors did not cause significant loss in velocity compared to the damage to the ice required in order to prevent these errors from occurring. Similarly when observing other athletes, ignoring the possibility of illegal material being the reason and staying with the hope that the sport is fair, how is this possible? The cases have no trend in body shape. Either it was a genuine error that happened to occur in a section of the track that did not sacrifice significant energy or momentum to the sled / athlete system or the sled / athlete system has a more optimum setup allowing the sled to continue to gather speed.

## 2.7 Sled Styles and Manufacturing

### 2.7.1 Sled Styles Used by Elite Athletes

There are a few sled manufacturers with consistent success at the highest racing level that athletes favour. There are two styles of particular interest. Firstly is a sled that will be called *Sled A* in this thesis and follows the geometry and saddle configuration of the FIBT schematics very closely. Secondly a sled that will be termed *Sled B* that has an alternative saddle design fabricated from a single piece of steel plate cut to an H-shape and mounted at the midsection of the frame, (Fig 2.6)

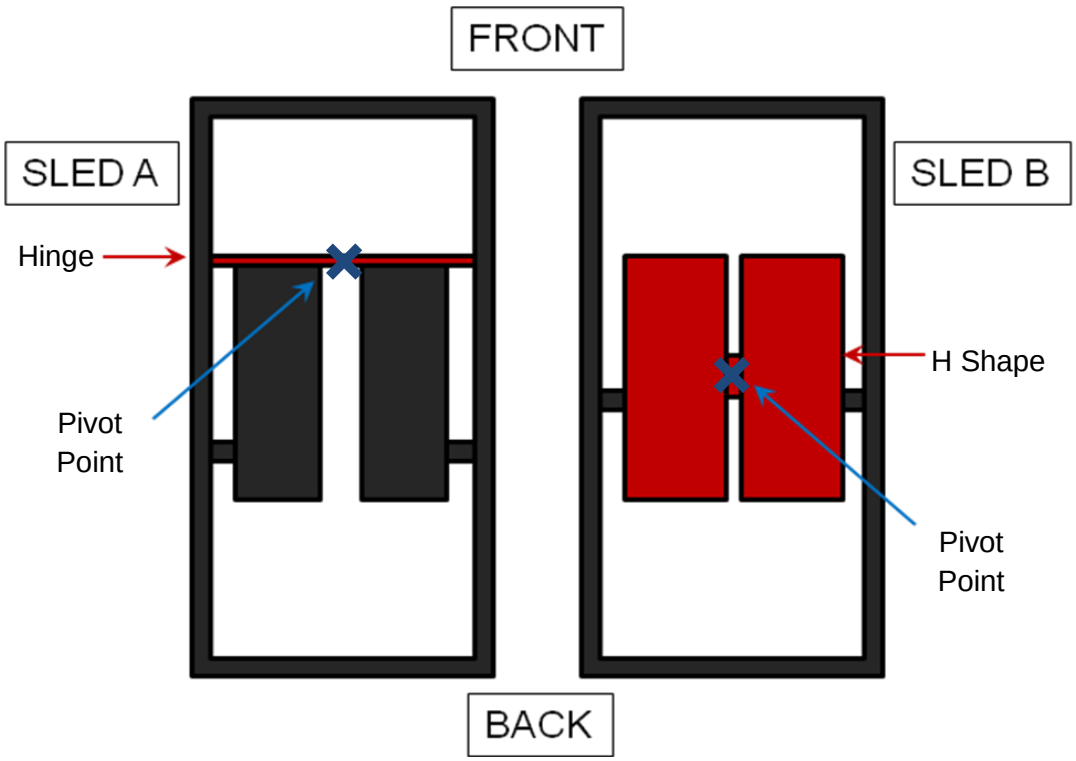


**Figure 2.6 – Simplified Diagram showing the pivot points of Sled A with a hinge at the front of the saddle plates and Sled B with an H-Shape saddle plate.**

Sled A has been the more popular in recent times although one particular manufacturer's choice of material and specific saddle geometry consistently produced the best results on the World Cup. Athletes using Sled B also have successful results at the highest level and upon comparison of these two shows the use of differing materials for the frame construction. Sled A is made from a CrMo (4130), Sled B from a stainless steel. The resulting frames have different dimensions to ensure the structural robustness is achieved with these materials.

Sled B is one of the most rigid produced but the placement and geometry of the saddle has proven very successful. The two halves of the saddle being cut from a single steel plate, connected at the mid-point which forms a strong structural frame, the diagonal twisting still possible and governed by the rigidity of the midsection. There is little scope for adjustments within the frame. The rectangular frame thickness of this type of sled is typically 8mm for the longbars and 5mm for the crossbars.

Sled A has a more flexible saddle plate design. The two halves are hinged onto a cross bar towards the front of the sled and loosely bolted to the long bars at the rear of the saddle plates. The long bars are thinner (6mm at thinnest but reinforced at end-points up to 9mm at thickest). The width bars are also thinner, machined into an I-Beam cross-section (min 3mm – max 6mm). The result is a frame that has less torsional rigidity, however with the saddle pivot towards the front of the sled results in a more knee-dominant steering, discussed further in Section 2.8. Even the use of shoulders will create a greater shift in contact patch towards the rear of the sled.

Many athletes view Sled B as being stiffer, that is with more resistance to flex on the diagonal, and conclude that it is less responsive to Sled A. However this is not correct,

although the more central pivot point reduces the distance and therefore also the turning moment from forces applied by the knees, it is still sufficient to steer using the knees and the consequence for shoulder steering is greater sensitivity as the distance to the pivot point is increased. First thoughts when taking these factors into consideration may be that Sled B would be a more popular choice for elite athletes, however in practice the general view is that Sled B is less responsive at slower speeds.

In recent times the Sled A style sled has become dominant on the International racing circuit, possibly through availability and cost but also by having this greater knee steering capabilities enabling novice and intermediate athletes to progress faster than if they were to begin on Sled B. Like many sports, athletes can become accustomed to particular pieces of equipment and so if they begin on a Sled A style sled it is likely that they will stay with a similar frame design. It should be noted that major championships have been won on both.

### *2.7.2 Sled Manufacturing*

The sport of skeleton does not have the commercial interest of say cycling, skiing, tennis racquets. There are other manufactures, a number who follow similar specifications to Sled A. Historically the equipment adapted through trial and error, not through significant engineering input. There are still athletes that will compete on hybrid sleds constructed from leftover spare parts in home workshops.

Ryan Davenport has made the largest contribution to the availability of equipment in the sport. Coming from an engineering background and involvement in drag racing he was also twice World Champion and many athletes have since had success on his equipment.

The success of Bromley Technologies was previously mentioned, who have a unique and highly secretive sled from extensive research since 1995. FES, a German sports Engineering company are also highly confidential and further engineering programs have begun in Canada and USA since the 2010 Olympics. Walser manufactures exceptional skeleton sleds and also equipment for the historic sport of Cresta from which skeleton originated. Since skeleton was reintroduced to the Olympics in 2002 there has also been involvement from McLaren and Ferrari.

### *2.7.3 Primary Test Sled Used in this Work*

The primary test sled for the following studies will be Sled C, (Fig 2.7). It is of German construction and based on the Sled A style frame and so has scope for investigating adjustments to the saddle. Although a similar construction to Sled A it has very different characteristics. The main differences being:

1) Material: Sled C uses a 304 stainless, 8mm thick for the longitudinal and 3mm thick for the transverse. There have been cases of the Sled C frame failing in use likely from fatigue.

2) Saddle Placement: the saddle of Sled A is shorter and so has a larger distance from the corner blocks to the saddle fixing points where it is mounted to the frame. The saddle plate of Sled C is longer and fixed closer to the corner blocks creating a bracing affect and stiffens the frame, (Fig 2.7).

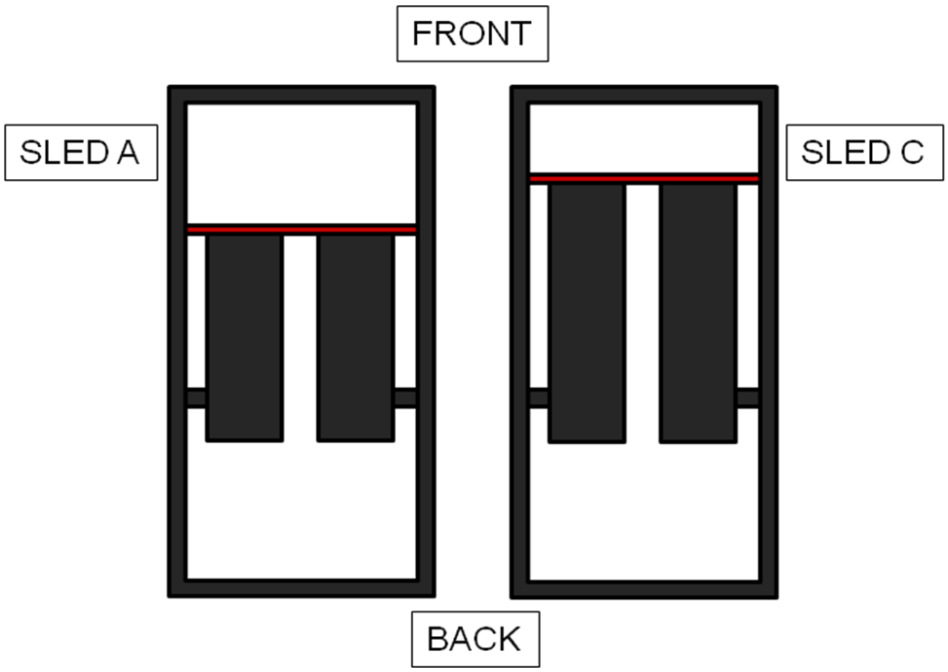


**Figure 2.7 – A comparison of Sled A and Sled C, highlighting the longer saddle plates of Sled C.**

## *2.8 Sliding: How a Sled Turns*

There are many methods of steering a skeleton sled depending on the type of sled or the athlete's physical characteristics and personal choice of driving style. Here I present current views, commonly held by athletes and coaches, on how a frame responds and what an athlete is ultimately trying to achieve. In steering a skeleton sled there is a delay in its response. Whilst in flat sections of the track the athlete is unable to create rapid alterations to the sleds direction of motion. The runners have little interaction with the ice surface on these flat sections and the athlete's main form of control is to create slight drifts by tilting a head to one side or leaning the whole body. Dragging a toe pivots the sled about the centre of gravity but also sacrifices speed in the process and is generally thought to be an excessive steer, only to be used if the shift in sleds orientation

is crucial for the following section of track. Excessive movements cause the sled to rotate and skid thereby losing significant speed in the process.

The sled is most responsive at the entries and exits of corners and it is at these points that the greatest precision is required. The curves are banked and begin with an *entry fillet*. This is a contoured build-up of ice that enables the sled to travel from the flat region of the track onto the banked wall of the curve and similarly an exit fillet at the end of the curve. The entry fillet can extend well before the curve begins giving a smooth path onto the curve, or start close to where the curve begins resulting in a steep path. As a sled travels along the entry fillet the sled and athlete begin to experience increasing centrifugal force from the rotational motion because of the increase in the track profile curvature. The orientation of the sled alters under this centrifugal force. In short curves the sled will travel down the exit fillet as the track straightens. In longer curves an oscillating motion is observed. This can be understood in a similar way to a snowboard generating height by angling through a halfpipe (Fig 2.8). That is if the athlete were able to turn the sled sufficiently at the very start of the curve then it would follow a flat line in the same way that were a snowboarder to turn the snowboard straight down the belly of the halfpipe then it would follow a straight path down the belly. However, due to the relatively blunt runner-ice interaction there are very few situations where the athlete would be able to turn the sled sufficiently to travel the flat line without excessive skidding on the ice surface.

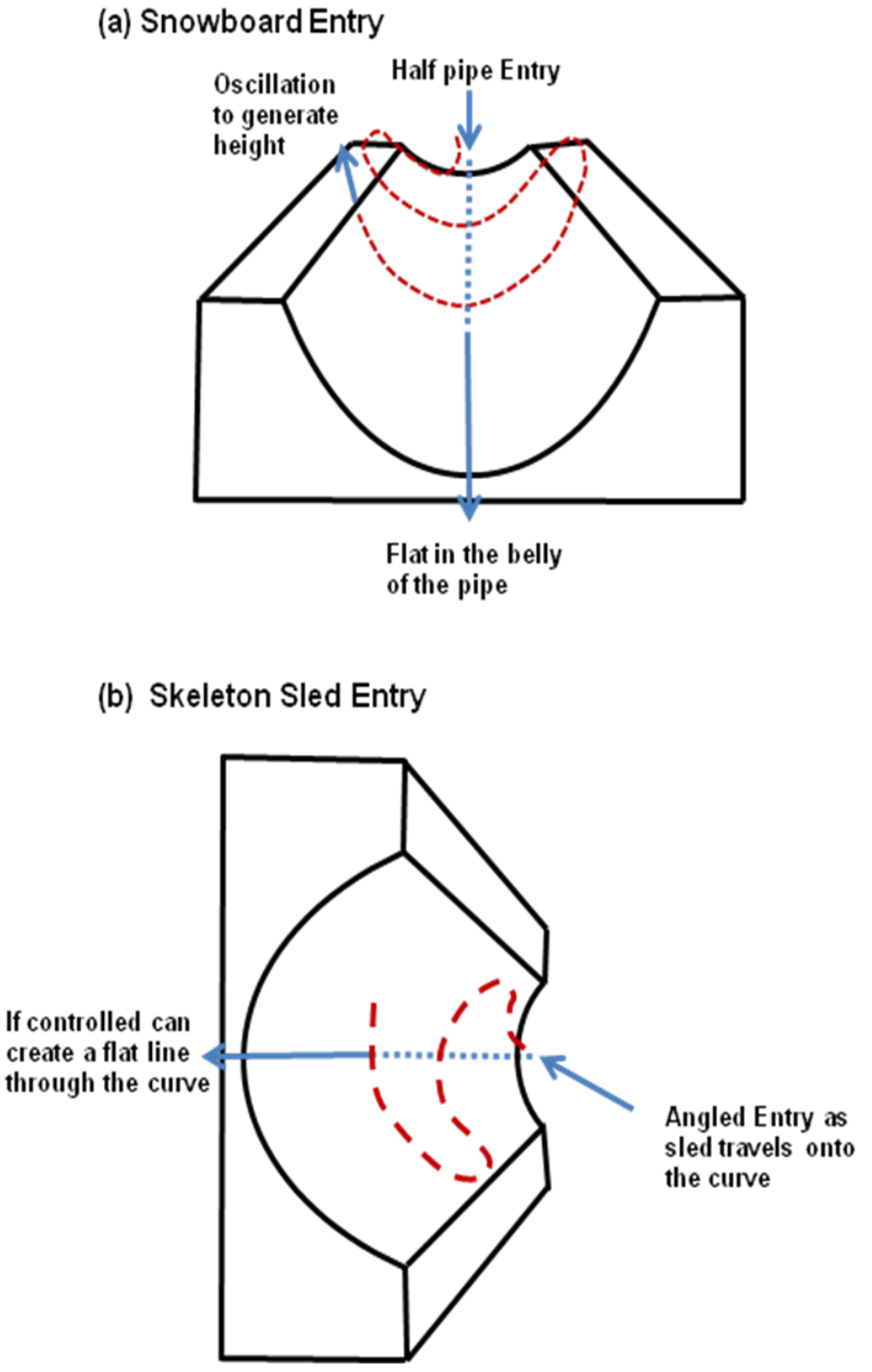


**Figure 2.8 - Oscillations within a bobsleigh track curve can be envisaged in a similar way as the motion of a snowboard in a half-pipe.**

Were the sled to enter angled away from the curve direction then it would result in a steeper trajectory onto the curve. A skeleton sled has a delayed response and typically achieves a height that exceeds the flat "perfect" line through the corner. If the athlete were not to respond at all the sled would climb excessively in height onto the corner. By continuing to climb in height the centrifugal force becomes insufficient to maintain the vertical position. The gravitational contribution overcomes that of the centrifugal force and the frictional contact with the ice and the sled begins a downward motion, (Fig 2.9)

If the curve continues once the sled has dropped below the centre line of the profile the centrifugal force builds again and a second oscillation occurs. This oscillating motion is one of the first elements an athlete must learn to feel and control, for the geometry of the track is rarely such that letting the sled run through the corner will result in a smooth exit. In practice, the downturn of the oscillation can cause the sled to exit the curve at an angle, resulting in a poor entry to the following curve or even impact with the track wall. It is typical that subsequent oscillations are greater in magnitude than the previous oscillations as it can be thought of as a second curve that the sled enters with an angled entry, as discussed above.

As the athlete makes their initial approach to a curve they aim to set a position in the track that best allows the sled to smoothly rise onto the corner. This is not only aiming for the entry point to rise up the fillet but also the entry angle. For a particular entry velocity there can be an optimum position and angle such that the sled flows through the curve with minimal interaction from the athlete in order to achieve a smooth exit and efficient trajectory onto the next curve. Setting this entry position and angle alone does not necessarily mean that no further work must be undertaken by the athlete for the remainder of the curve (although that would be the ideal scenario) but it is the time where an athlete has the best opportunity to alter the sleds trajectory through the curve.

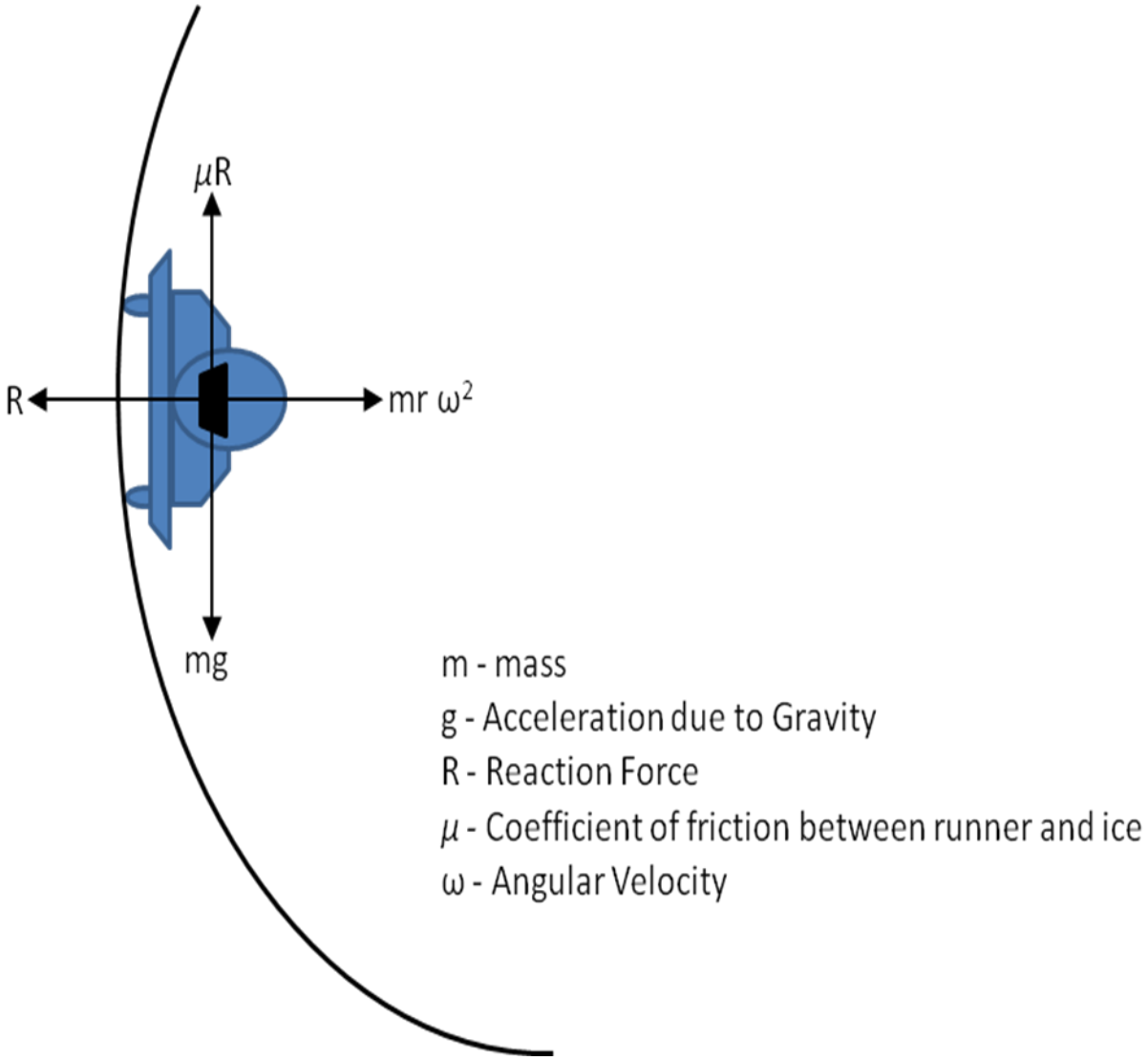


**Figure 2.9 - Force diagram of skeleton sled and athlete whilst in a curve.**

As the sled travels along the entry fillet any twist in the sleds frame alters the contact patch between the runners and the ice enabling angular changes in the sleds orientation. The curve does not necessarily begin to turn where the entry fillet commences and is typically straight at the initial rise of the fillet. Once the corner begins to turn the centrifugal force builds and it is at this point where an athlete can greatly alter the sleds

trajectory by creating an asymmetry in the contact patch through controlling the deformation of the sled frame.

Shorter corners only have a single oscillation where the fall of the sled as the centrifugal force lifts coincides with the end of the curve. Longer curves may have two, or even three oscillations and don't necessarily end on a smooth downward oscillation. Failure to set a required angle at the beginning of the curve could result in the sled dropping out with a bumpy exit. Multiple oscillation corners present the opportunity for continued work throughout the corner as the centrifugal force builds and lifts. For many curves the midpoint, where the g-force is greatest, is so large that movements by the athlete have very little affect.

Putting aside t intricacies of curve profile, entry and exit fillets, a general approach to controlling these oscillations is to either steer down at the beginning, reducing the height achieved by the sled and resulting in a longer, flatter oscillation, or by holding the high point preventing the sled from dropping too soon off the oscillation, again resulting in a further distance travelled. I should emphasise that in practice the reality is more likely to be a combination of multiple, subtle steers used as well as careful sled angle control upon entry. As long curves have multiple oscillations the approach to traversing a section of the track will vary from athlete to athlete.

Typical steering approaches are:

1) Knee steering: with the rear of the runners having the spine, an obvious method of steering is to apply force to the frame with a knee. This flexes the frame along the diagonal creating an asymmetry in the contact patch with the ice. This increases the running length of the spine on one side of the sled, and reduces it on the other, for example force from a left knee turns the sled left.

2) Shoulder steering: this works in tandem with knee steering as to apply force with a single knee the athlete's body must be rigid enough, essentially bracing with the opposite shoulder. This could also work in reverse applying force with just a single shoulder, bracing with the knees. Here, force from a left shoulder would turn the sled to the right

3) Shoulder and knee steering: for a more aggressive steer, force from opposite knee and shoulder causes maximum twist in the sled frame, so a left knee and right shoulder would provide maximum flex and turn the sled left.

4) Mass transfer: The frame doesn't necessarily have to be twisted to turn the sled. Leaning with the left shoulder can result in the sled turning to the left. This can confuse novice athletes as it is not immediately obvious as there is no image of the sled deformation but results from turning moments from the centre of gravity combined with the orientation of the sled on the tracks curved profile.

In summary, the literature review shows research in the push start, aerodynamics, frictional contact with the ice, trajectory and frame response are all beneficial to improve overall performance. Accounting for the rules and restrictions set by the FIBT reduces the benefit in aerodynamic or ice friction research. The remaining three areas become the focus of this thesis.

Previous push start studies are mostly focused on physical attributes and overall push performance. In Chapter 3 I investigate the application of an accelerometer within the

sled to analyse the push start in more detail and quantify phases that will aid the athlete to target aspects of their push start that need further training and ultimately improve their performance.

# 3 THE PUSH START

The skeleton descent commences from a push start and although the start alone will not win the race it is crucial for a successful skeleton descent. If there is too great a speed deficit after the push start it can become impossible to out perform athletes with a faster start through driving technique and therefore is an important element of much of an athlete's training. To determine how best to instrument a sled such that the trajectory and frame response can be investigated requires a thorough understanding of the limitations posed by the space available within the sled and also the effectiveness of sensors that are applied.

This chapter examines the push start of a skeleton bobsleigh run using accelerometers, timing information, video records and track geometry details to quantify the dynamics and identify the different phases of a skeleton start. By examining the mechanics that govern these phases the characteristics of a good push start can be established. The data obtained provides detailed information on the performance of a skeleton athlete during a push start, and will allow athletes to target specific areas for training and improvement.

## *3.1 Phases of the Push Start*

A skeleton push start can be viewed as being in four phases, which are shown in Fig 3.1. During the early stages of the descent, the athlete:

A. *Drives* off a fixed starting block with as much force as possible.

B. Continues to *accelerate* by running alongside the sled until they can run no faster.

C. *Loads* onto the sled with a dive, landing in a head-first, face-down position, flat on the sled.

D. Settles into the *race position*, in which subtle movements and flexing of the sled are used to control the remainder of the descent.

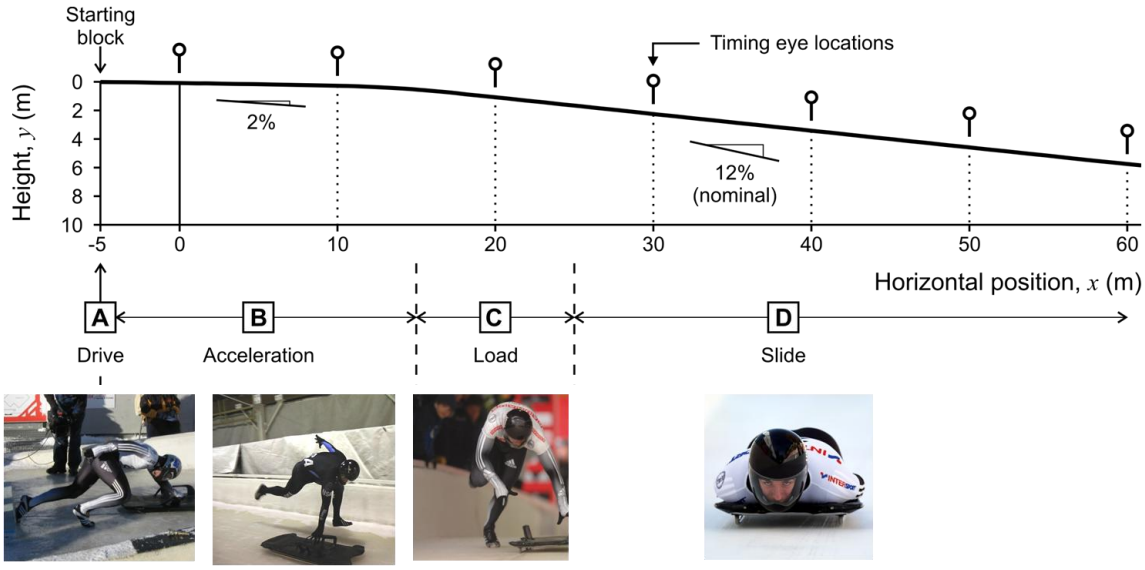


**Figure 3.1 - The vertical profile of a push track, showing the four phases of a push start.**

The push start is only a small part of the overall run, but the interaction between the sled and athlete during the start has a strong influence on the final descent time, and it is consequently a particular focus of a skeleton athlete's training. An athlete's success in the push start is partly a result of their physical power and the speed required to accelerate the sled; however, an athlete who can accelerate quickly in an upright sprinting position will not necessarily produce a good push start due to the bent-over position whilst pushing the sled. Good technique is essential during all stages of a push start. The push start is particularly prone to errors in technique under race conditions as technique can deteriorate when attempting to maximise power output and doing so under

pressure of competition. Once the athlete has learnt the basic push start, training involves biomechanical drills to refine their technique and give maximum efficiency to minimise any chance of error in a race.

Push start technique varies from athlete to athlete, but one important distinction is whether an athlete grasps the sled with both hands or only one hand during the drive and acceleration phases. A two-handed push start is the more traditional technique and is more stable than a single-handed start; however, grasping the sled with both hands whilst running to one side requires the athlete's spine to twist, making it more difficult to drive the sled forward. A two-handed push may also result in sideways flicking of the feet, and increased bobbing motion compared to a one-handed push, consequently experienced athletes nowadays adopt a single-handed push start technique, but two-handed push starts are used to gain balance and confidence during initial training. The majority of World Cup and Olympic athletes now use the one-handed technique. The few that still use two handed typically have longer arms and flexible backs so the athlete's power can still be applied in the forwards direction.

### *3.2 Push Tracks*

Athletes train on "push tracks", which are short, straight tracks that have the same geometry as the early sections of full race-tracks. Push tracks have well defined vertical gradients, no horizontal curves, are equipped with a greater number of "timing eyes" than full tracks, and the controlled indoor environment helps maintain consistent ice conditions. They thus allow well-controlled experimental work.

The vertical profile of a push track (Fig 3.1) is set by the Federation Internationale de Bobsleigh et de Tobogganing. It must not exceed 2% for the first 15m, but then steepens to a nominal 12%. The position of the crest and the gradients vary from track to track. Two push tracks were used during this study: the Calgary Ice House track (track C) and

Torino Olympic Park track (track T). The maximum gradients were measured as 11.7% on track C and 10.5% on track T.

The ice on push tracks is prepared by shaving the existing ice flat, cutting a single groove to accommodate a single runner, and spritzing with water to give a smooth finish. The groove allows the athlete to accelerate in a straight line and is cut for a distance far further than an athlete would run. The refrigeration system maintains as constant an ice temperature as possible with approximate daily fluctuation from -1ºC to -3ºC. The preparation is the same as on race tracks; however, the controlled environment of an internal push track helps minimise track deterioration between each run.

Both tracks C and T have timing eyes at 10m intervals, as shown in Fig 3.1. Timing information is routinely recorded for all push track descents, and is used to assess the success of a skeleton start in terms of (a) the time taken to reach the last timing eye and (b) the velocity measured at the final timing eye. Timing starts when the sled passes the first timing eye, and consequently this is used as the datum for time and position in the current study. On a push track, the starting block is positioned 5m before the first timing eye (Fig 3.1). On a full skeleton track, however, the first timing eye would be 15m after the starting blocks, the equivalent of the 2$^{nd}$ timing eye on a push track.

## *3.3 Experimental Description*

### *3.3.1 Instrumentation and Data Analysis*

A single skeleton sled and runners with a standard cut were used during this study. The sled used was Sled C as discussed in Chapter 2. A triaxial accelerometer, Crossbow CXL10LP3, was attached towards the rear of the frame of the sled (Fig 3.2), so that the device recorded the sled acceleration. Data was logged at 100Hz per channel using the Race Technology DL1 data logger, allowing frequencies up to 50Hz to be recorded

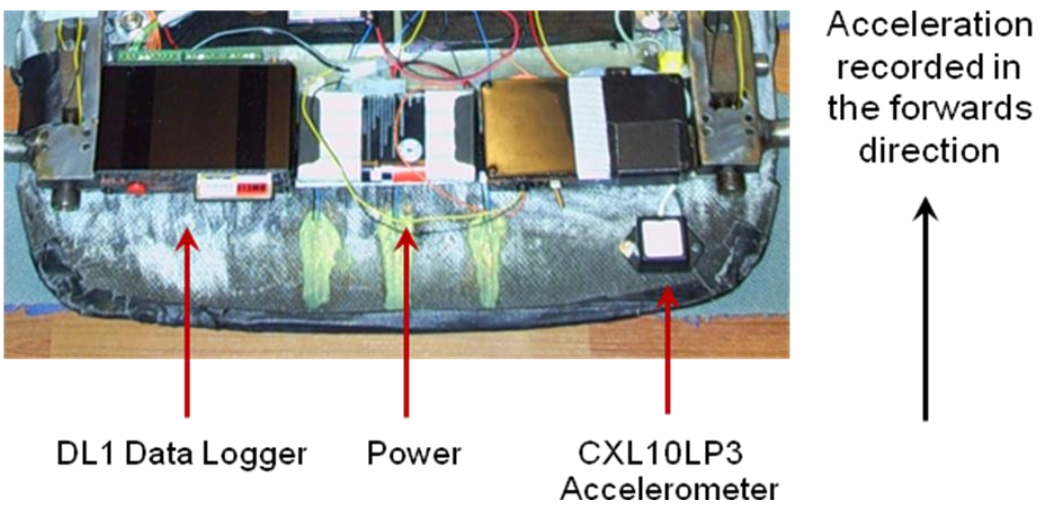


**Figure 3.2 – Location of Instrumentation installed at the rear of the sled in this study.**

accurately according to Nyquist Theory, Horowitz P and Hill W (1989)**.** The data logger and accelerometer were equipped with stand-alone power sources that allowed them to be fitted inside the sled without any interference to either the athlete or the aerodynamics of the sled.

The accelerometer was orientated to measure the accelerations in the three orthogonal directions relative to the sled (Fig 3.2), but only the horizontal forwards acceleration will be examined in this chapter. The measured slope angle of the push track (Fig 3.1) was used to determine the horizontal acceleration from the accelerations recorded relative to the sled, and to compensate for the shift in gravitational contribution with track gradient. The acceleration was then integrated numerically to calculate the velocity throughout the push start. This was achieved by beginning with the first data point and dividing the calibrated acceleration signal by the sampling rate producing the associated velocity. The cumulative summation of this calculation through all the data points recorded enables the velocity increase in time to be calculated. Similarly, repeating this integration method to the now velocity data points results in the position of the sled. An example of the resulting plots of acceleration, velocity and position against time are

shown in Fig 3.3. Using the known split times measured at the 10m intervals provides confidence in the calibration of the accelerometer and double integration process of the data, by overlaying the split time data to the double integrated position plot, which will be described in further detail below. Note that all athletes loaded onto the sled between 10m and 20m, and consequently the first two timing eyes recorded the passing of the front of the sled, whereas the remaining timing eyes recorded the front of the athlete's helmet. The timing eye positions have been adjusted to take this into account. Video footage was also recorded for all runs, and this was used to determine footfall times, which are also plotted in Fig 3.3.

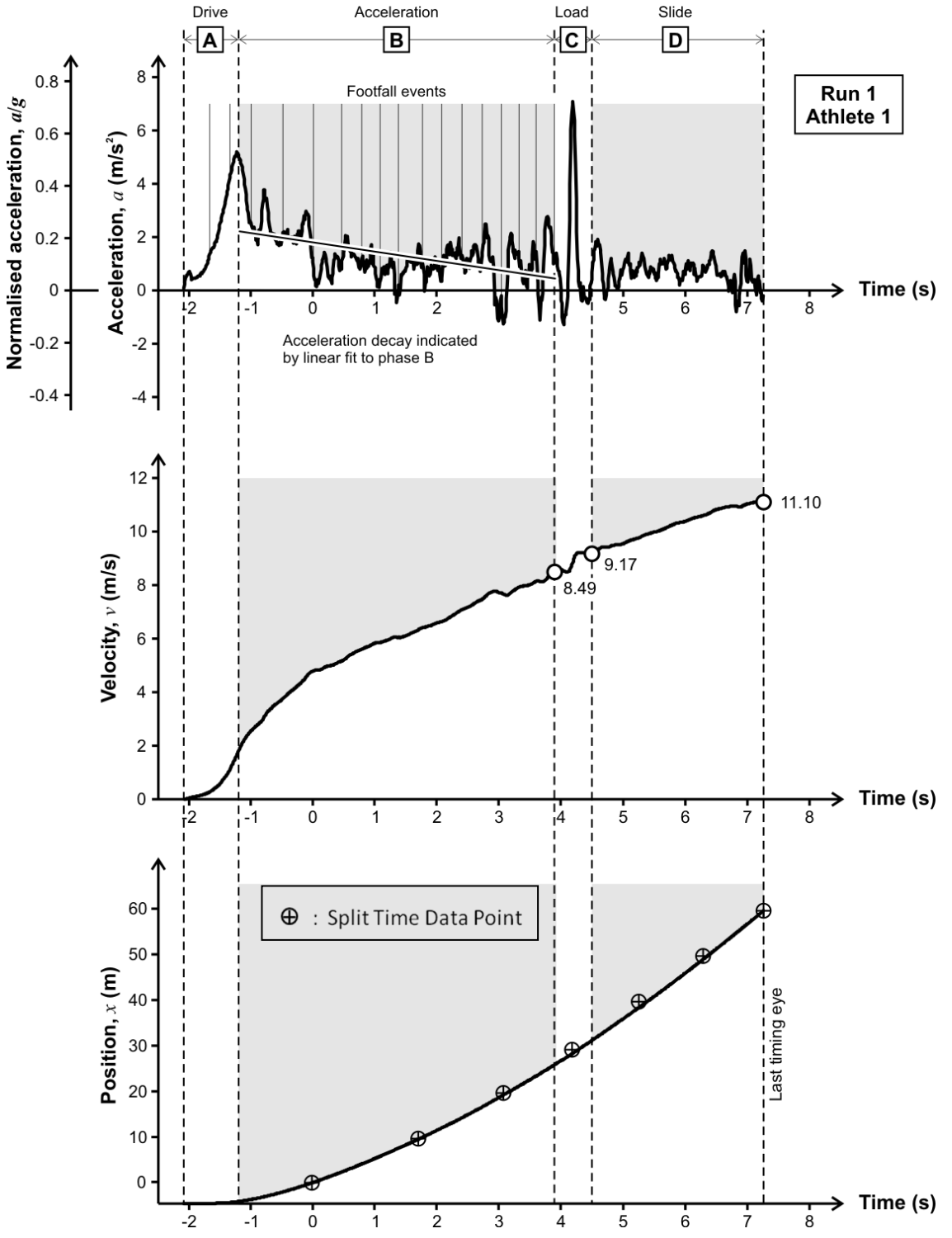


**Figure 3.3 – An example of the recorded acceleration data and its double integration to determine the velocity and position of the athlete with time (Run 1, athlete 1, at track T).**

### 3.3.2 The Athletes

Four male skeleton athletes took part in this study, three of whom were experienced internationally competitive athletes. The fourth was a recreational skeleton athlete, who has been regularly involved in the sport, but who has not undergone rigorous push start training. Push start potential is traditionally assessed in terms of an athlete's power and their sprinting ability. Power can be assessed using a power clean weightlifting exercise, and sprinting ability is assessed in terms of a 30 m track sprint where stride frequency can also be considered and any relevance for the biomechanics suited to a push start. Table 3.1 lists the athletes' mass, power, and sprint performance, but note that this is only intended as an indication of their relative performance and physical characteristics.

| Athlete | Mass | Power* | Frequency** |
|---|---|---|---|
| 1 | High | High | Low |
| 2 | Low | Mid | Mid |
| 3 | Mid | Low | High |
| 4 | Recreational athlete | | |

* Maximum power tested through power clean weightlifting.

** Stride frequency during a 30m track sprint.

**Table 3.1 - The characteristics of the four athletes tested.**

Table 3.2 summarises the push start runs that are presented in this chapter. Runs 1 to 4 took place on track T. They compare the performance of athletes 1, 2 and 3, with two runs by athlete 2 to investigate athlete variation between different runs. The remaining two runs (5 and 6) took place on track C, and compare the performance of athlete 2 (experienced) and athlete 4 (recreational). The runs were conducted in the order they are listed.

| Run number | 1 | 2 | 3 | 4 | 5 | 6 |
|---|---|---|---|---|---|---|
| Athlete | 1 | 2 | 2 | 3 | 2 | 4 |
| Track | T | T | T | T | C | C |

**Table 3.2 - A summary of the runs studied in this chapter.**

### *3.4 A Typical Push Start*

The results from a typical skeleton push start are shown in Fig 3.3 for Run 1. This figure plots the horizontal acceleration, velocity, and position obtained from the accelerometer data, together with footfall times obtained from the video footage, and timing eye measurements. The plot of horizontal position demonstrates good agreement between the accelerometer data and the timing eye data.

The acceleration trace in Fig 3.3 consists of four phases that correlate with the actions of an athlete when starting a skeleton bobsleigh race (Fig 3.1).

*Phase A* is the initial acceleration or *drive* as the athlete starts from stationary by pushing off the starting block. The starting block is 5 m ahead of the timing eye, but the front of the sled (which triggers the first timing eye and hence the start of the timed run) is some distance ahead of the starting block. This distance varies from athlete to athlete depending upon their starting stance, which might involve two feet on the block, or a

split stance with one foot on the block. The initial drive typically takes place over the first two strides.

The athlete continues to *accelerate* the sled during *Phase B* whilst running along side it. The acceleration diminishes until their maximum sprint speed is reached and it becomes increasingly difficult to match the velocity of the sled. Fig 3.3 shows pulses in the sled acceleration during this phase, in which the footfall events generally occur when the sled acceleration is a minimum. The combination of the athlete's leg and body motion drives the sled forward, leading to a peak in the sled acceleration trace; however, there is not a direct match between footfall times and the peak sled acceleration, because the motion of the athlete's body does not transmit their forwards acceleration to the sled instantaneously. At higher velocity, the athlete's sprint is less balanced and the correlation between footfall and acceleration peak is lost, resulting in negative accelerations being recorded towards the end of Phase B. The net acceleration remains positive, but the negative acceleration troughs and the momentary drop in velocity at 3s indicate that the athlete has reached their maximum sprint speed, and that the athlete should load on to the sled. The time at which an athlete decides to load depends upon personal choice, experience and the feeling that they are no longer accelerating the sled, but the correct time can be difficult to judge.

*Phase C* is when the athlete loads on to the sled. *Loading* involves diving onto the sled and landing in race position. A successful load will increase the velocity of the sled; for example, in Fig 3.3 the velocity increases from 8.5 m/s to 9.2 m/s. The loading process is complex, involving sudden changes in sled acceleration that vary depending upon the athlete's loading style. In general, there are three significant components to the loading process:

- The start of the load is defined by the athlete's final footfall, which they use to *launch* their dive on to the sled (at around 4s in Fig 3.3). At the same time,

they may need to change their hold on the sled, for example, from one-handed pushing to a two-handed load. The launching action and change of hand hold results in a short period of deceleration of the sled at the start of the load.

- When the athlete lands, their *forward momentum* is transferred to the sled. A successful launch means that they will have a higher velocity than the sled; hence there is a sharp peak in the sled acceleration and a step change in the sled velocity when they land (Fig 3.3). The momentum transfer and hence the sled acceleration will depend upon the athlete's mass.

- The athlete also has *vertical momentum*, which must be dissipated upon landing. This momentarily increases the vertical force between the ice and sled, increases the runner-ice friction, and results in a brief period of deceleration. A heavy landing is thus detrimental to the loading phase.

Finally, *Phase D* starts once the athlete is settled into race position on the sled. Here, acceleration is governed by only gravity, wind resistance and frictional contact between the ice and the sled-slider system. The fluctuations in acceleration during the sliding phase result from irregularities in the ice surface, but the acceleration trace is also dependent upon damping between the sled and athlete, which in turn depends upon how relaxed the athlete is on the sled.

### *3.4.1 Quantifying Push Start Performance*

The two aims of a push start are to reach the last timing eye in the shortest possible time, and to do so with the greatest velocity. These key indicators of overall push start performance are plotted for each run in Fig 3.4. The different runs will be compared in detail below, but at this point it is worth noting that:

- The two runs at track C (Runs 5 & 6) were quicker than the four runs at track T, due to the slightly steeper track and different environmental and ice conditions.

- Runs 1 to 4 are presented in order of decreasing overall performance, rather than chronological order. Runs 2 and 3 have consequently been swapped in the figure, because this allows trends to be spotted in other indicators of push start performance that will be presented below.

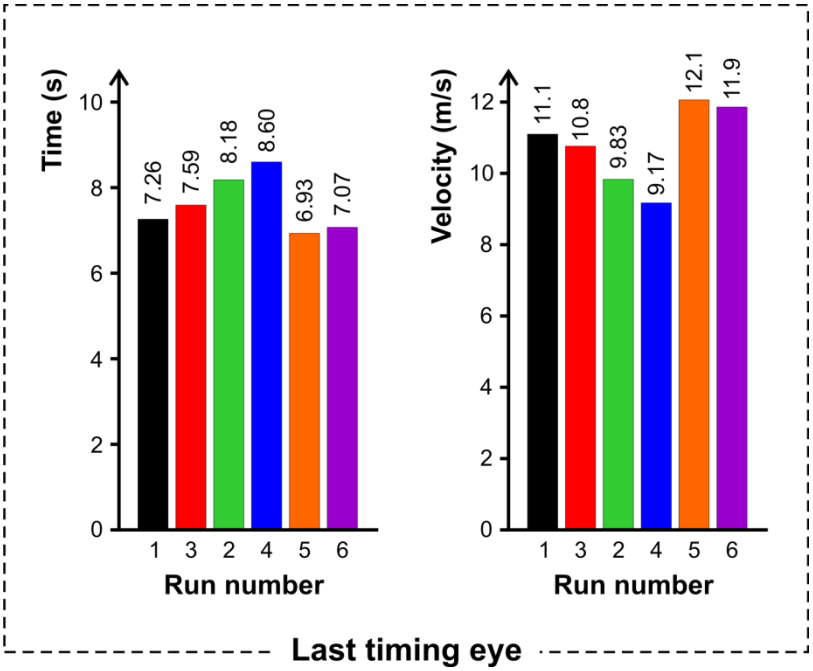


**Figure 3.4 – Indicators of overall push start performance, the total time taken to reach the final timing eye (left) and the velocity achieved at the final timing eye (right).**

The time and velocity through the last timing eye are good indicators of overall push start performance, but they do not tell an athlete whether there is a particular phase of their push start that they should work on during training. The acceleration data (such as Fig 3.3) can be used to derive other indicators of performance that relate to specific phases of the push start, and these are shown in Figs. 3.5 & 3.6.

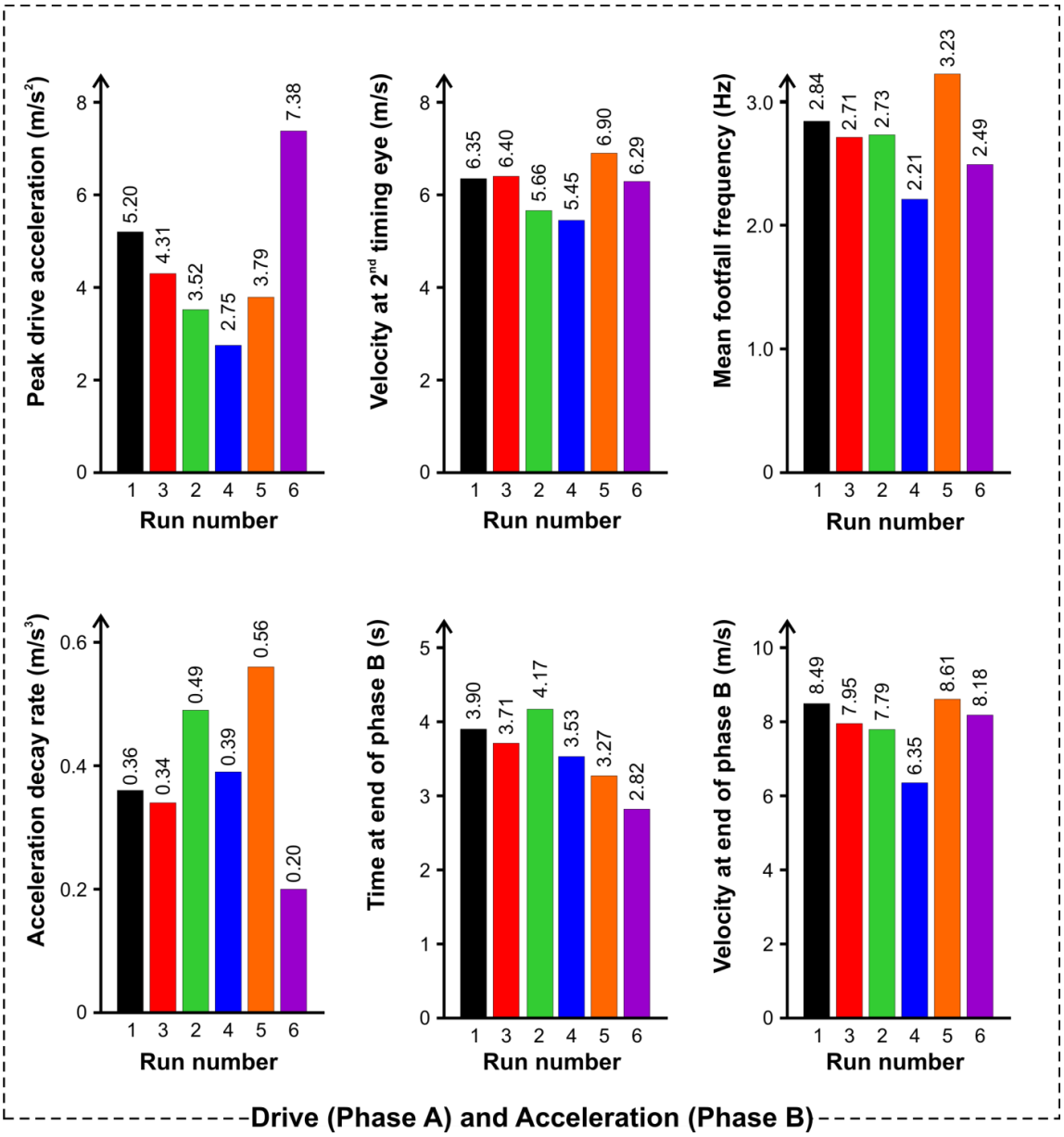


**Figure 3.5 - Indicators of athlete performance during the drive and acceleration phases of a push start where the drive, Phase A, can be quantified using the peak acceleration and velocity at the 2nd timing eye. The acceleration decay rate and footfall frequency can provide information as to the subsequent acceleration, Phase B, and when considered with the time and velocity at end of Phase B indicates the success at accelerating the sled.**

Fig 3.5 quantifies athlete performance during the drive (A) and acceleration (B) phases of the push start. The drive off the starting block is characterised by the peak initial acceleration resulting from the first two strides, and the velocity through the 2$^{nd}$ timing eye. Footfall frequency from a track sprint (Table 3.1) is commonly used to assess athlete performance, so Fig 3.5 plots the mean footfall frequency recorded during phases A & B of each push start. During phase B, the athlete's ability to accelerate the sled reduces as its velocity increases, and this is characterised by an acceleration decay rate that is the gradient of a linear least squares fit to the acceleration data. Phase B ends when the athlete decides that they cannot accelerate the sled further, and this is characterised by the time and velocity of the sled at the final footfall.

Fig 3.6 quantifies athlete performance during loading (phase C). It includes the maximum acceleration (associated with the transfer of forward momentum to the sled) and minimum acceleration (due to increased runner friction as the athlete lands). The change in velocity during loading, the load duration, and the resulting mean acceleration are also given, and their ability to characterise overall loading performance is discussed below.

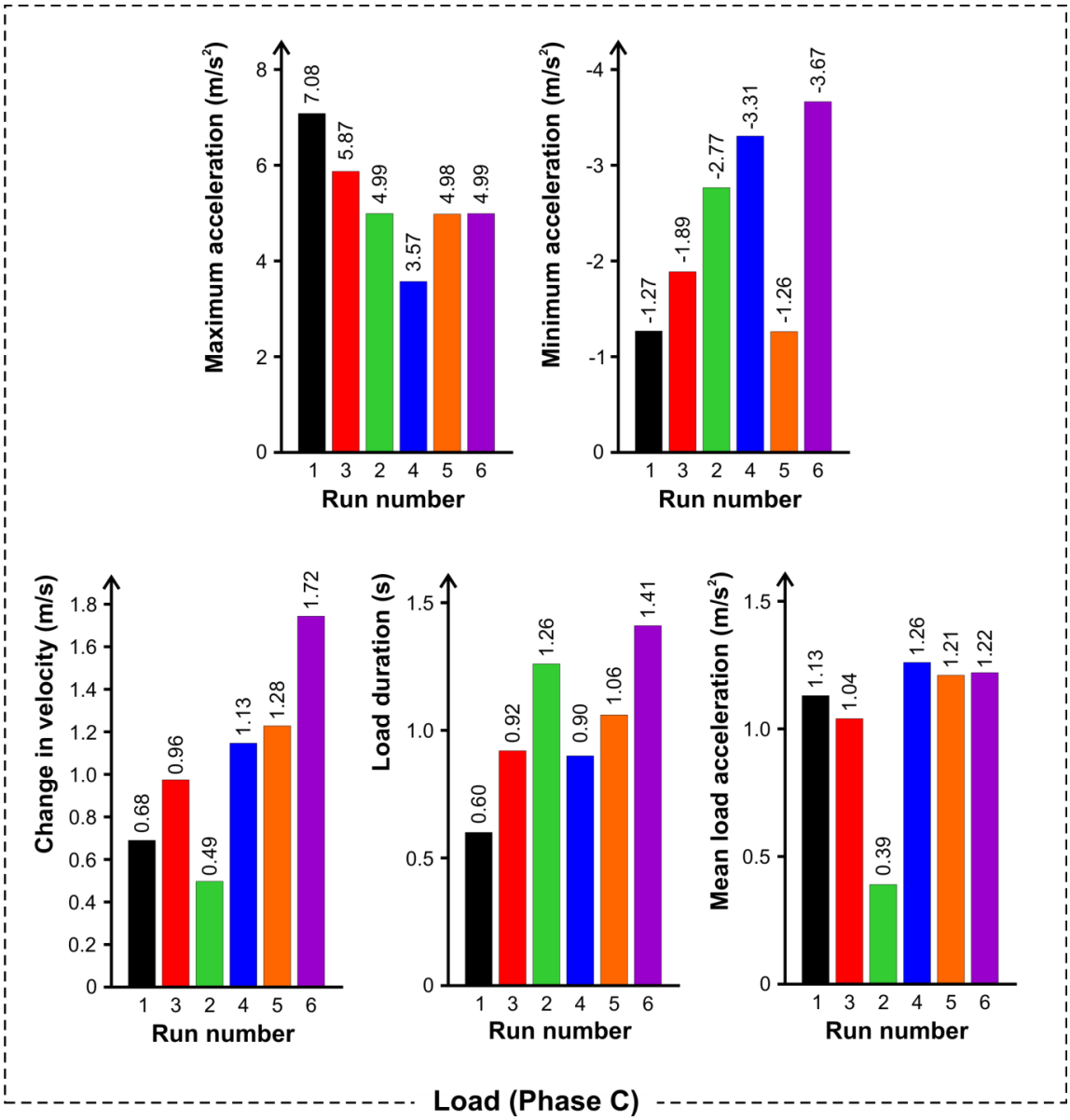


**Figure 3.6 - Indicators of athlete performance during the loading phase of a push start. Maximum acceleration for the transfer of forwards momentum and minimum acceleration from increased runner friction as the athlete lands. Change in velocity during loading, the load duration, and the resulting mean acceleration are also shown.**

## 3.5 Comparison of Athletes and Tracks

The data obtained from Run 1 has already been introduced in Fig 3.3. Similar data was obtained for each of the other five runs. These data are shown in Figs. 3.7, 3.8 & 3.9, in which the athlete's performance is presented in terms of acceleration plotted against both time and position, and velocity plotted against position. Position has not been plotted against time in these figures, but there was good agreement with the timing eye data (as in Fig 3.3). The data from each of the runs is discussed in more detail below.

### 3.5.1 Run 1: Athlete 1 at Track T

Athlete 1 was the fastest starter in this study, with both the shortest time to the last timing eye and the greatest velocity through the last timing eye for track T (Fig 3.4). Athlete 1 started with two feet on the starting block and rolled the sled forwards slightly before very strong acceleration off the starting block (Phase A, Fig 3.3). The initial acceleration was applied smoothly over two strides, giving a continuous acceleration trace up to a peak of 5.2 $m/s^2$ (Fig 3.5). During phase B, athlete 1's acceleration decays (at 0.36 $m/s^3$), but the sled is still being accelerated until the athlete decides to load at 3.9 s, when their velocity is 8.49 m/s (Fig 3.5). The deceleration at 3 s (Fig 3.3) is probably due to a poor footfall and momentary lack of balance that indicates that the athlete was approaching their maximum speed. Athlete 1's load (phase C) was well executed, with a high peak loading acceleration of 7.08 $m/s^2$ and minimal deceleration (1.27 $m/s^2$) that together indicate a good landing on the sled and a smooth transfer of forward momentum. These were accompanied by a velocity increase of 0.68 m/s (Figs 3.3 & 3.6).

### 3.5.2 Runs 2 and 4: Athletes 2 and 3 at Track T

Fig 3.7 compares Run 2 by athlete 2 and Run 4 by athlete 3. Athlete 3 was the weakest of the starters tested at track T, and consequently Run 4 took the longest time (8.60 s) to

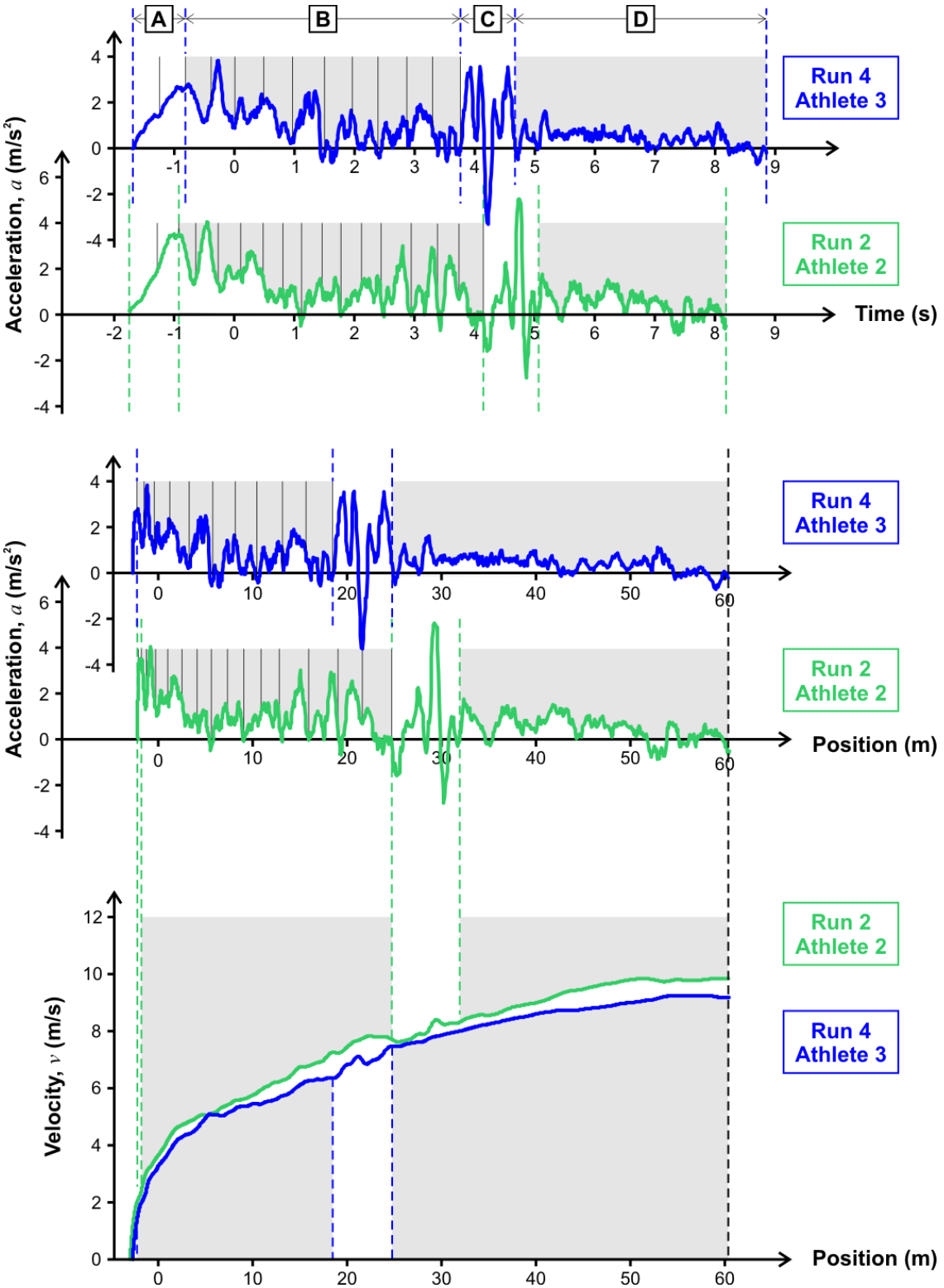


**Figure 3.7 – A comparison of two different athletes at track T, in terms of acceleration, velocity and push start phases.**

reach the last timing eye. Run 2 was 0.42 s quicker, as shown in both Fig 3.4 and the velocity trace in Fig 3.7. Neither run is as fast as Run 1 (by athlete 1).

During the initial drive (Phase A), Run 2 involved greater acceleration from the starting block, with a peak acceleration of 3.52 $m/s^2$ after two footfalls compared to 2.75 $m/s^2$ in Run 4 (Fig 3.5). This was lower than the 5.20 $m/s^2$ peak acceleration generated during Run 1; furthermore, there are secondary, higher, peaks after the third footfall during both Runs 2 and 4, indicating that they did not make good use of the purchase provided by the starting block during their initial drive.

Athlete 3 was unable to sustain acceleration during phase B of Run 4, and their acceleration decays more quickly (0.53 $m/s^3$) than Run 2 (0.37 $m/s^3$, Fig 3.5). Run 4 only had 12 steps before loading, whereas Runs 1 and 2 had 16 and 17 steps respectively. Run 4 also suffered from momentary deceleration due to a poor footfall at 1.5 s, and a load at a lower velocity compared to Runs 1 or 2 (Fig 3.5).

Both of the runs shown in Fig 3.7 have more complex loading phase (C) traces than Run 1 (Fig 3.3). Run 2's load involved higher peak acceleration (4.99 $m/s^2$) and a smaller deceleration (2.77 $m/s^2$) than Run 4, for which the load was dominated by a large deceleration spike of 3.31 $m/s^2$ due to a heavy landing on the sled (Fig 3.6).

Despite the apparently poor peak acceleration and deceleration, Run 4 had the highest increase in velocity during the loading phase of any run on track T (Fig 3.6), because there were three acceleration peaks during the load phase (Fig 3.7), and not just a single peak. Run 4 was also the strongest load performance based upon the mean acceleration during loading, although the differences between Runs 1, 2 and 4 are less pronounced based on this measure, due to the wide variation in the duration of loading (Fig 3.6). The

use of these performance indicators during the load phase are discussed in more detail below.

### *3.5.3 Runs 2 and 3: Two Runs by Athlete 2, Track T*

Fig 3.8 compares two consecutive runs by the same athlete on the same track. Run 3 was completed 0.59 s quicker than Run 2 (Fig 3.4), which is a notable improvement in performance given that typical push start variations under race conditions are in the region of 0.1 s. The improvement in performance on Run 3 occurred during the drive and load phases of the push start shown in Fig 3.8.

During the initial drive (phase A), the initial acceleration and velocity through the 2$^{nd}$ timing eye were higher for Run 3 than Run 2 (Fig 3.5). The peak acceleration for Run 2 did not occur during the first two footfalls that define phase A, but instead occurred after the third footfall, indicating poor use of the starting block. The acceleration phase (B) was similar for the two runs, with similar acceleration decay rates (Fig 3.5). The maximum sprint velocity just prior to loading was also similar for the two runs (7.79 and 7.95 m/s$^2$); however, loading took place later for Run 2 due to the poor initial acceleration, after two additional footfalls.

During the load phase (C), both runs show a peak in acceleration due to the transfer of forward momentum, followed by deceleration during landing (Fig 3.8). The Run 3 load was better executed, with a higher maximum acceleration and lower deceleration, resulting in a greater increase in velocity and mean acceleration during the loading phase.

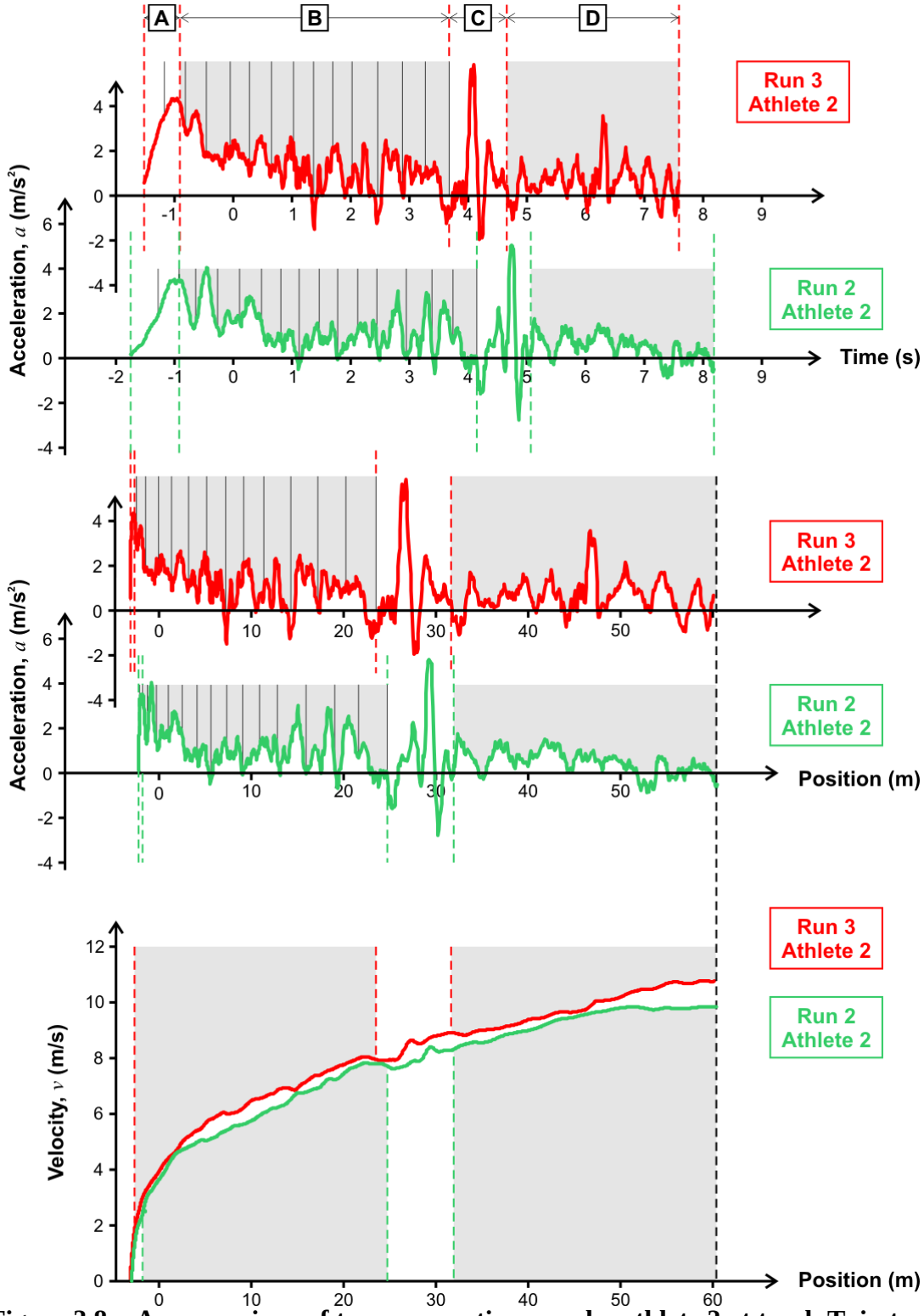


**Figure 3.8 – A comparison of two consecutive runs by athlete 2 at track T, in terms of acceleration, velocity and push start phases.**

### 3.5.4 Runs 5 and 6: Athletes 2 and 4 at Track C

The last two runs took place on track C, and compare the performance of athlete 2 with a recreational athlete, athlete 4 (Fig 3.9). Athlete 4 used a two-handed push start, which (as discussed above) is more traditional and stable than a single-handed push start. Athlete 2 (and all of the runs at track T) used the more efficient single-handed push start technique, although this was one of the first times that athlete 2 had practised a single-handed start on ice.

Athlete 4 (Run 6) made an exceptionally strong drive off the start block (phase A), with the largest peak acceleration (7.38 $m/s^2$) recorded during any of the runs (Fig 3.5) due to the greater stability afforded by a two-handed push start. However, this peak initial acceleration is not sustained, and it is athlete 2 (Run 5) who is fastest through the $2^{nd}$ timing eye. Athlete 4 was not nearly as effective as athlete 2 during the subsequent acceleration phase (B). Their acceleration decay rate was low (Fig 3.5), but this is because their mean acceleration was low throughout phase B (Fig 3.9). Each of athlete 4's footfalls was accompanied by a momentary deceleration of the sled, indicating that athlete 4 was running beside the accelerating sled without providing additional forwards drive.

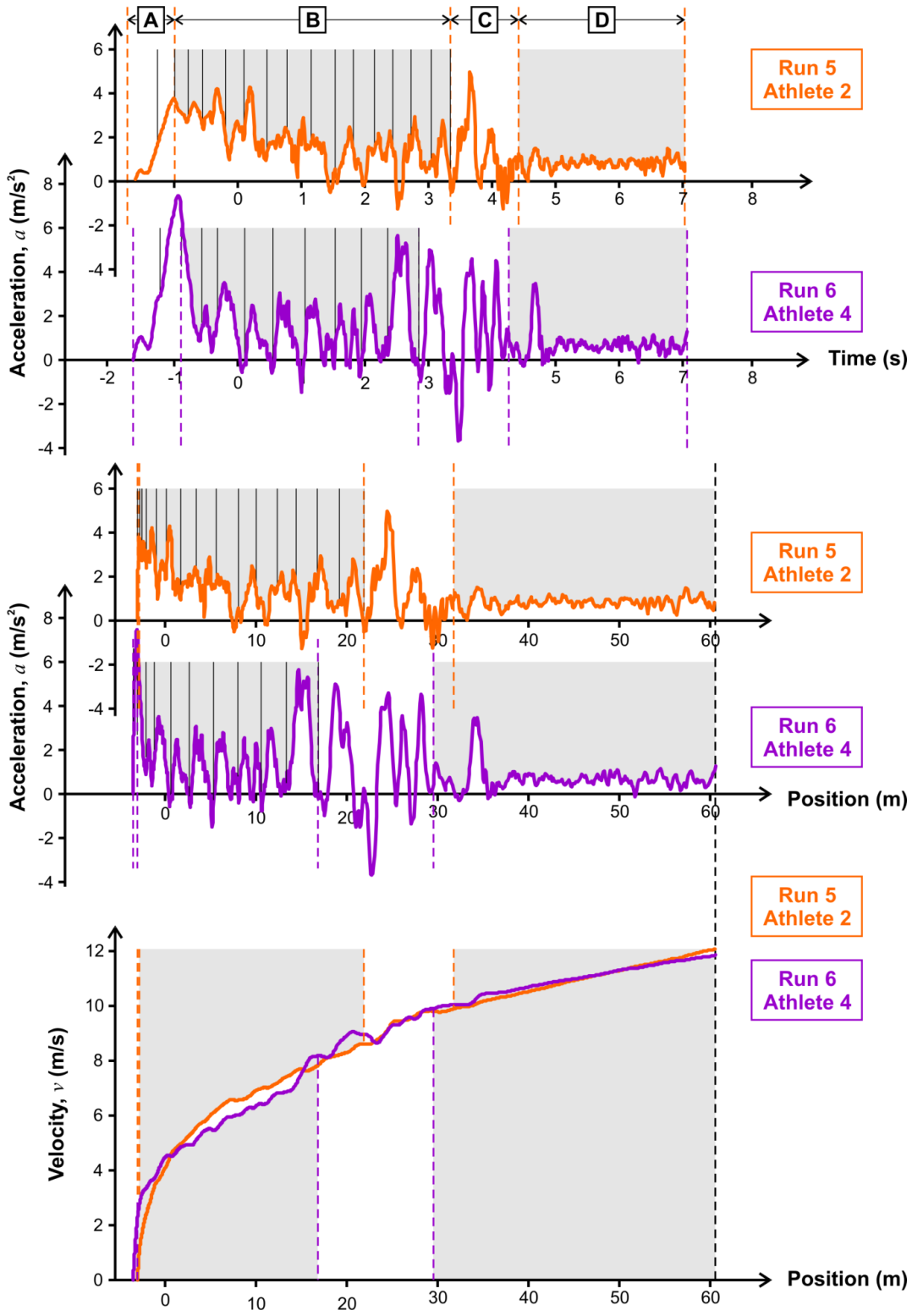


**Figure 3.9 – A comparison of the push starts of an experienced athlete 2 and an inexperienced athlete 4 at track C, in terms of acceleration and velocity data.**

### 3.6 The Use of Push Track Data to Improve Athlete Performance

Examination of the data in the preceding section identified significant variability in the accelerations and velocities achieved by different athletes, by the same athlete on different runs, and between the two different tracks. How can a skeleton athlete use this data to improve their push start performance?

A detailed examination of the recorded data (similar to that in the previous section) can be conducted to identify the phases of the push start upon which an athlete should focus their training. Fig 3.10 presents the velocity vs. position performance of all six runs on a single plot, and by way of example, this shows that the velocities of athletes 1 and 2 (Run 2) are similar during the first half of the push start, but athlete 2 has a comparatively poor load and loses speed as a result.

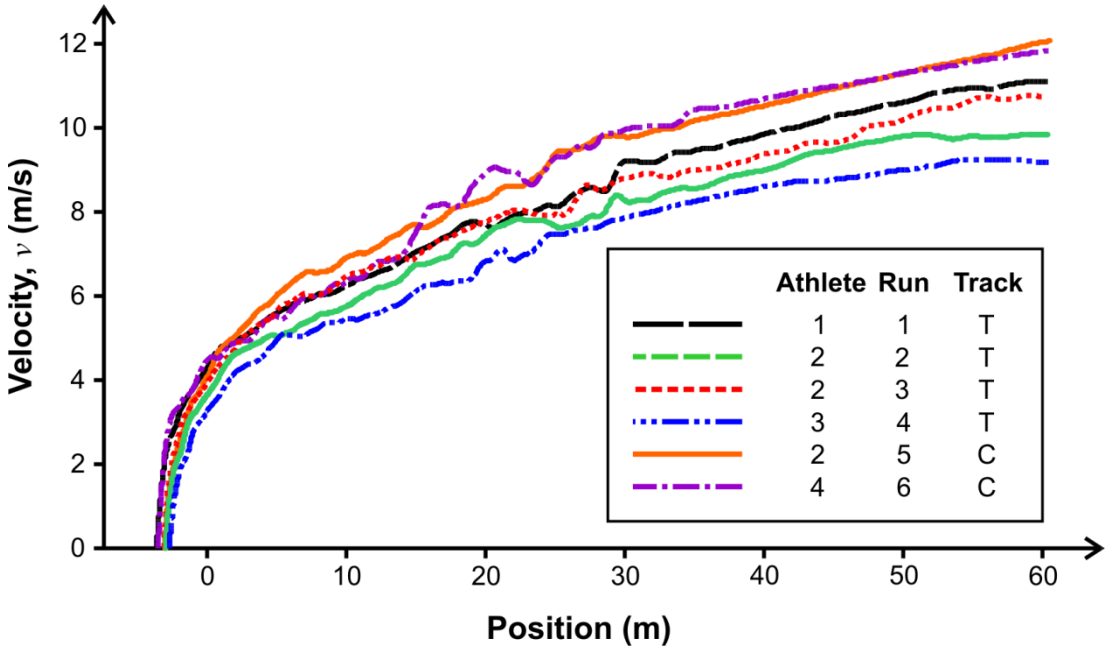


**Figure 3.10 – A comparison of all six push starts in terms of the athlete velocity with position.**

These detailed comparisons are a useful training aid; however, an instrumented sled is not usually available. Instrumentation cannot be fitted under race conditions, and an athlete will not want to modify their favoured race sled to allow an accelerometer unit to be fitted. It is therefore useful to examine the recorded data to see how other indicators of performance can be used in training.

Despite Run 3 being noticeably quicker than Run 2, it is possible to use the recorded data to spot opportunities for further improvement. In particular, there are two heavy footfalls during which the sled decelerates. The first (at 8 m) corresponding to a wide step as the velocity increases, something athlete 2 in particular was trying to improve. The second (at 14 m) occurs at the crest of the track and suggest a loss of balance due to the change in the track gradient. Furthermore, athlete 2's last footfall prior to loading involves a longer contact than athlete 1; however, it is not clear whether this last footfall is an opportunity to improve athlete 2's push start performance, or whether it is due to a difference in loading style.

### *3.6.1 Indicators of Performance During the Drive and Acceleration Phases*

Fig 3.5 shows possible indicators of push start performance in the drive and acceleration phases. The runs are in the same order as Fig 3.4, so good indicators of performance will show a similar trend to Fig 3.4.

A strong initial acceleration off the starting block is an important part of a push start, correlating well with overall performance (Fig 3.5). It must be followed, however, by sustained acceleration; it has already been noted that the recreational athlete 4 had the highest drive acceleration, but was subsequently unable to accelerate the sled further before loading. The velocity through the 2$^{nd}$ timing eye is commonly used as an indication of the quality of the drive out of the starting block (in the absence of

accelerometer data); however, it can be seen from Fig 3.5 that this does not correlate so well with overall performance. Athlete 1's velocity through the 2nd timing eye is slower than athlete 2 (Run 3), despite having a stronger initial drive and better overall performance.

It was previously noted that the mass, power and stride frequency of an athlete are used to assess the ability of an athlete (Table 3.1). It is interesting to compare the mean footfall frequency recorded during the tests with the footfall frequency assessed during 30m track sprints. The athlete's footfall frequency on a flat track (Table 3.1) correlates well with overall performance, but the footfall frequencies recorded during the tests were very different. This is because a track sprint is conducted with the body upright, whereas the body is bent over during a push start, suggesting that the track sprint frequency is not a reliable indicator of performance during a push start.

The acceleration phase ends when the athlete can run no faster, and it can be seen from Fig 3.6 that the best athletes are able to run faster before loading. The time (and position) that loading occurs at, however, varies from run to run as the higher velocity generally results in further distances covered.

### *3.6.2 Indicators of Performance During the Loading Phase*

Loading onto the sled is a particularly critical stage of the push start. The velocity fluctuations that occur during loading are clearly visible in Fig 3.10. It has already been noted that the load performance is particularly important in differentiating the performance of athletes 1 and 2; it can also be seen that the changes in velocity during loading play an important part in the athletes' runs.

Maximising the change in velocity during loading is thus the key outcome of a successful load, but this is difficult to measure, principally because of the difficulty of

establishing the duration of the load phase. In the current analysis, the start of the load was taken as the last footfall from the video footage; the end of the load was taken once the athlete was flat on the sled. Whilst Fig 3.10 shows significant variations in velocity during loading, the changes in velocity calculated during the loading phase (Fig 3.6) do not correlate with athlete performance. Each athlete has a different loading style that takes a different amount of time, and there is also a period of settling-in after landing on the sled. Consequently, it is not possible to consistently assess the change in velocity during loading.

The maximum acceleration (due to transfer of forward momentum) and the minimum acceleration (resulting from landing) do directly affect overall push start performance, but these would not normally be available during training. Timing eye data does not give information on load performance (the eyes are too widely spaced, and each athlete loads at a different position and speed), and hence the only data available during this critical phase is qualitative from video footage observations of loading style. Accelerometer data would hence be of benefit to skeleton athletes, allowing them to study and improve their loading performance.

## *3.7 CONCLUSIONS*

The push start is critical to a successful skeleton bobsleigh descent. Whilst it does not dictate medal positions, medals cannot be won without a good push start. The key objectives of the push start are to minimise the starting time and maximise the starting velocity, as assessed at a fixed timing eye. This chapter has examined the push start in detail by instrumenting a skeleton sled with an accelerometer, combined with more traditional data in the form of timing eye results and video analysis (which provided footfall times). The resulting forward acceleration and velocity data allows a detailed assessment of an athlete's push start performance, allowing them to pinpoint the particular phase of the push start on which they need to focus their training.

The six recorded runs demonstrated the importance of all phases of the push start (the initial drive, additional acceleration, and a smooth loading). They showed the benefit of traditional indicators of push start performance (such as using the velocity through the second timing eye as an indicator of a successful initial drive); however, it also suggested that other indicators (such as using footfall frequency during a flat track sprint) are less relevant to the push start unless taking consideration of athlete build. Furthermore, the traditional performance indicators do not provide sufficiently detailed data to quantify the success of the loading phase. The accelerometer data and subsequent analysis reported in this study provides this detailed data, and is thus of benefit in skeleton bobsleigh push start training.

# 4 TRAJECTORY ANALYSIS OF THE KOENIGSSEE INTERNATIONAL RACE TRACK

The following chapter investigates the trajectory of a skeleton bobsleigh down the Koenigssee bobsleigh track in Germany. Koenigssee is regularly featured at the highest level on the World Cup racing circuit. It has unique characteristics that make it difficult to both accumulate speed and also maintain it through technical regions of the track.

Having established that the use of a single axis accelerometer within the sled can provide information of benefit to the athlete (Chapter 3) it follows that gains could be made upon analysing a full descent in this way. The push start study highlights the need for accurate track geometry and frequent timing eye positioning in order to fully calibrate the sled's motion, of which there is far less information available over the length of the full track and the dynamics are more complex because of the geometry of the track. A tri-axial accelerometer was installed inside a skeleton sled and multiple runs taken down the international race track in Koenigssee. Examination of data from the upper region of the track shows key features that aid in accumulating velocity whilst detailed analysis of the mid-section, in particular the "Kreisle" curve, provides evidence for specific characteristics between a successful descent and a poorly executed descent.

As outlined previously, a good push start is crucial to provide the opportunity to win a race but will not be the only determining factor in the final position. After the actual pushing phase, typically complete after 25 m, there still remains around 1200 - 1600 m of track where athlete driving error will rapidly deplete any gains made during the push start. If the athlete were to allow the sled to follow the natural line of the track, with the overall trajectory governed by the rotational dynamics that the geometry of the curve dictates, there would inevitably be impacts with the side walls as the tracks are not

designed to allow movement to flow forgivingly, and they are becoming increasingly more technical. Every steer / movement the athlete makes to correct the sleds orientation does so by damaging the ice surface and so excessive movements can result in a loss of velocity. Ideally the athlete must therefore steer only when the angular correction to the sled can maintain the velocity or, depending on the track geometry, increase it.

This study isolates key sections of the Koenigssee track and uses accelerometers, timing eye data, video footage (captured from the trackside) and track geometry to identify characteristics of curve trajectory. The data analysis and correlation to velocity / time data can assist an athlete in optimising their driving ability and improve their performance. I link qualitative data taken from personal notes to the quantitative data captured by the instrumentation.

### *4.1 The Koenigssee Race Track*

An overhead track map of the track at Koenigssee is shown in (Fig 4.1). Timing eyes are located at intervals along the track as are two speed traps providing split times and velocity data which are made available to the athletes. The distance from the starting block to the crest is one of the shortest of all tracks and also decreases in gradient shortly after the athlete has *loaded* onto the sled. This results in start times which are tightly packed and a smaller margin between the fastest and slowest starter in the field. Consequently it is of great importance to drive the optimum trajectory and, if an error is made, correct as efficiently as possible. To add motivation to improving the success of the descent it is also the shortest track to regularly feature on the World Cup circuit at only 1185 m in length (2010 – for skeleton) increasing the need to maximise driving efficiency and minimise error.

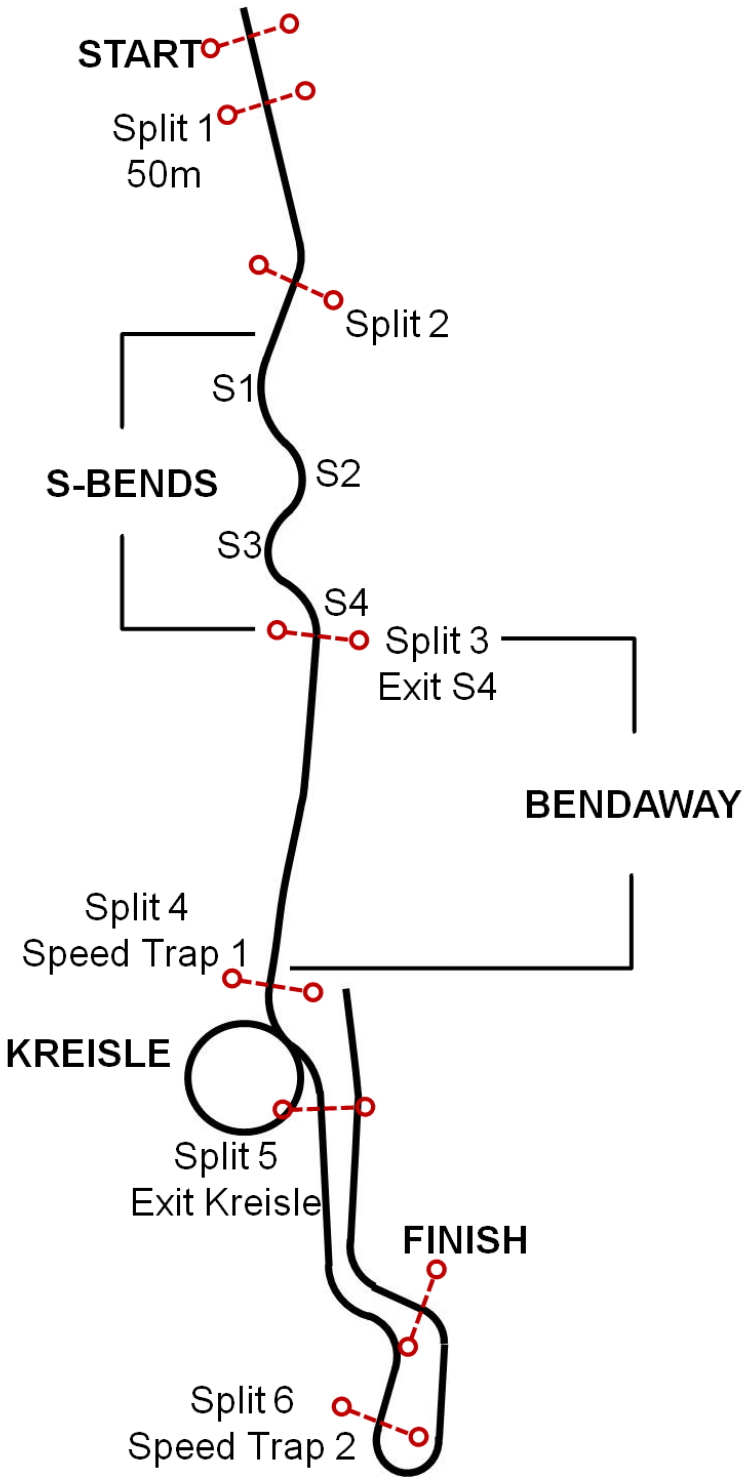


**Figure 4.1 - Overhead track map of the Koegnissee international race track indicating S Bends, Bendaway and Kreisle; timing eye and speed trap locations are also shown.**

### *4.2 Experimental Set Up: The Skeleton Sled Instrumentation Used*

The sled used for this study was Sled A with a *standard* set of runners in contact with the ice. I was the test athlete and the data obtained and analysed was recorded during open training in 2008 with four descents in total analysed here. Additional results from the 2010 World Cup in my qualification for the Olympic Games are commented upon.

A tri-axial accelerometer, Crossbow CXL10LP3, was attached to the sled mounted rigidly to the saddle so that the device recorded the sled acceleration. The accelerometer was orientated to measure the accelerations in the three orthogonal axis relative to the sled shown in (Fig 4.2a).

Data was logged at 100 Hz per channel, so that frequencies up to 40 Hz could be recorded accurately, according to Nyquist Theory, Horowitz P and Hill W (1989)**.** The data logger, Race Technology DL1, and accelerometer were equipped with stand-alone power sources that allowed them to be fitted inside the sled without any interference to either the athlete or the aerodynamics of the sled.

### *4.3 Results*

#### *4.3.1 Identifying Characteristic Accelerometer Signatures: S-Bends, Bendaway and Kreisle*

This study is split into three sections of interest. Raw accelerometer output from all 3-axis during a run at Koenigssee (Fig 4.2b) was used to identify these sections.

With the accelerometer rigidly attached to the saddle the data is in the reference frame of the sled. As the sled travels through the banked curves the contribution to measured acceleration due to gravity will shift from one axis to another.

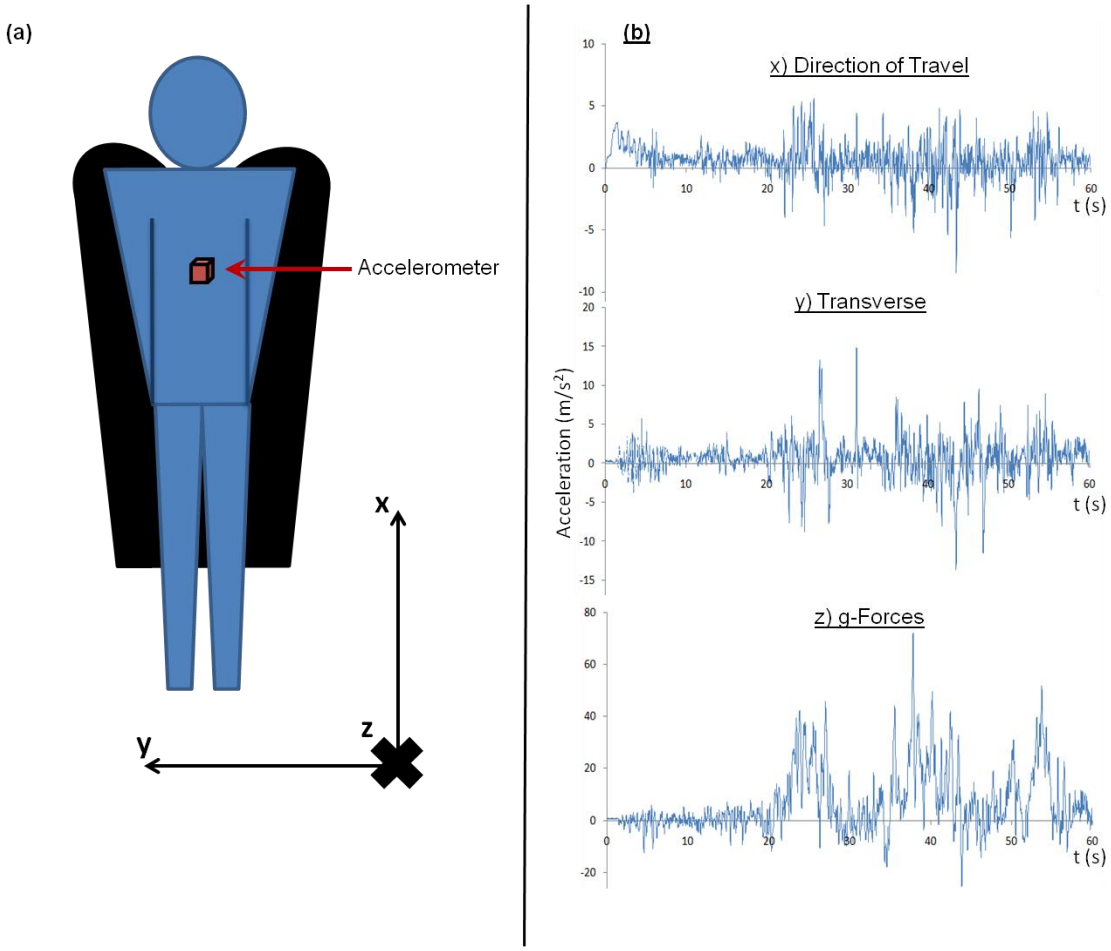


**Figure 4.2a - The accelerometer was installed inside the sled located under the athlete's chest and firmly attached to the saddle such that it recorded in the reference frame of the sled. The orientation was such that x is positive in the forwards direction, y is positive to the left and z is positive downwards into the track.**

**Figure 4.2b - Accelerometer output for the x, y, z axes for a whole run down the Koenigssee track. Calibration factors have been applied to convert the accelerometer output from voltage into acceleration. In curves the sled rotates so the z axis of the accelerometer is no longer vertically downwards, which causes distinct changes in the z axis acceleration data as the gravitational contribution shifts to the y axis. This aids identification of the specific curve locations that are used for further analysis.**

At this stage the motivation is to identify key sections of the track where information may be gained in order to benefit the athlete. Linking the time stamping of curve locations to the accelerometer output is best identified by not applying a correction for acceleration due to gravity as it highlights rapid shifts in sled orientation; so although the y-axis is labelled $m/s^2$ this is purely to indicate a guide to the magnitude of accelerations and will differ by up to 9.81 $m/s^2$ depending on the specific location on the track.

Comparison of the direction of travel output in Fig 4.2b to the push start study, (Chapter 3), shows the characteristic peaks expected due to the footfall from a push start in the first 5 s. After this initial push phase the remainder of the output in direction of travel is dominated by noise of the sled vibrations and peaks / troughs are predominantly due to the sled angling up / down as it enters and exits curves. This is as expected as the greatest acceleration in the forwards direction is from the initial explosion of power from stationary off the starting block. It would be a futile exercise to attempt to gain information on athlete performance from the remainder of the output in the forwards direction as without precise track geometry or sled location on a comparable sampling rate, the accumulation of errors exceeds the potential gain of information to the athlete. Even with accurate track geometry the ice profile differs from the underlying structure and often is significantly thicker in the latter part of the season. It follows that double integrating for sled velocity and position is not indicative of the actual outcome in this direction. Of course the forwards velocity is important in terms of race performance however the accelerometer output in this direction has little to offer in feedback to the athlete.

Of greater significance is the output from the z-axis. Perpendicular to the sled this shows the magnitude of g-forces experienced within the corners during a run. Again the raw output is noisy, (Fig 4.2b) indicative of the harshness of the interaction between the sled and the ice surface. The magnitude of acceleration is useful for confirming velocity data using rotational dynamics.

The y-axis, transverse (left / right), output is the most beneficial to the athlete as it is strongly correlated to the sled entering and exiting curves. The variations of these accelerations are immediately apparent due to a near zero output while the sled is travelling in the forwards direction as there is no transverse acceleration, whereas upon entering / exiting curves the sled not only travels in this direction but also has the primary gravitational shift in this direction as the sled's reference frame rotates.

Upon comparison with video footage, captured at the side of the track by my track coach - Jill Roberts née Anderson, and split time data the bend locations can be seen in the transverse output, from which three sections are of particular interest due to the significant shift in magnitude of accelerometer output and the potential to alter the sleds trajectory at these locations, (Fig 4.3):

*a)* *S-Bends*
*b)* *Bendaway*
*c)* *Kreisle*

Unfiltered and filtered raw data is shown in Fig 4.3. The post processing is described in detail in section 4.3.2. For the remainder of this chapter all results will show the filtered output.

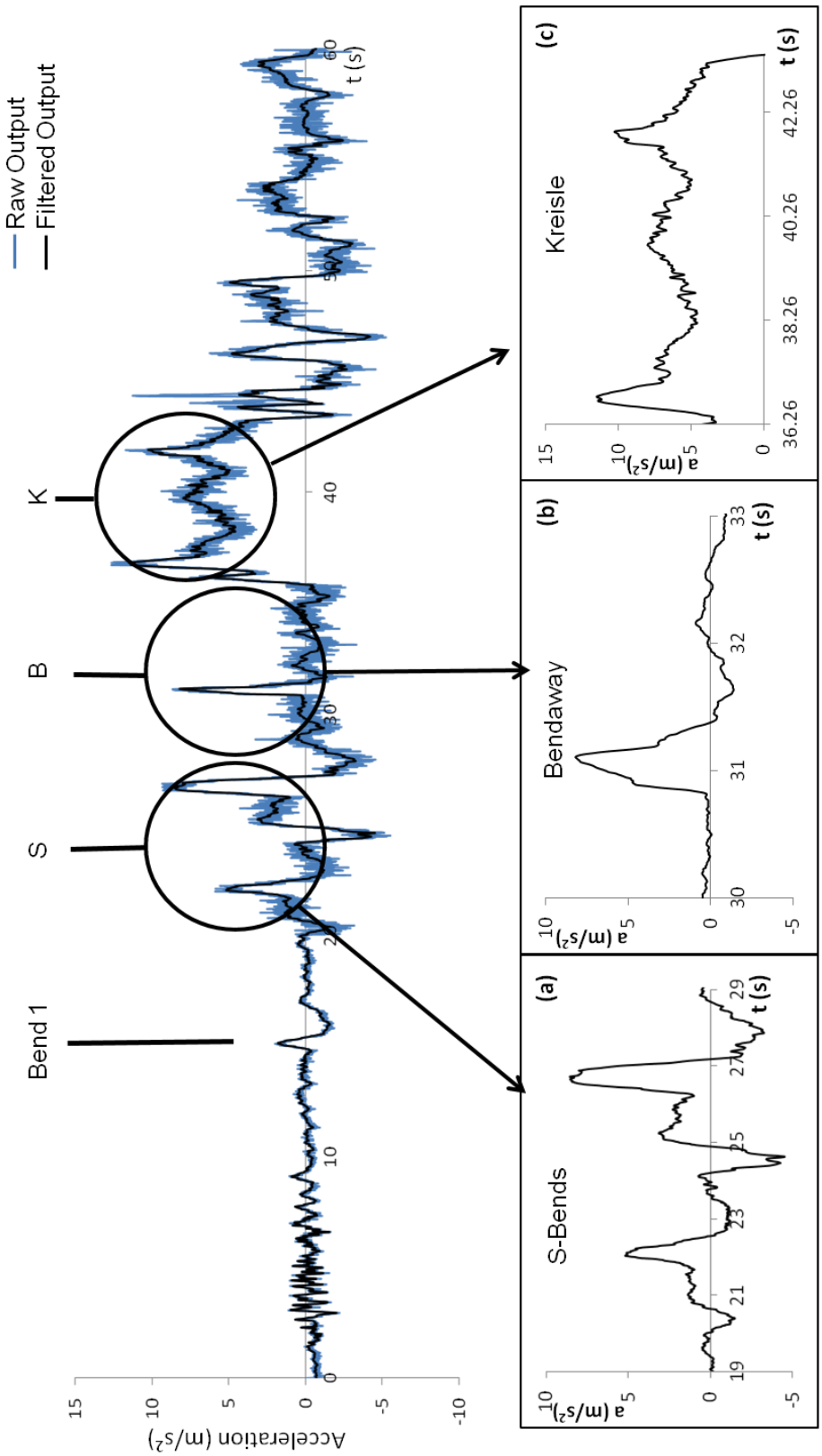


**Figure 4.3 - Raw accelerometer output from the transverse, y axis. The curve locations are identified by applying a low pass filter and comparing to split time data and video footage. Using the filtered output three regions of interest are highlighted, a) S Bends, b) Bendaway and c) Kreisle.**

*(i) S-Bends:* located in the upper region of the track the S-Bends are a combination of 4 curves, aptly named due to the alternating direction of the curves and shortness of transitions between them creating S-shapes as can be seen in the overhead track map (Fig 4.1). The walls are banked such that the athlete will rotate a full 90 degrees regardless of entry angle. With such a short transition, (Fig 4.4), they can flow very easily from one to the other; often an athlete will compare split times recorded through the S-bends with runs that they felt they had steered with a similar approach and find significant differences in time taken with no clear indication as to the cause of the discrepancy. Elite athletes alter the high point of the sled's trajectory. That is, if the athlete were to let the sled run freely through the corner then the highest point would be at the apex or even towards the latter part of the curve (athlete observation – due to the geometry of the curves). By setting a particular entry angle and using an appropriate entry steer the athlete can achieve the high point of the trajectory earlier, not necessarily higher than the apex, resulting in a longer, straighter exit and a smoother transition into the following curve with less damage to the ice, (Fig 4.4b). During the transitions there is a sharp shift in the accelerometer output as the orientation of the sled rotates close to 180° and so the gravitational contribution switches direction, (Fig 4.4c). By examining the transverse accelerometer output without compensating for the shifting contribution due to gravity a ratio of sled fall time to sled rise time can be calculated and the athlete can determine where the high point was with respect to the curve apex, (Fig 4.4d). This can be extremely beneficial for athletes that do not have coaches present to give feedback (either because they have no coach at all or that their coach is at a different location on the track).

**Figure 4.4 - Transition between curves S2 and S3 in the S-Bends. Note the sharpness of the transition from S2 exit fillet to S3 entry fillet.**

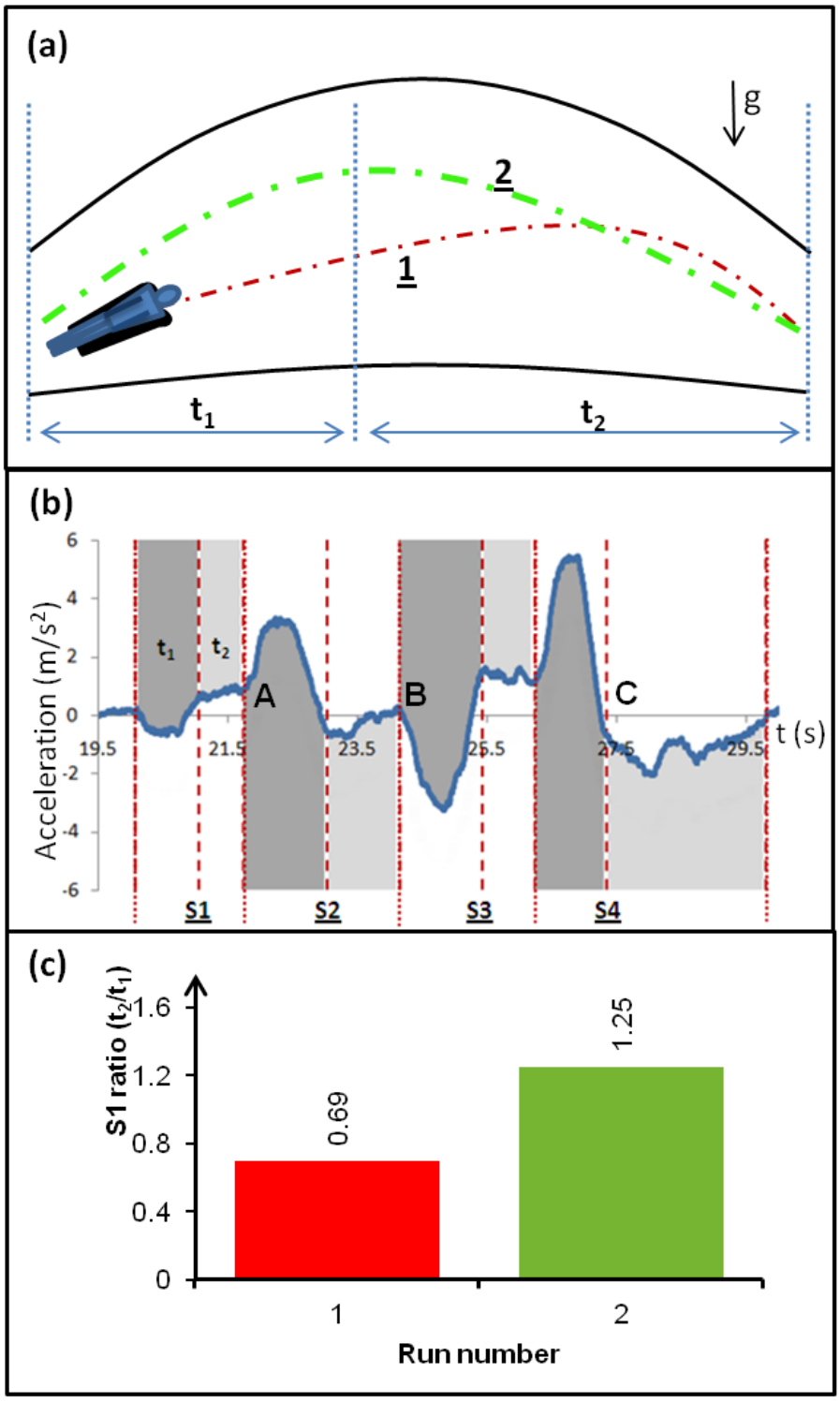


**Figure 4.5a – Vertical side view of S1 cross section (mirrored for time trace). Trajectory 1 has the high point later on in the curve, typical of an uncontrolled**

**entry. Trajectory 2 is that of a controlled entry to create the high point earlier in the curve thereby generating a longer, smoother exit line. The rise time being $t_1$ and the fall time $t_2$.**

**Figure 4.5b - Filtered accelerometer output from the transverse, y axis. The transition between S-Bends results in a sharp change in the sled's orientation which can be seen at points [A, B, C] as the gravitational contribution inverts. Within each curve trace a characteristic rise / fall can be observed from which times $t_1$ and $t_2$ can be calculated.**

**Figure 4.5c - The ratio of $t_2/t_1$ for Runs 1 and 2 through curve S1 plotted as a bar chart, the magnitude of which correlates to the location of the high point within the curve. Schematically trajectory 1 in Fig 4.5a corresponds to Run 1 and trajectory 2 corresponds to Run 2**

*(ii) Bendaway / Kink* is one of the first sections of the Koenigssee track that any athlete must master, from the novice on their first descent to the elite athlete racing on the World Cup circuit. As discussed in Chapter 2, a skeleton sled responds best on the entries and exits of corners. Koenigssee has an unusual portion of track from exit S4 all the way to the K-1 (a short curve before Kreisle) section that is almost straight, (Fig 4.6). It has no banked curves and therefore no centrifugal force and so the runners on the sled have very little *bite* on the ice surface. It bends to the right, then to the left and back to the right again. It is impossible to set an exit angle from S4 and be able to travel directly to the entry of K-1. Although it is possible to force the sled through the kinks using light toe touches on the ice and weight transference this is seen by most elite athletes as an inefficient method of control with high risk of forcing the sled into a skid where it slides laterally along the ice surface losing significant speed. Instead the path that requires least input by the athlete and allows the sled to accumulate velocity is to exit S4 aiming to allow the sled to glance off the wall at a particular point. There is a rounded profile to the ice where the floor meets the vertical wall which does soften the impact and rotates the sled slightly to the right. A glancing impact at a

specific point with the required force will rotate the sled sufficiently that the athlete can then travel all the way through the following two kinks to entry K-1 without touching the wall again. Athletes call it "*threading the needle*", (Fig 4.7). The point of this impact can be seen in the transverse accelerometer trace, along with any subsequent impacts and the magnitude of these correlate to the severity of the impact with the wall, (Fig 4.7).

**Figure 4.6 - View from the exit of S4, looking down the Bendaway track and Kreisle.**

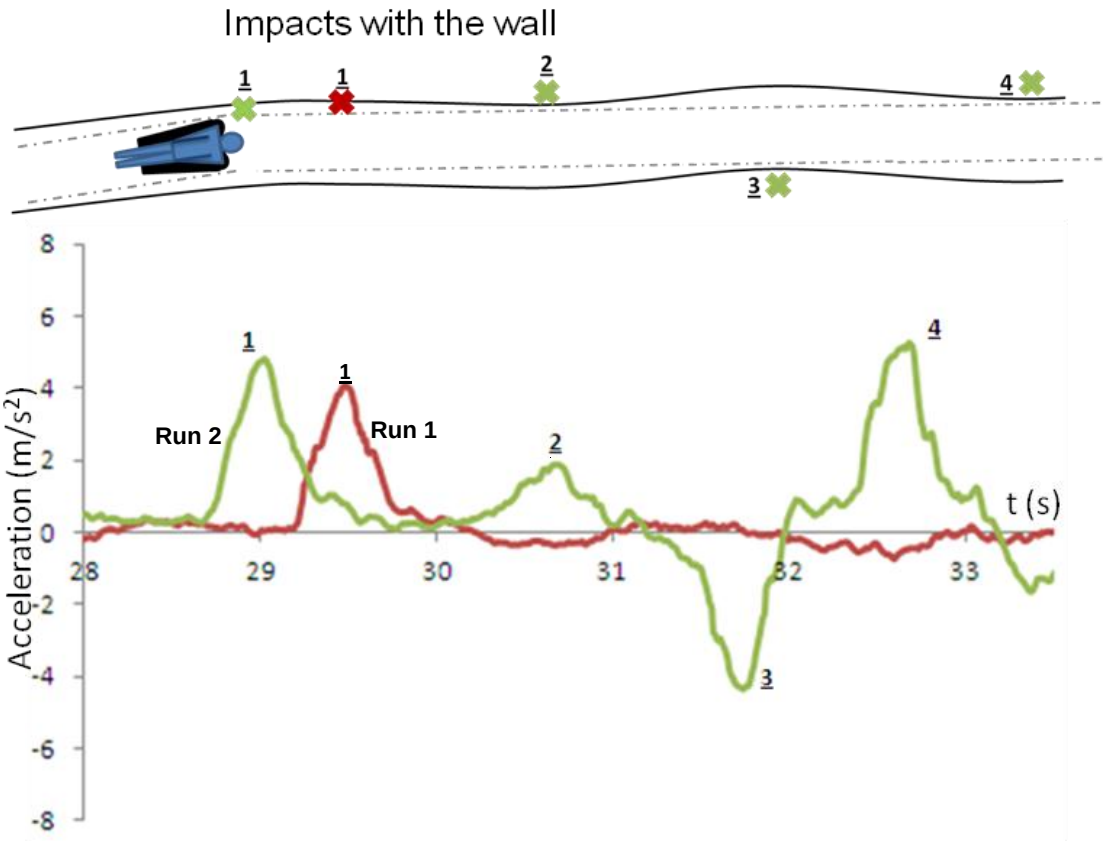


**Figure 4.7 – Top: diagram to show the process of "threading the needle" if an alteration to the sled's trajectory is achieved at a single touch at point [1]. Failure to touch at the right point can result in additional impacts, the most common result being at points [2, 3, 4]. Below: comparison of filtered output from the accelerometer y axis for two runs that show Run 1 successfully threading the needle, Run 2 failing to do so and the subsequent impacts observed.**

*(iii)Kreisle:* is one of the most technical curves in the entire racing circuit. It is corkscrew shaped turning a full 360°. The entry has a slight rise in height as the radius of curvature begins to increase while the majority of the curve has no vertical gradient until a steep drop where the track bends underneath itself at the exit, like a corkscrew. There is a speed trap prior to Kreisle and a second four curves afterwards, all of which are single oscillation with small vertical drop and relatively low difficulty for the athlete to maintain velocity should a good exit from Kreisle be achieved. The Kreisle is crucial to overall

performance as a poorly executed Kreisle can result in a loss of velocity – 3km/h (or more if the sled flips on the exit, Fig 4.8), whereas a controlled Kreisle performance will maintain the velocity and a well executed Kreisle will actually gain velocity – approx. 3km/h – in this section of the track.

**Figure 4.8 - Failure to control the oscillations in Kreisle can result in the sled flipping upside down on the exit.**

The sled's trajectory through Kreisle typically has 3 oscillations (Fig 4.9), although at slow speeds even this may not be enough to complete the curve which can result in the athlete hitting the right hand wall hard on the exit or even being scooped up by the fillet and flipped onto their backs. It is common for the entry and exit of the Kreisle to be covered with shades in order to prevent track deterioration from exposure to the sun. These shades

typically cover the first oscillation rise, the fall of the second oscillation and the entire third oscillation. This makes it difficult to visually analyse specifics of the athlete's trajectory at the crucial sections where the most alteration to the trajectory, and therefore gains, can be made. These oscillations can however be identified (Fig 4.9) and later analysed in the accelerometer output.

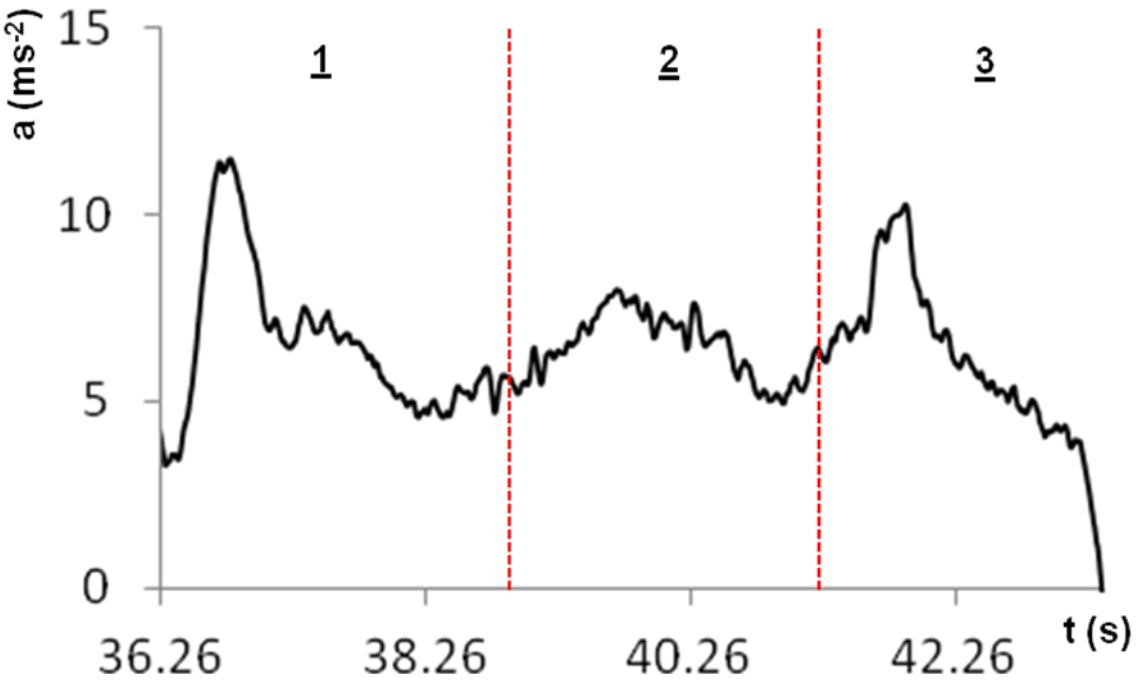


**Figure 4.9 – Filtered accelerometer output from the transverse axis during Kreisle. Oscillation [1, 2, 3] are indicated and were determined using oscillation duration from video capture. Further analysis can be applied, post processing is described in section 4.3.2.**

### *4.3.2 Post Processing of Accelerometer Data*

The push start study, (Chapter 2) shows that for specific sled location to be accurately determined using an accelerometer required both accurate track geometry and multiple timing eye data points (every 10 m) for calibration. When taking into account that the ice thickness on the track can vary considerably throughout the season, usually thicker in the later months, so much so that experienced athletes have alternate approaches for different surface preparations, means it would be a futile exercise to attempt to use track geometry alone to calibrate the accelerometer's orientation through the banked curves over a full descent. Using an additional gyroscopic sensor to measure rate of rotation may assist in plotting sled trajectory, however a suitable gyroscopic sensor would not have fitted inside the sled without causing the surface that the athlete lies on to be adjusted.

This study investigates the outcome of four runs, the processing steps applied to the data in order to determine the characteristics of each run are:

i) S-Bends:

- Calibration factors applied to the y-axis to convert voltage output into acceleration. Although no contribution due to gravity will be corrected as the sled's orientation shifts in the curves, this process centres the output on the zero line when no acceleration is experienced in this direction and enables identification of entry / exit points.
- A low pass filter is applied. The cut off frequency used was 10 Hz in order to reduce the noise on the output signal.
- S-Bend transitions are identified from the shift in gravitational contribution creating the sharper peaks in the output.
- The fall time and rise time is calculated within each curve and the corresponding ratio calculated.

ii) Bendaway:

- The first two steps are as for the S-Bends. Once the low pass filter is applied the impacts are clearly identified.
- From inspecting the timing and magnitude of wall impacts it can be determined whether it was too soon, too late or too hard an impact. Consideration must be given to the S Bend trajectory in order to gauge velocity through the Bendaway.

iii) Kreisle:

The difficulty in maintaining or gaining velocity through Kreisle provides extra motivation to understand the factors affecting a trajectory through this curve in more detail. It aids the analysis that further information is available in this region of the track. Entry velocity is provided from a speed trap on the track, this enables the longitudinal axis to be fully calibrated. Track geometry, inferred from visual inspection and photographs, enables the lateral axis to be fully calibrated, including axial shift of gravitational contribution. Video footage captured by Jill Anderson provides oscillation length and duration information. With this additional data the following post-processing methodology was applied:

- Again the first two steps stated in i) S-Bends were applied to centre and filter the y axis output.
- Using track geometry an approximation of entry / exit axial rotation was used to correct for the shifting gravitational contribution to the accelerometer.
- A centreline can be identified in the output, from which duration of oscillation can be measured and compared with video footage to confirm output is centred.

The data can now be used to analyse the oscillations and the overall affect of the Kreisle trajectory.

### *4.3.3 Quantifying Accelerometer Output From the Four Runs*

After a training session is complete the athlete receives a timesheet with split times and speed trap data. Typically the first information viewed is the push start time and total descent time. The values for which are shown in Fig 4.10. Once an initial measure of success has been identified a closer inspection of the split times is made to rate the performance at different sections of the track. From the accelerometer data, Fig 4.3a shows the S-Bend processed output and Fig 4.11 quantifies the fall to rise time ratios. Similarly, Fig 4.12 plots the data for the Bendaway and Fig 4.13 for the Kreisle data including velocity comparison before and after Kreisle.

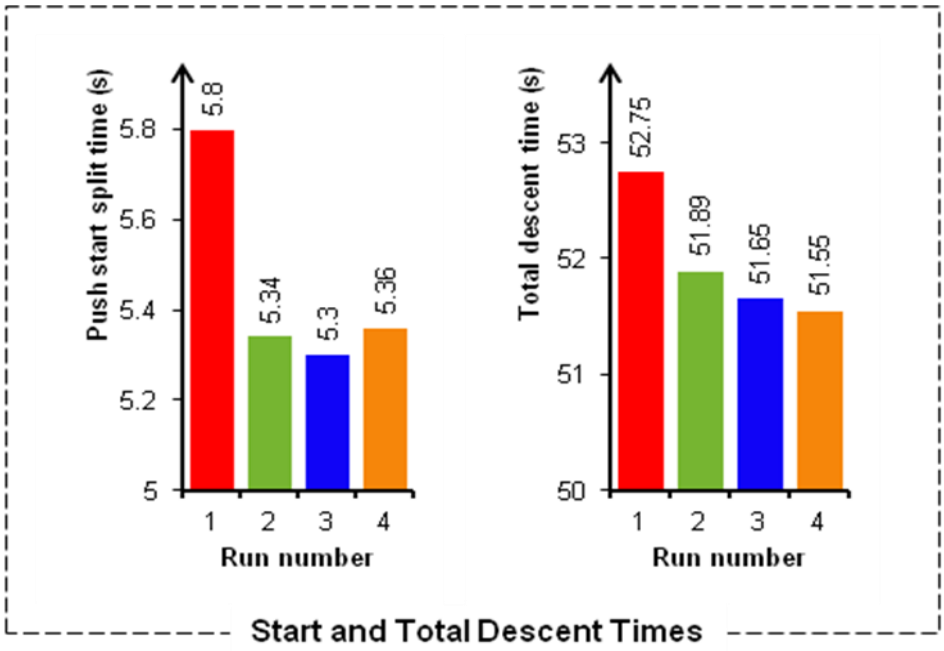


**Figure 4.10 – Indicators of performance over the push start and full descent. This highlights that the fastest push start does not achieve the fastest descent time.**

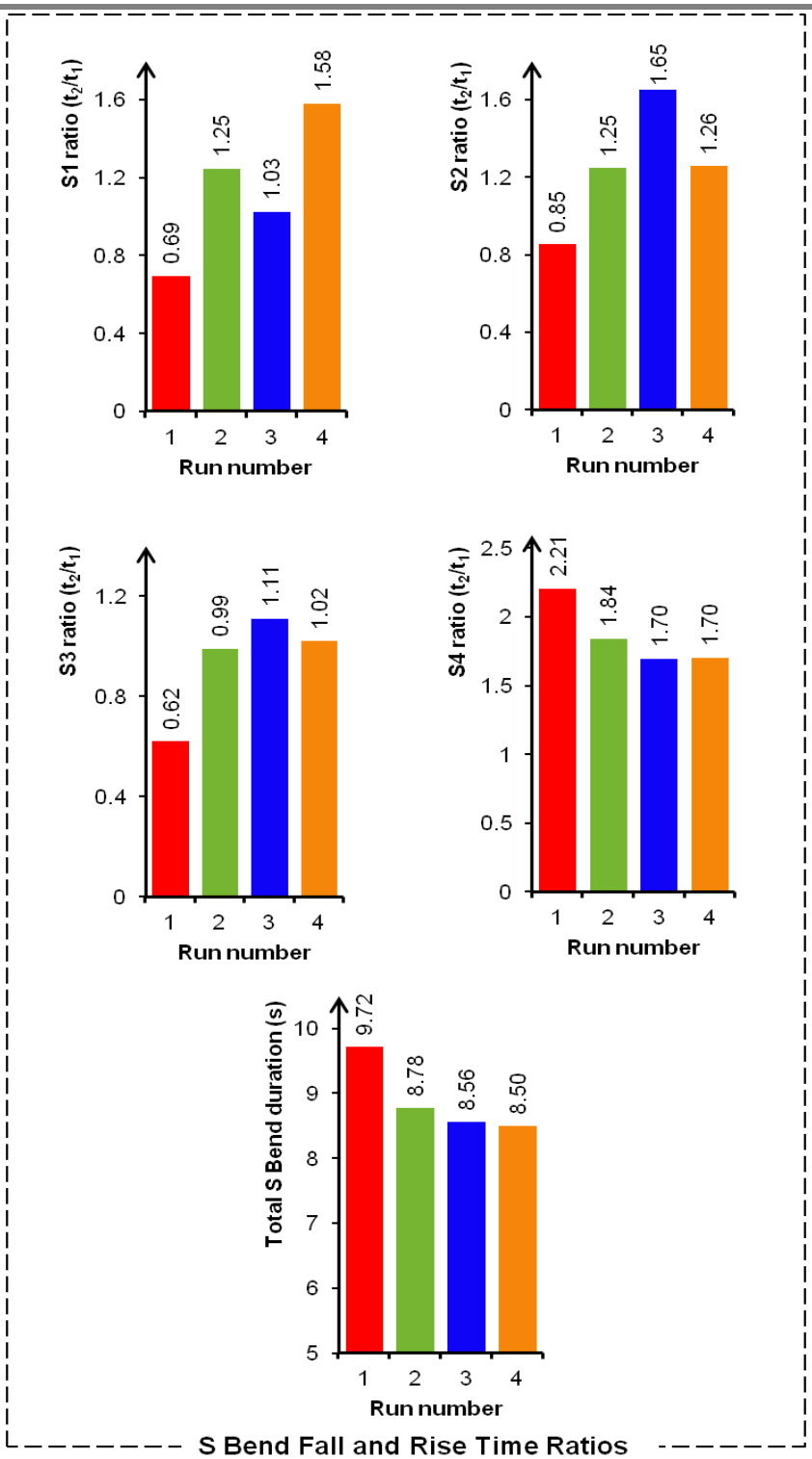


**Figure 4.11 – Indicators of performance during the S-Bends. The relative magnitudes should be considered to determine athlete performance and will be discussed in section 4.4.**

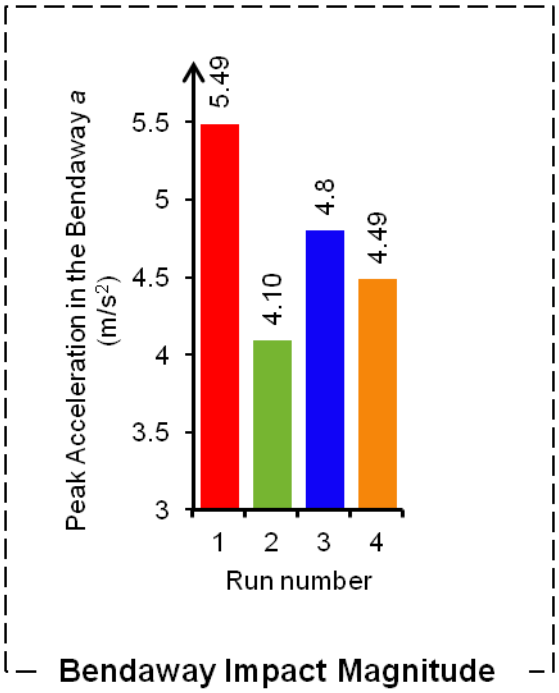


**Figure 4.12 – Indicator of performance during the Bendaway is shown using the magnitude of the first impact acceleration recorded in the Bendaway.**

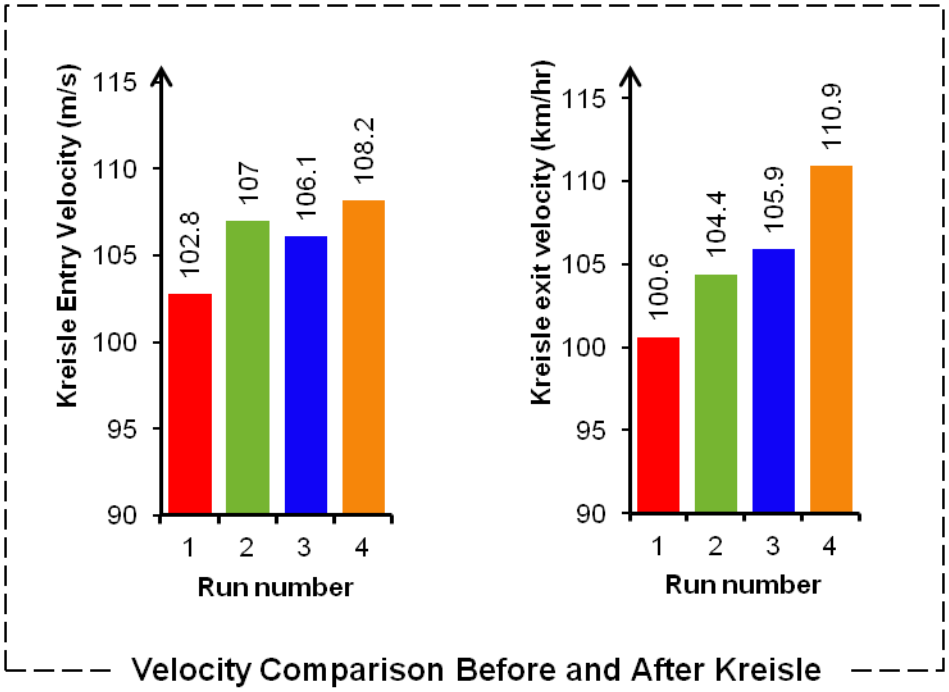


**Figure 4.13 – Indicator of performance during the Kreisle is shown using the velocity recorded before and after Kreisle.**

### *4.4 Discussion*

The three sections of interest are best understood by viewing a whole descent, accounting for push start times and how the sections interrelate. (Fig 4.10) plots a comparison of push start and total descent time for each run. The runs are presented in an order of increasing overall performance. As can be seen the fastest start time does not achieve the fastest descent time. An indicator as to where time is gained, or lost, can be seen by comparing the velocity before and after Kreisle, (Fig 4.13). This clearly shows that speed is lost on both Run 1 and Run 2, -2.2 km/h and -2.6 km/h respectively. The speed of Run 3 stays fairly constant with a marginal loss of -0.2 km/h whereas Run 4 makes an improvement of 2.7 km/h. To understand why this occurred we can look in more detail at the accelerometer output to determine how speed is generated in the upper region of the track, and then gained or lost through Kreisle. This is discussed in more detail below.

#### *4.4.1 Comparison of Multiple Runs*

Here I will compare how the characteristics identified above vary for each run, how the data correlates with my experience as the athlete and how the combination of this quantitative and qualitative data may aid in improving performance.

i) *S-Bends:* The above processing was applied and the $t_2/t_1$ ratios calculated for each of the S-Bends and for each of the four runs, (Fig 4.11). With athlete experience suggesting that the natural high point to be forced earlier in the corner would suggest a higher $t_2/t_1$ ratio is the goal. The exception being S4 as it is the final curve of the S-Bend sequence and unlike the other S-Bends that are optimally driven with a smooth crossover into a curve in the opposite direction, S4 exits into the level section of track leading onto the Bendaway. In this instance too high a ratio would imply too early a high point and the sled will likely skid and stay on the curve too long resulting in the exit fillet

pushing the sled over towards the right wall on the exit. Each of the four runs will now be considered in detail.

Run 1: overall the sled was allowed to follow the natural line determined by the geometry of the track. This sets a baseline for the ratios and therefore is an indicator as to how the runs are affected as the highpoint of the trajectory is shifted within the curves. The outcome is that the $t_2/t_1$ ratios are the lowest of all the four runs for S1, S2 and S3 with values of 0.69, 0.85 and 0.62 respectively implying the apex is towards the far end of the curves. S4 being the exception and here is too high, with a value of 2.21, due to the sled turning sharply on the entry after a steep exit from S3 and then requiring a lot of work by the athlete on the exit fillet to prevent the sled and athlete hitting the right wall. Feedback from athlete experience was that the sled's position on the exit of each S-bend was too high and therefore scraped / skidded on the ice surface between the curves instead of flowing. It should be noted that due to snow fall prior to the session, the push start for Run 1 is significantly slower than Runs 2, 3 and 4 which had the resultant effect of lower trajectories in general through the S-Bends because of the lower velocity.

Run 2: compared to Run 1, the $t_2/t_1$ ratios for S1 – S3 are significantly higher indicating the highpoint was achieved sooner in the curve. The resultant S4 has a lower $t_2/t_1$ ratio and athlete feedback is that the exit required far less work to control the exit. The overall S Bend duration was 0.94 s shorter than Run 1 (Fig 4.11) which is a gain of 0.48 s when accounting for the push deficit. Of course with such different start times and the clearing snow fall this is difficult to put into context as a significant gain over Run 1. This can be compared to less experienced athletes in the same training session, (Table 4.1) who from a similar push start travelled the 2 to 3 split section 0.29 s

slower than the instrumented sled implying the instrumented sled trajectory was more optimal to generating velocity.

| SPLIT | 1 | 2 | 3 |
|---|---|---|---|
| LOCATION | Push Start | Exit 1 | Exit S4 |
| ATHLETE 1 (Instrumented Sled), time (s) | 5.34 | 12.47 | 21.58 |
| ATHLETE 2, time (s) | 5.33 | 12.49 | 21.89 |

**Table 4.1 – Comparison of the first three split times recorded in Run 2 for the instrumented sled, ATHLETE 1, and a less experienced ATHLETE 2 training in the same session. Both have comparable push starts. ATHLETE 2 takes 0.29 s longer to travel from split 2 to split 3 than ATHLETE 1.**

Run 3: again this run shows a higher set of $t_2$/t1 ratios for S1 – S3 than for Run 1. However, the S2 ratio is almost double that of Run 1. Athlete feedback felt S1 to S2 was smooth but S2 – S3 experienced some scraping / skidding of the runners on the ice. Inspection of the ratios show that S1 for Run 3 was less than Run 2, so despite it feeling smooth the sled will still have been high on the end of S1 creating a very steep uptake into S2 and creating the high S2 ratio. This suggests that an upper level of ratio can also indicate the overall success of previous ratios. By then being too high too soon in S2 forces the sled to run flat and long through S2 and scrape into S3. Scraping often resets the sleds trajectory and the following S4 is actually not too bad with athlete feedback showing minimal work required to control the exit.

Run 4: the ratios are very similar to Run 2 with the exception of S1 which is significantly higher at 1.58. On this occasion the height is generated by athlete steering and not poor crossovers as seen in Run 3 S1-S2, the result

was smooth transitions through all the S-Bends and the shortest total S-bend duration. Fig 4.14 shows an overlap of accelerometer output for all four runs and shows that Run 3 arrives at S1 first and will be assumed to be travelling with the highest velocity due to having the fastest push start and the simplicity of the only bend prior to the S-Bends. In order of decreasing velocity it is followed by Run 2, Run 4 and finally Run 1, which is consistent with the push start times. Through the whole S bend section it clearly shows Run 4 catches up with Run 2 and comparison of total S bend duration for Run 3 and Run 4, (Fig 4.11), shows that Run 4 takes 0.06 s less time which is even more significant considering the push start was 0.06 s slower. Not only did athlete feedback feel smooth transitions throughout but the steering also seemed effortless and not forced which is a good indicator of steering at optimum points within the curves.

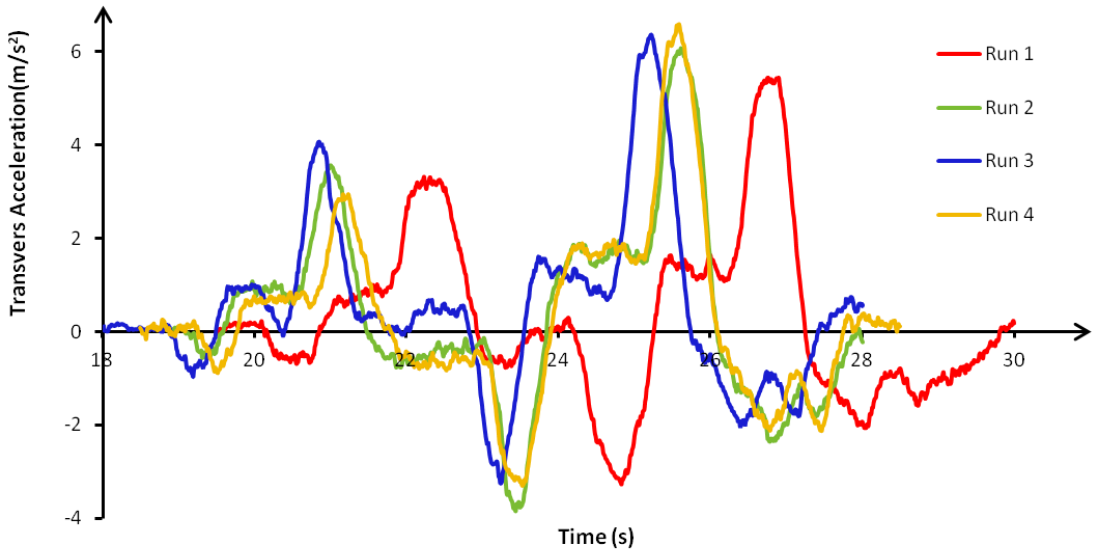


**Figure 4.14 – Filtered accelerometer output for all four runs through the S-Bends. Run 1 has the slowest start and so occurs latest in the time trace. Run 3 is the first to enter the S-Bends as this is the Run with the fastest push start. Run 2 enters the S-Bends before Run 4 however they exit at approximately the same time.**

ii) *Bendaway:* Fig 4.12 showed the peak acceleration at point of impact. Fig 4.15 shows the accelerometer output for each of the four runs.

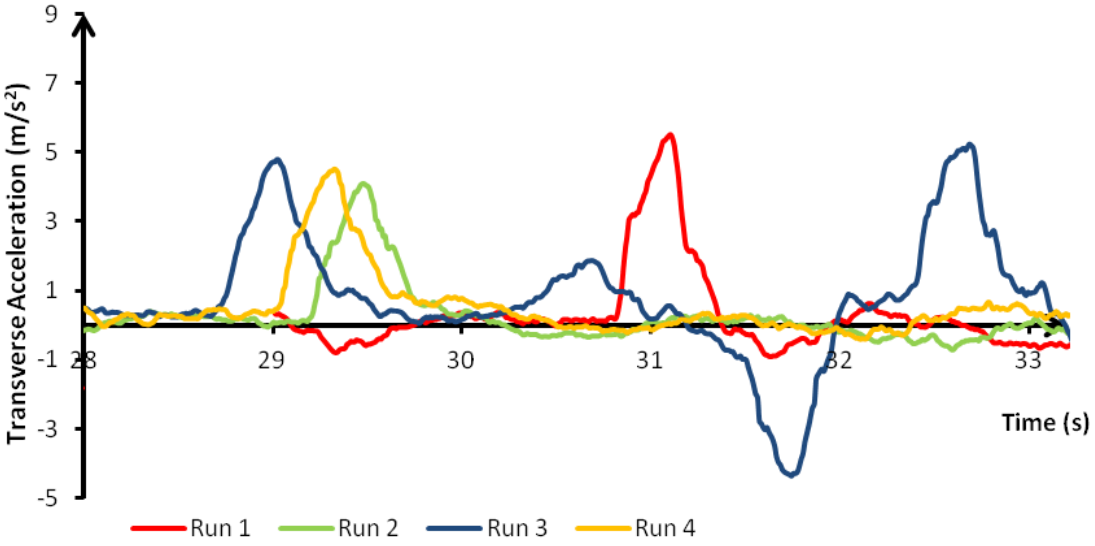


**Figure 4.15 – Filtered accelerometer output for all four runs at the Bendaway. Run 1, 2 and 4 all successfully *thread the needle* with only one impact. Run 3 fails and has a total of four impacts with the walls.**

Run 1: With the slowest start velocity and S-bend duration the impact in the Bendaway occurs at the latest time of the four runs. The magnitude of the acceleration peak is the largest of the four with a value of 5.49 $m/s^2$. However during the run I felt the impact was going to occur further down the Bendaway than desired, resulting from exiting S4 on the right hand wall, therefore a harder impact would be required to turn the sled adequately to clear the left wall further along the Bendaway, (Fig 4.7 point 2). The result was successfully threading the needle.

Run 2 and Run 4: The peak acceleration of Run 4s impact occurs before that of Run 2 in the time trace, which is expected due to the higher exit velocity

from S4 having reduced the gap to Run 2 during the S-Bends. The peak magnitudes of acceleration are 4.10 m/s$^2$ for Run 2 and 4.49 m/s$^2$ for Run 4. A larger impact for Run 4 is possibly due to the higher exit velocity from S4, however unknowns in the precise sled orientation make it difficult to ascertain for certain. Following the impact both runs successfully thread the needle.

Run 3: Fig 4.14 shows Run 3 touches the wall sooner than Run 4 in the Bendaway. The time between impacts of Run 3 and Run 4 in the Bendaway is equivalent to the difference in time exiting S4. With Run 3 having a higher velocity implies it impacts in the Bendaway too soon. The peak at impact is largest of the 4 runs at 4.8 m/s$^2$, (Fig 4.12). However, this was not sufficient to alter the sled's trajectory at this early point in the Bendaway. The consequence is failure to thread the needle with further impacts, (Fig 4.7 [2, 3, 4]).

iii) *Kreisle*: A comparison of calibrated, filtered and gravitational compensated accelerometer outputs are plotted in Fig 4.15 for all four runs. The three oscillations are indicated on each with a peak and trough level also highlighted in the third oscillation, the values of which are plotted in Fig 4.16 and can be used as an indicator of oscillation control. From an athlete perspective the track rising on the entry makes it difficult to determine whether the rising sensation is the track geometry or the beginning of an oscillation from the building centrifugal force. This is crucial as it sets up the remainder of the curve and if missed it makes it difficult to correct and can dictate how much work is required by the athlete in order to maximise velocity.

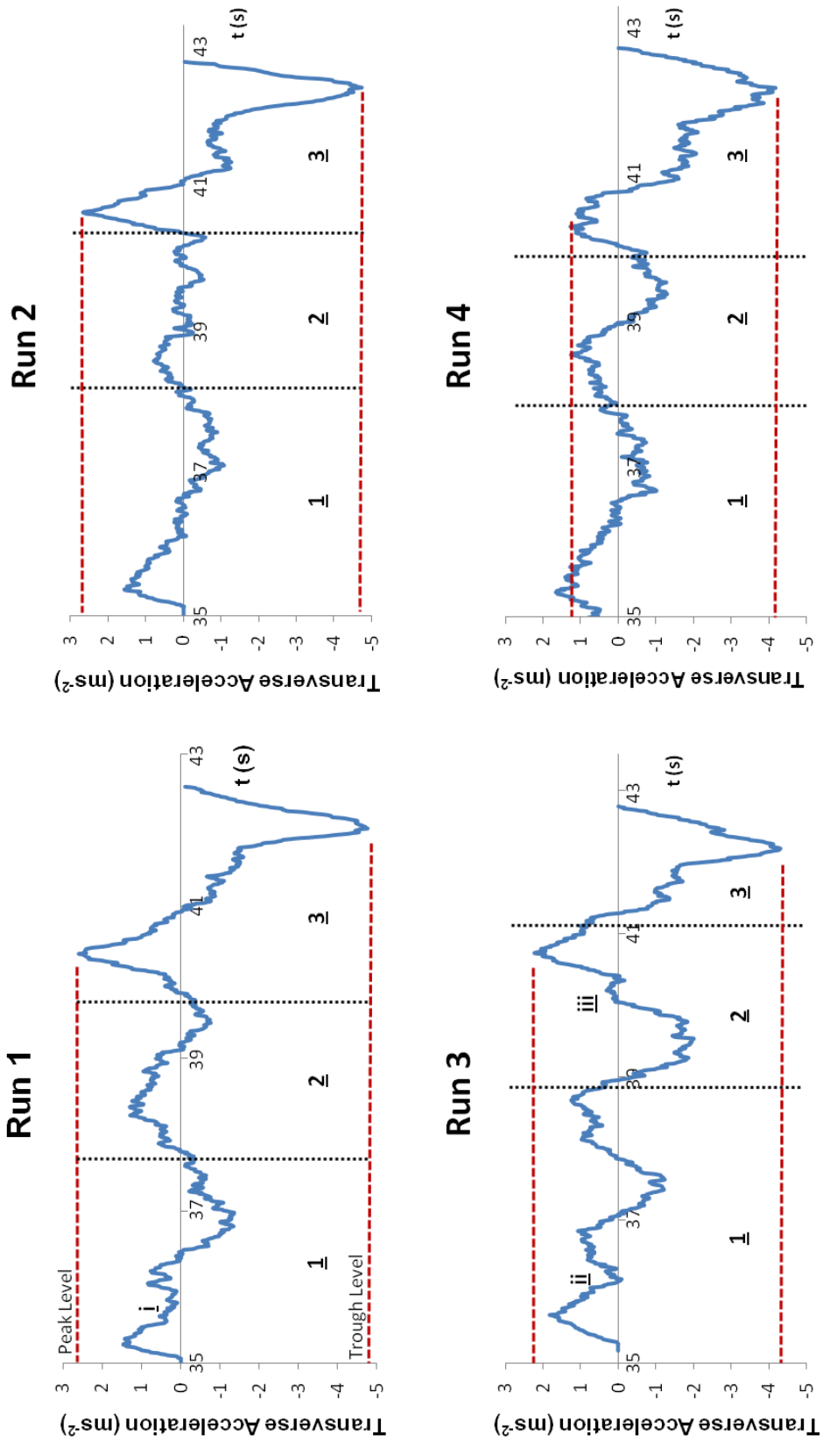


**Figure 4.16 - Filtered and calibrated transverse accelerometer output for all four runs through the Kreisle Curve. The oscillations [1, 2, 3] are indicated as are the peak and trough acceleration levels for the 3rd oscillation. Significant characteristics are also highlighted with errors on entry at points [i, ii] in Run 1 and Run 3 respectively and correction steer at point [iii] in Run 3.**

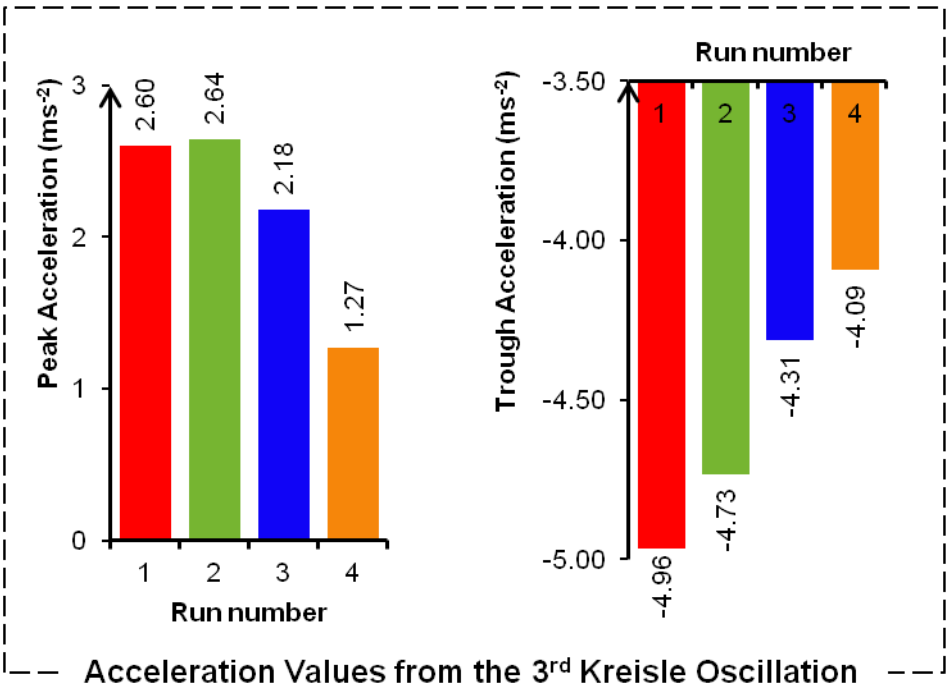


**Figure 4.17 – Magnitudes of peak and trough acceleration levels recorded in the 3rd oscillation for all four runs.**

Run 1: A dip in the acceleration can be seen at [i] in Fig 4.15 Run 1, which shows the sled did not smoothly rise onto the curve. This suggests that the sled was pushed off the entry fillet before the radius of curve increased and the sled was unable to make a smooth transition along the entry fillet to the curve wall. The peak and trough levels in the third oscillation are 2.6 $ms^{-2}$ and -4.96 $ms^{-2}$. The peak is correlated to the height the sled rises to from which the sled "freefalls" off the corner as the radius of curvature reduces and the Kreisle exit drops below the Kreisle entry. The trough value is the largest recorded and the peak value is almost equivalent to the largest, seen in Run 2, indicating poor oscillation control. The result being a loss of -2.6 km/h, Fig 4.13.

Run 2: The entry shows a smooth trace compared to Run 1. The peak and trough levels are again large with 2.64 $ms^{-2}$ and -4.73 $ms^{-2}$ respectively. Despite a better entry the oscillation control was unsuccessful, the peak and trough levels verify this, and again resulted in a loss of velocity, -2.9 km/h.

Run 3: Similarly to Run 1, Fig 4.15 shows a dip in accelerometer output as the track rises at the Kreisle entry for Run 3 [ii]. On this occasion however I forced the sled into a skid as the third oscillation commenced. This created a sharp alteration to the sleds trajectory to match the curve profile and can be seen at point [iii]. The outcome was a far smoother exit and managed to maintain velocity with only a -0.2 km/h loss.

Run 4: This time the entry is similar to Run 2 showing a smooth transition onto the Kreisle. The third oscillation peak and trough levels are the lowest recorded, 1.27 $ms^{-2}$ and -4.09 $ms^{-2}$. The outcome was a gain in velocity of 2.7 km/h.

## *4.5 Conclusions*

The athlete with the fastest push start time does not consistently achieve the fastest descent time. The requirement for the athlete to continue to accumulate and maintain speed during a descent provides motivation to quantify athlete performance at key points within the track. At the Koenigssee track the curves studied were S-Bends, Bendaway and Kreisle. The most beneficial accelerometer output for monitoring trajectory was determined to be in the transverse direction. It shows significant changes in acceleration as the sled travels in and out of the corners. It is at these points where the athlete has the greatest scope for altering trajectory.

Using the accelerometer output in the transverse direction through the S-Bends enabled a ratio of sled fall to rise time to be calculated. From this we can infer where the highest

point was achieved within the curve. Upon considering the relative magnitudes we can then conclude the effectiveness of athlete steering in order to achieve smooth transitions and generate velocity in the forwards direction.

Races can be won and lost in the Bendaway if the athlete fails to *thread the needle.* Being able to determine the optimum location and magnitude of impact with the wall in order to achieve this is often difficult to monitor efficiently. Using the transverse accelerometer output provides quantitative data to aid the athlete in deciding the optimum location for the fastest descent.

The Kreisle curve is one of the most difficult on the entire racing circuit. Utilising additional data available from speed traps, video capture and track geometry enables the orientation of the sled to be calibrated with a rotation approximation. The transverse accelerometer output can be used to identify smoothness of entry onto the Kreisle curve. Angled entries to Kreisle as a result of a right to left crossover from the K-1 exit can cause the sled to be pushed off the entry fillet to Kreisle. Without a smooth entry to Kreisle the subsequent oscillations can be more difficult to control. Corrections can be applied within the Kreisle, the example here being skidding the sled at the start of the 3$^{rd}$ oscillation and correcting the alignment on the curve for a smooth exit. This is presented quantitatively and I used the 3$^{rd}$ oscillation control in the 2010 World Cup. Electronic instrumentation is not allowed in official FIBT events, however an increased awareness was gained from previous training. Achieving a successful exit from the Kreisle based on the low point between the 2$^{nd}$ and 3$^{rd}$ oscillations, the TV commentary referred to my manoeuvre as a *power slide* from which I achieved the 16$^{th}$ fastest descent in the World Cup. These subtleties in sled trajectory are difficult to capture visually. By combining the quantitative data with qualitative feedback enables optimum trajectories to be determined and aided in a significant result in my qualification for the 2010 Winter Olympic Games.

# 5 SLED DYNAMICS AT THE LAKE PLACID INTERNATIONAL RACE TRACK

Chapter 4 showed a tri-axial accelerometer mounted within a skeleton sled during a descent. The data collected could be analysed to determine various aspects of the overall trajectory. Using knowledge of general steering approaches this data could be interpreted to infer the effect of the athlete's movements on the sled velocity. An accelerometer however does not provide information as to the deformation of the frame that occurs as the athlete attempts to steer the sled.

In this chapter information gained from strain gauges fixed to the frame of the sled is presented. Using rosettes of strain gauges on the long bars and cross bars enables the flex of the frame to be quantified as the sled gathers speed and travels through the curves. Data was recorded at the Lake Placid Olympic Park. Of Particular interest is the top section of the track including bends 1, 2 and 3. This is due to skeleton sleds having less response at lower velocities as the curves have the lowest g-forces making it more difficult to control them. Additionally any errors in this region of the track will be less forgiving with a higher likelihood of skidding.

The stiffness of the frame of the test sled used could be altered. Data was collected for two settings of stiffness, referred to from now on as *stiff* and *loose*. The subsequent analysis quantifies the difference between the two sled setups and the results related to both overall descent success and personal feedback on sled response.

## 5.1 The Lake Placid Track

The Lake Placid Olympic Sports Complex features regularly on the international racing calendar and has held the World Championships twice in the last 4 years (2009 and 2012). A track map of the Lake Placid track is shown in (Fig 5.1).

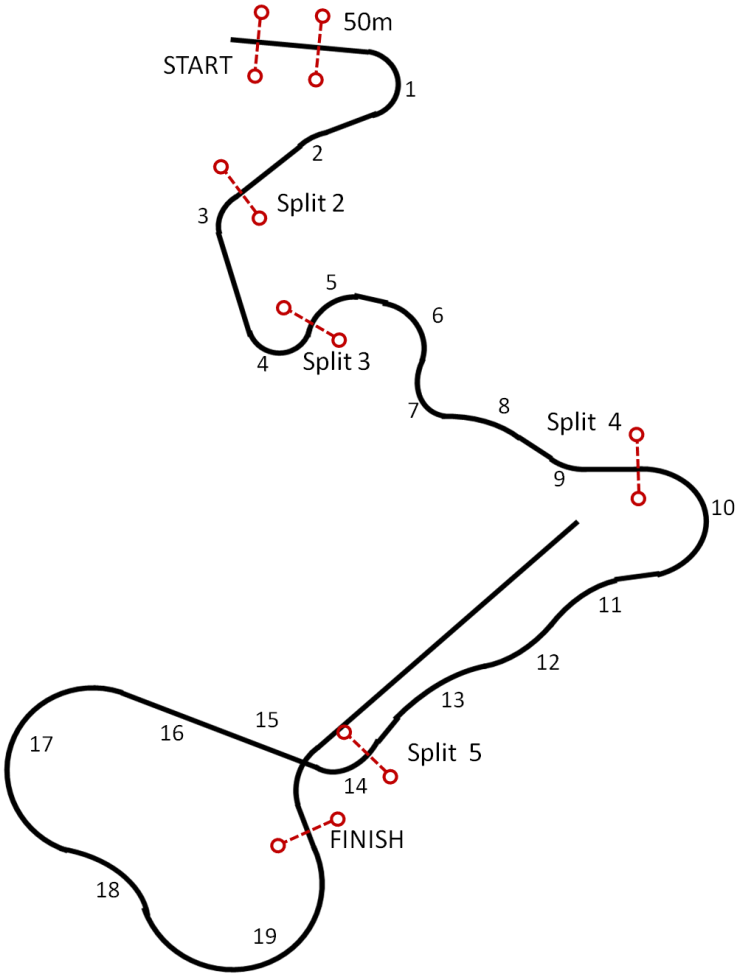


**Figure 5.1 – Track Map of the Lake Placid Olympic Complex. Timing eye locations are indicated and the bends numbered from the start, 1 to 19.**

## *5.2 Curve Characteristics and General Steering Approach*

Of key interest is the upper region of the track, curves 1, 2 and 3. The main focus at this stage of the descent is to allow the sled to use the velocity generated during the push start and continue to accelerate under the influence of gravity. Steering is therefore kept minimal both in quantity of steers and magnitude of steering force applied by the athlete.

A generalised view on steering through this region of the track follows. There are many possible approaches and that chosen will depend on the specifics of the ice profile. Throughout the racing season the ice thickness varies. Typically only a few centimetres thick at the start of the season (2-3 cm, athletes must inspect the track before training to ensure no concrete is showing through) and can increase to 30 cm over the course of the winter with the greatest variation observed on the entry and exit fillets.

The first point of interest is exit curve 1. Depending on the velocity accumulated through the push start and the ice profile of the curve results in a natural line on the exit that can vary between two extremes. The first being to exit the curve early, presenting an angled trajectory towards the left wall. The second being to stay on the curve too long and the exit fillet pushing the sled out with an angled trajectory towards the right wall, (Fig 5.2). The athlete may decide to alter the trajectory at the entry or midpoint of the curve to create a clean direct transition to the second curve. Here the use of knee steering only on the exit is investigated. This enables results to be interpreted with confidence limiting errors from unplanned body movements.

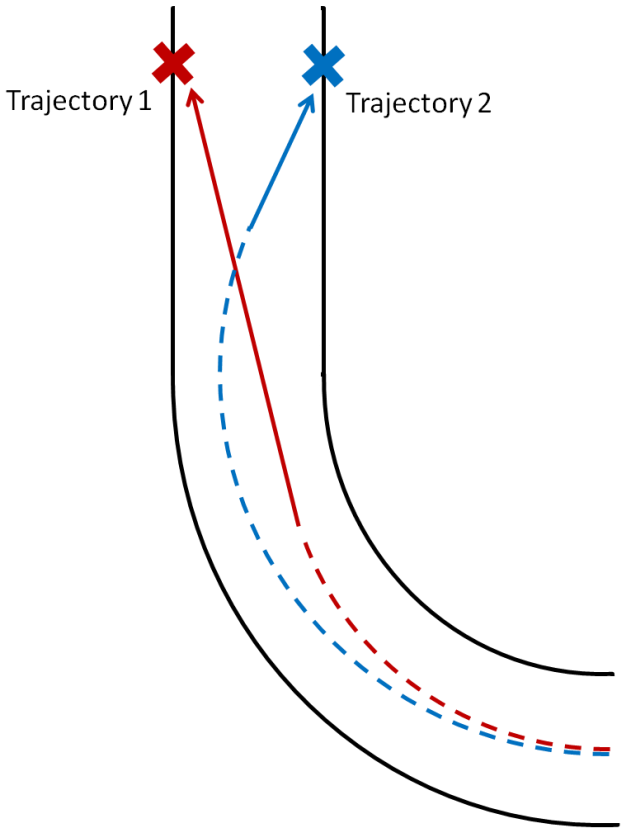


**Figure 5.2 – Overhead view of exit curve 1. The profile has been flattened to highlight two trajectories. Trajectory 1 shows the sled leaving the curve early with an impact on the left wall. Trajectory 2 is the far extreme with the sled staying on the curve too long and the exit fillet sending it over to the right wall.**

The second point of interest is the control of the second curve and the subsequent trajectory through curve 3. Curve 2 has a very small radius, appearing as a slight raised bank of ice. Novice athletes may underestimate the importance of the trajectory through this curve. It is relatively simple to travel through curve 2 to curve 3 without any impacts with the walls. Curve 3 however is a short curve with a tight radius. The geometry of curve 3 usually results in the sled exiting on a right to left trajectory and hitting the left wall, (Fig 5.3). This is not necessarily a bad event to occur. With curve 4 also being to the left, taking the touch to the wall on the exit of curve 3 can push the sled over to be positioned ideally towards the right of the track for entry to curve 4.

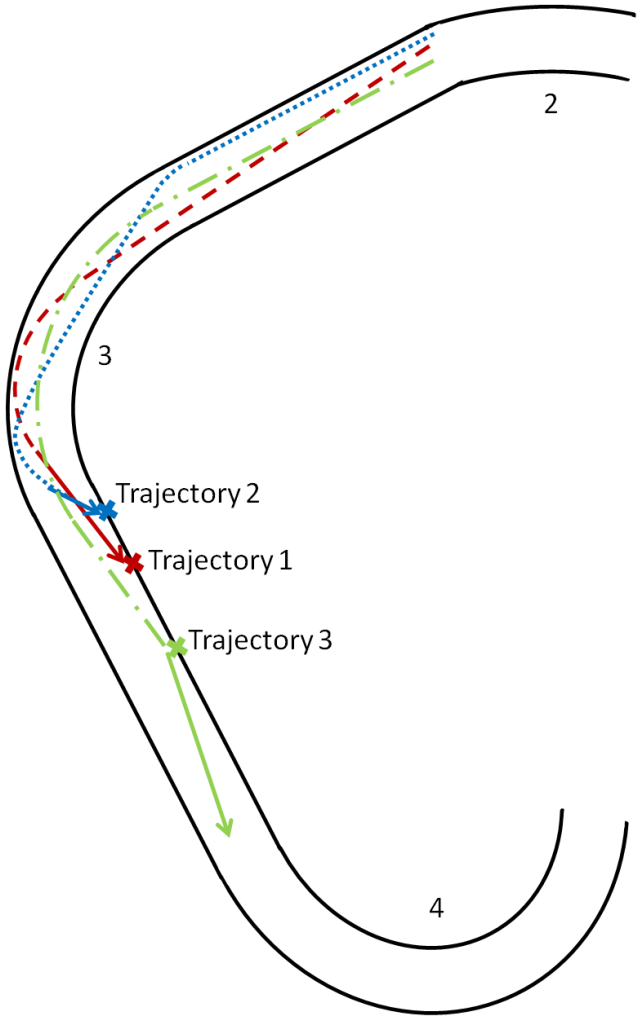


**Figure 5.3 – Overhead view showing possible trajectories from exit curve 2 to entry curve 4. Trajectory 1 leaves curve 2 angled right to left resulting in a high point late on in curve 3 and a heavy impact on exiting curve 3. Trajectory 2 travels parallel to the wall on exiting curve 2 and is pushed away from the wall as the entry fillet to curve 3 begins, again resulting in late height and an impact on the exit of curve 3. Trajectory 3 shows a midpoint between these two trajectories, the specifics depend on the shape of the ice fillets, and has a glance with the left wall on exit curve 3 that enables a good entry position to curve 4 to be achieved.**

Too hard an impact will lose velocity and likely result in skidding or even ricocheting off the right wall also. A gentle glance sacrifices minimal velocity and can be controlled for an optimum entry to curve 4. Although it is possible to steer heavily through curve 3 for a clean exit it should be noted that the track record was achieved by taking the glance off of the left wall.

The path of minimal steering in this section is usually achieved using curve 2 to set an entry position to curve 3 that then uses the geometry of curve 3 to do the work of altering the sleds trajectory requiring minimal input from the athlete. Extremes for possible exits from curve 2 are:

Trajectory 1 (Fig 5.3) - Exiting curve 2 with a right to left trajectory will send the sled late into curve 3 and create a sharp turn at the latter stage of the corner and a heavy impact with the left wall,

Trajectory 2 – The sled travels close and parallel to the right wall from exit curve 2. The entry fillet of curve 3 pushes the sled away from the corner before it has begun. This would again angle the sled towards a sharp turn at the latter stage of the corner and a heavy impact with the left wall.

Trajectory 3 - The specific details for controlling the trajectory through this section of the track depends on the shaving of the ice profile and will be somewhere between these two extremes with a gentle glance on exit 3.

This highlights how the exit trajectory from curve 2 has subsequent impact on the ease of controlling curve 3 and entry to curve 4. It is therefore of interest to measure the effectiveness of steering response of the sled through curve 2.

## 5.3 Experimental Setup

### 5.3.1 Strain Gauges and the Wheatstone Bridge

In order to quantify the deformation of the sled frame during a run requires the application of strain gauges. The gauges need to be connected in a suitable circuit and an excitation voltage applied in order to measure the movement of the frame. Here I present the electrical setup used for the dynamic tests at the Lake Placid track.

The strain gauges are applied directly to the frame, with a suitable adhesive, such that as the frame bends the gauge experiences tension or compression. Small changes to the gauges geometry results in a change in the resistance, $R$, as there is a mutual dependency with the relation:

$$R = \rho \frac{l}{A} \qquad \text{(Eq. 5.1)}$$

where $\rho$ is the resistivity of the conductor, $l$ is the length and $A$ the cross sectional area. This in turn can be used to determine the strain, $\varepsilon$, of the frame by logging the change in resistance, $\Delta R$, as the deformation occurs:

$$k.\varepsilon = \frac{\Delta R}{R_0} \qquad \text{(Eq. 5.2)}$$

with $k$ being a constant called the gauge factor and $R_o$ the steady state resistance.

The changes in resistance are small and the values are detected best when aligned in a Wheatstone bridge, (Fig 5.4).

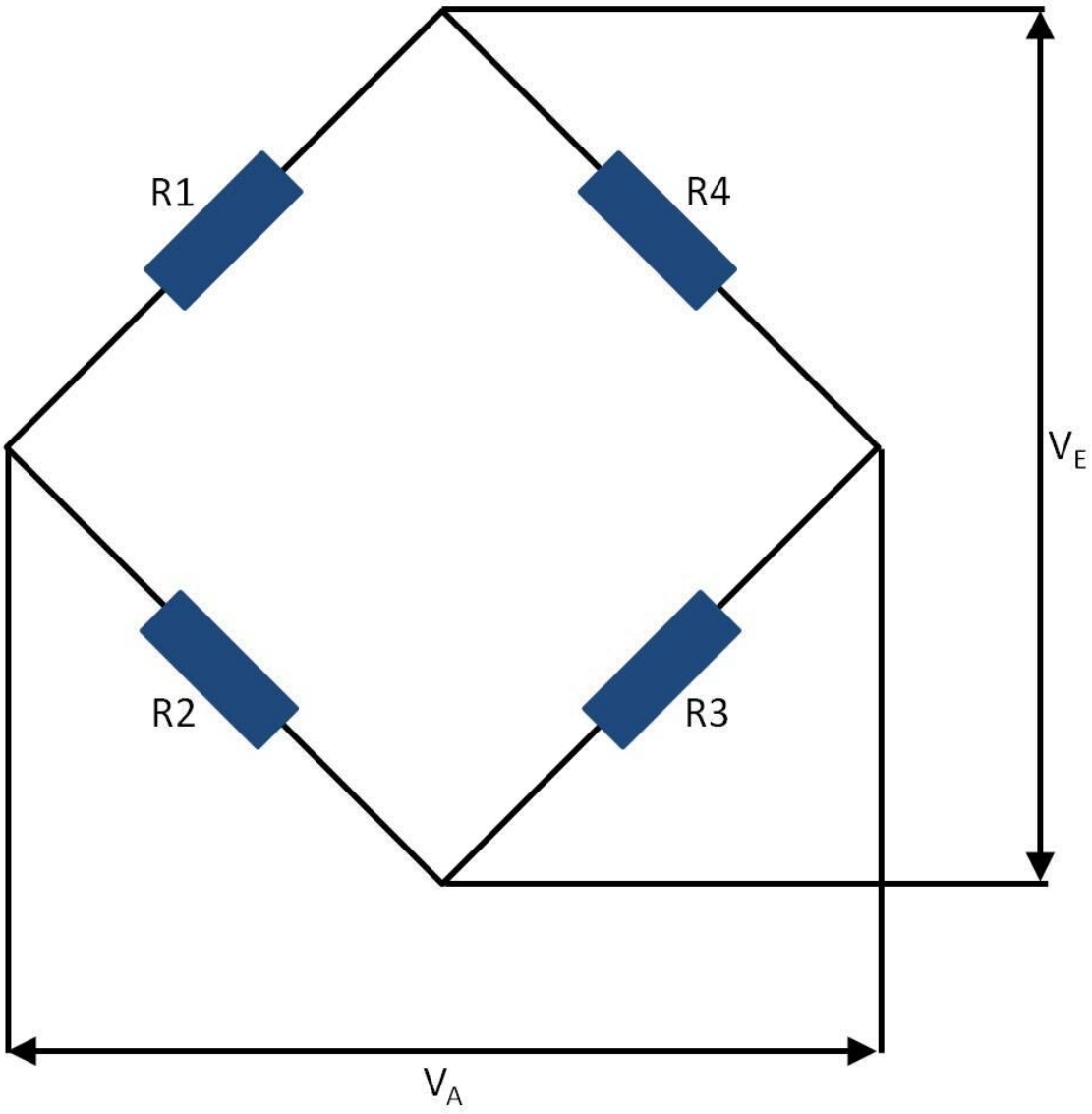


**Figure 5.4 – Schematic of a Wheatstone bridge where R1, R2, R3, R4 are resistors, $V_E$ is the excitation voltage and $V_A$ the resulting output voltage.**

The configuration of a Wheatstone bridge creates a direct relationship between the excitation voltage and the output voltage with a dependency on the resistors:

$$\frac{V_A}{V_E} = \frac{R1}{R1+R2} - \frac{R4}{R3+R4} \quad \text{(Eq. 5.3)}$$

This is useful for measuring the resistance of strain gauges as any change that occurs in R1, R2, R3, R4 results in Eq 5.3 becoming:

$$\frac{V_A}{V_E} = \frac{\Delta R1}{R1} - \frac{\Delta R2}{R2} + \frac{\Delta R3}{R3} - \frac{\Delta R4}{R4} \quad \text{(Eq. 5.4)}$$

So that this can be applied to the investigation of frame deformation at a single point a half Wheatstone bridge is formed where R3 and R4 are fixed resistors of known resistance. R1 and R2 are both strain gauges, R1 the test gauge and R2 a *dummy* gauge. The purpose of the dummy gauge is to compensate for temperature fluctuations. While the test gauge, R1, is fixed to the frame the dummy gauge is fixed to a neutral plate of identical material that will not be exposed to any deformation. In the event of thermal expansion / contraction both the test and dummy gauge outputs will scale and the bridge will remain balanced. The output voltage will only vary if the test gauge is exposed to any tension or compression from the deformation of the frame.

With the twist of the frame being of interest the strain gauges can be applied in rosettes. Here as a configuration of three strain gauges orientated at 45° to each other, (Fig 5.5). By measuring the resistance changes at these angular variations provides information as to the directional flexing of the frame. Each of the gauges in the rosette requires a dummy gauge and two fixed resistors to complete the half bridge so that the output from individual test gauges can be recorded at every location.

### *5.3.2 Sled Setup*

Sled C, introduced in Chapter 2, was used as the test sled for this study. *Standard* runners were fitted to it as these were suitable for the ice conditions in Lake Placid at the time of data collection. Upon inspection of the frame, locations were determined for strain gauge placement. Recall that the rectangular section of the frame is formed from the corner blocks and comprising of long bars, and cross bars. A rosette of strain gauges was fixed to the underside of the front cross bar at the midpoint, (Fig 5.5a). The rear cross bar previously had a hole machined into the exact centre point and so two rosettes of strain gauges were fixed equidistant from this hole. Again on the underside of the cross bar and had a separation of 6 cm, (Fig 5.5b). The long bars of Sled C have a distinct profile, having a width of 4 cm where they meet the corner blocks and a narrower 3 cm midsection. Here the rosette of strain gauges was applied to the underside of both the long bars at the centre point of the narrow section as it is anticipated that this region will have the greatest deflection.

**(a)**

**(b)**

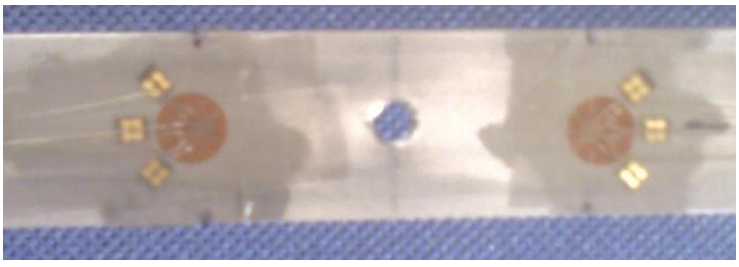

**Figure 5.5 – Photos showing the strain gauges attached to the steel frame. (a) is the front cross bar and (b) the rear cross bar.**

The locations of all the strain gauges attached to the frame are shown in Fig 5.6. The notation used for the remainder of this chapter is also indicated.

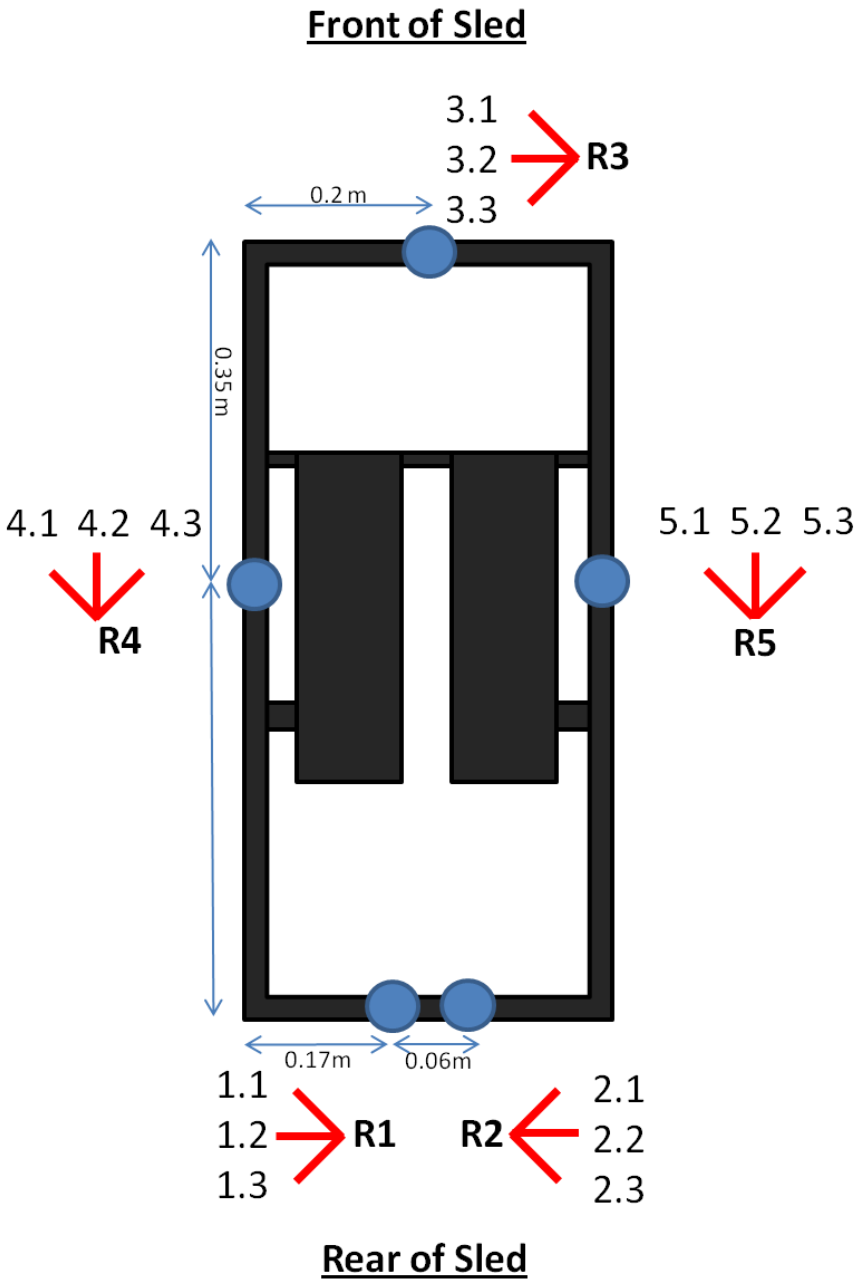


**Figure 5.6 - Overhead schematic of the steel frame indicating the placement of the strain gauges and the labelling used for each rosette for the remainder of this chapter.**

Each gauge was incorporated into a half Wheatstone bridge circuit, utilising a dummy gauge on an isolated steel plate to compensate for any thermal expansion / contraction. The Wheatstone bridge had a ±5V applied resulting in a 0V to 5V output as required for the Race Technology DL1 data logger. An accelerometer was also used to measure the acceleration in the forwards direction which enabled the signature trace of the push start to be used as a time stamp for all the data recorded. The experimental set up is shown in Figure 5.7.

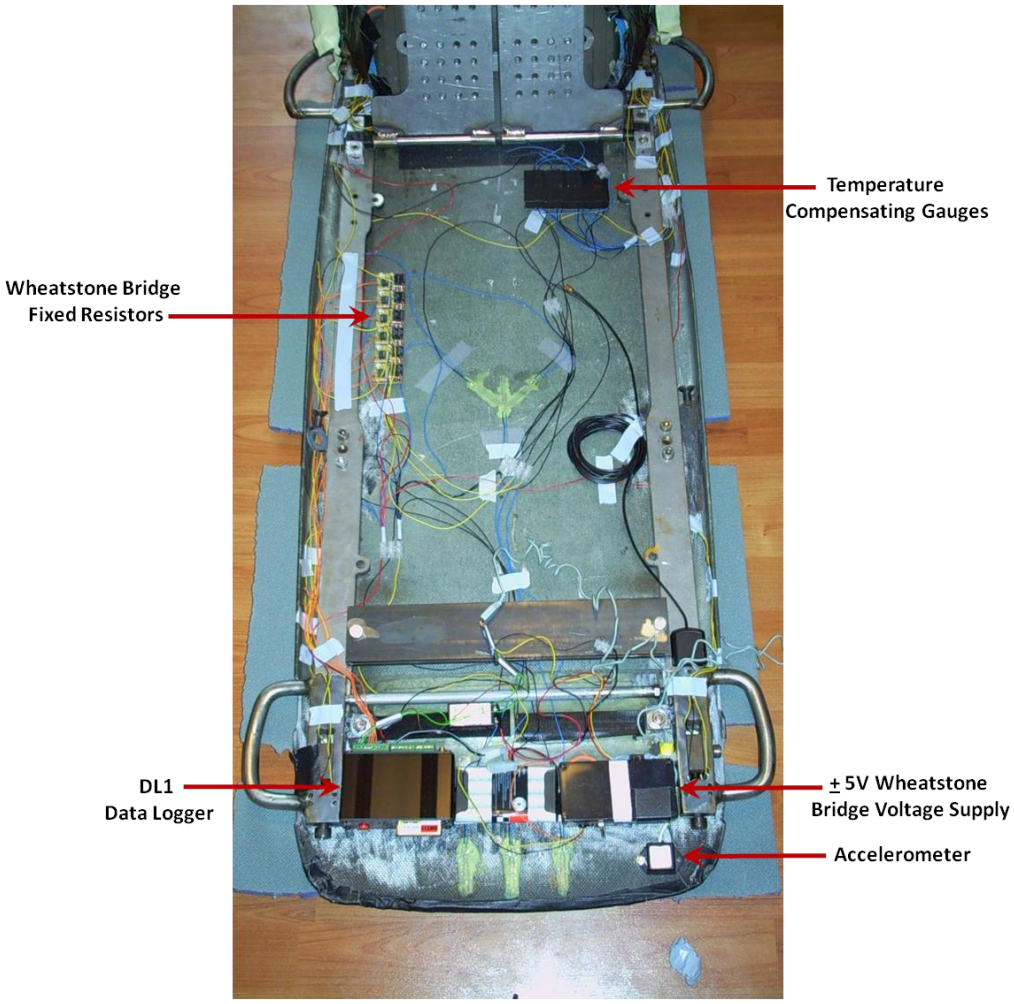


**Figure 5.7 – The experimental setup within the sled used for static and dynamic testing. The data logger, voltage supply, Wheatstone bridge resistors, temperature compensating gauges and accelerometer are indicated.**

The modification to Sled C to alter the stiffness was achieved using the bolts fixing the rear of the saddle plates. The "*stiff*" frame setup was with these bolts firmly secure*. The "*loose*" frame setup achieved by replacing the bolts with equivalent diameter but 2 cm longer in length. This extra bolt length enables the saddle plates to pivot on the front hinge of the saddle and the rear of the saddle plates move freely in the vertical direction and therefore the cross and long bars can flex to a greater extent. The longer bolt length was limited to 2 cm as this prevented Sled C frame distorting beyond the elastic limit.

(* secure meaning *finger tight*. Excessive tightening creates tension in the frame and can result in an uneven distortion. This is a common mistake made by athletes at all levels.)

### *5.3.3 Static Testing*

To be able to interpret the dynamic data recorded on the track a set of static tests were conducted. The test sled was set up as it would be for use on the track. Runners were attached to the frame and runner tension applied (to a *rock* of 10 mm, equivalent to that used during the dynamic tests). The sled was fixed at three of the corners by applying weights to prevent movement at those points. The free corner was supported so that the frame was in a level state of equilibrium and four Linear Displacement Potentiometers (LDPs) configured around this free corner (Fig. 5.8). The strain gauges were connected, again in a half Wheatstone bridge formation.

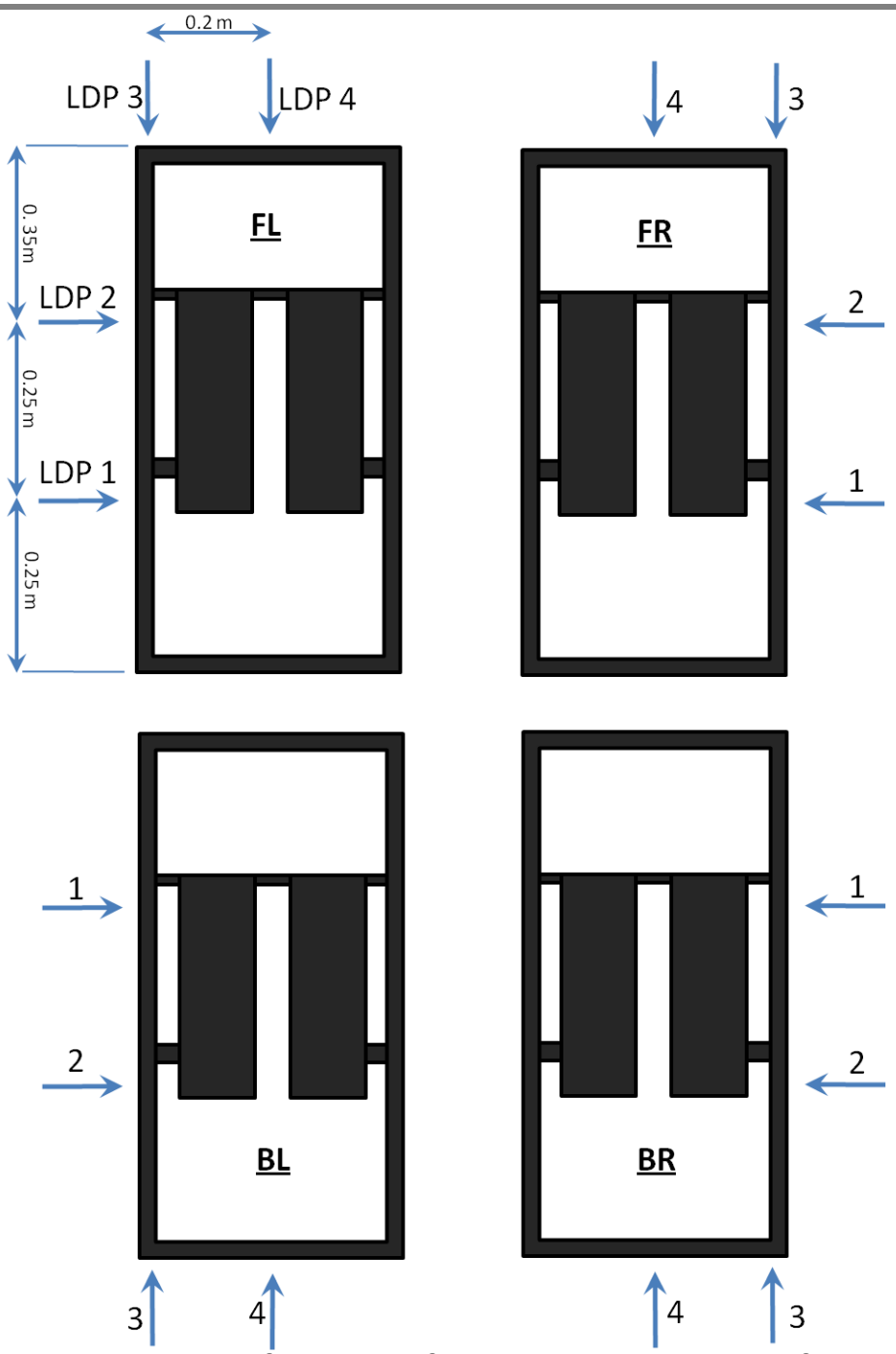


**Figure 5.8 – Locations of the LDPs for the static testing. The full length of the frame is 0.95 m. Due to the clamping of the fixed corners the length free to move was 0.85 m and the LDPs were positioned at the free corner and at 0.35 m, 0.25 m along the long bar. The midpoint of the cross bar was used for the final LDP.**

The support for the free corner was then removed and the frame allowed to flex under the weight of the sled. Once settled in a steady state a further 2 kg was applied to the corner, allowed to settle once more and then followed by a further 2 kg. This process was recorded for each rosette of strain gauges for both the *stiff* and *loose* frame setup and then repeated for the remaining three corners of the frame until all configurations had been tested. The free corners are labelled FL, FR, BL, BR corresponding to the Front, Back, Left and Right of the frame as viewed from above.

### *5.3.4 Dynamic Testing*

The dynamic tests on the Lake Placid track were carried out over three different days. This is due to the DL1 data logger having 8 single ended inputs enabling two rosettes of strain gauges and the forwards direction of an accelerometer to be recorded. The harshness of the environment experienced during a descent resulted in numerous failures, either due to connections coming loose or strain gauges permanently damaged / too noisy to analyse. The additional channel was used to determine whether any noisy gauges were potentially useful. Summary of data recorded for each day is shown in Table 5.1

| Day | Run | Frame | Strain Gauge Number | | | | | | | | | | | |
|---|---|---|---|---|---|---|---|---|---|---|---|---|---|---|
| | | | R1.1 | R1.3 | R2.1 | R2.3 | R3.1 | R3.2 | R4.1 | R4.2 | R4.3 | R5.1 | R5.2 | R5.3 |
| **1** | 1 | S | X | X | X | X | | | | | | | | |
| | 2 | S | X | X | X | X | | | | | | | | |
| | 3 | L | X | X | X | X | | | | | | | | |
| **2** | 1 | S | | | | | X | X | | | | | | |
| | 2 | S | | | | | X | X | | | | | | |
| | 3 | L | | | | | X | X | | | | | | |
| **3** | 1 | S | | | | | | | X | X | X | X | X | X |
| | 2 | S | | | | | | | X | | X | X | X | X |
| | 3 | L | | | | | | | X | | X | X | X | X |
| | 4 | L | | | | | | | X | | X | X | X | X |

**Table 5.1 – Summary of data recorded over three days of testing. The number of descents taken each day and the corresponding active strain gauges are shown. The stiffness of the frame is indicated by S – Stiff, L – Loose.**

## *5.4 Results*

### *5.4.1 LDP and Strain Gauge Static Test Results*

Fig. 5.9 shows the LDP data recorded for a *loose* frame with the Front Right (FR) corner unconstrained. From the linear relation we can infer that when the support is removed but no additional mass applied is equivalent to a point mass of 2 kg placed at the corner and the subsequent added mass therefore relating to 4kg and 6 kg. Table 5.2 shows the numerical results and highlights this relation to mass which will now be expressed as steps of 2 kg, 4 kg, 6kg.

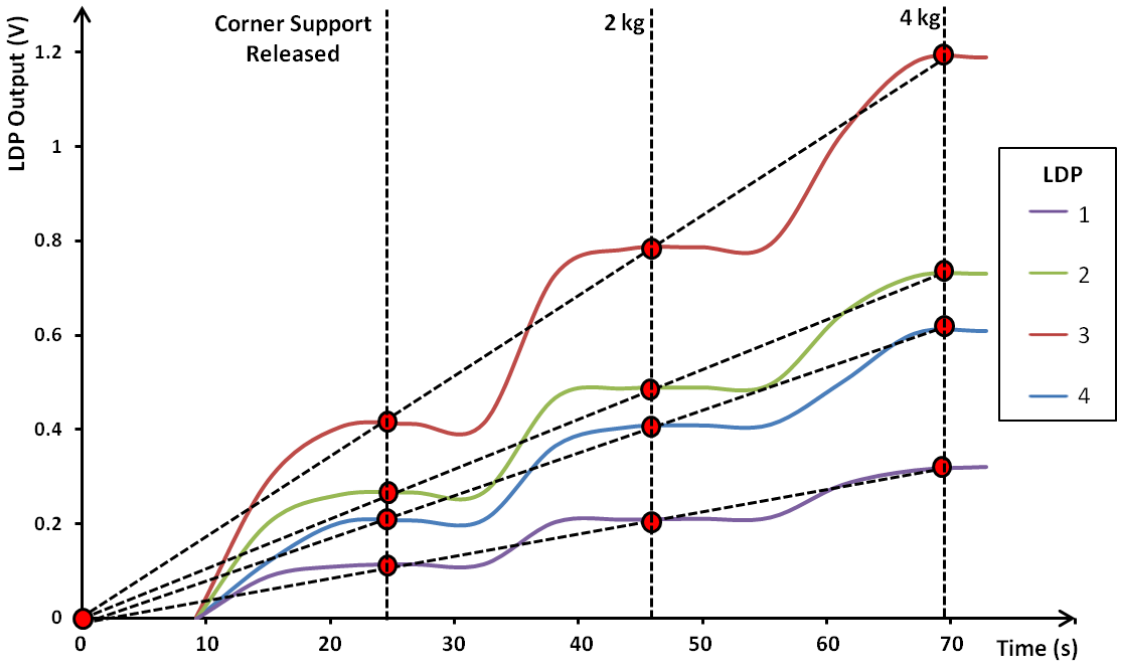


**Figure 5.9 – Plot showing the LDP results carried out at the Front Right of the sled with a *loose* frame.**

| Test : FR Loose | | | | |
|---|---|---|---|---|
| LDP Position | Weight Applied (kg) | LDP Output (V) | Displacement (m) | Twist Angle (°) |
| 1 | 0 | 0.00 | 0.0000 | 0.00 |
| | SLED (2) | 0.12 | 0.0012 | 0.27 |
| | 2 | 0.23 | 0.0023 | 0.52 |
| | 4 | 0.34 | 0.0034 | 0.77 |
| **2** | 0 | 0.00 | 0.0000 | 0.00 |
| | SLED (2) | 0.25 | 0.0024 | 0.27 |
| | 2 (4) | 0.49 | 0.0047 | 0.53 |
| | 4 (6) | 0.72 | 0.0068 | 0.78 |
| **3** | 0 | 0.00 | 0.0000 | 0.00 |
| | SLED (2) | 0.40 | 0.0039 | 0.26 |
| | 2 (4) | 0.82 | 0.0080 | 0.54 |
| | 4 (6) | 1.21 | 0.0119 | 0.80 |
| **4** | 0 | 0.00 | 0.0000 | 0.00 |
| | SLED (2) | 0.20 | 0.0020 | 0.57 |
| | 2 (4) | 0.41 | 0.0041 | 1.16 |
| | 4 (6) | 0.60 | 0.0059 | 1.70 |

**Table 5.2**

| Test: FR Stiff | | | | |
|---|---|---|---|---|
| LDP Position | Weight Applied (kg) | LDP Output (V) | Displacement (m) | Twist Angle (°) |
| 1 | 0 | 0.00 | 0.0000 | 0.00 |
| | 2 | 0.08 | 0.0008 | 0.18 |
| | 4 | 0.16 | 0.0016 | 0.36 |
| | 6 | 0.24 | 0.0024 | 0.54 |
| **2** | 0 | 0.00 | 0.0000 | 0.00 |
| | 2 | 0.16 | 0.0015 | 0.17 |
| | 4 | 0.33 | 0.0031 | 0.36 |
| | 6 | 0.50 | 0.0048 | 0.54 |
| **3** | 0 | 0.00 | 0.0000 | 0.00 |
| | 2 | 0.27 | 0.0026 | 0.18 |
| | 4 | 0.55 | 0.0054 | 0.36 |
| | 6 | 0.81 | 0.0079 | 0.54 |
| **4** | 0 | 0.00 | 0.0000 | 0.00 |
| | 2 | 0.13 | 0.0013 | 0.37 |
| | 4 | 0.27 | 0.0027 | 0.77 |
| | 6 | 0.40 | 0.0040 | 1.13 |

**Table 5.3**

| Test: BR Loose | | | | |
|---|---|---|---|---|
| LDP Position | Weight Applied (kg) | LDP Output (V) | Displacement (m) | Twist Angle (°) |
| 1 | 0 | 0.00 | 0.0000 | 0.00 |
| | 2 | 0.22 | 0.0021 | 0.48 |
| | 4 | 0.43 | 0.0041 | 0.94 |
| | 6 | 0.65 | 0.0062 | 1.42 |
| **2** | 0 | 0.00 | 0.0000 | 0.00 |
| | 2 | 0.42 | 0.0042 | 0.48 |
| | 4 | 0.83 | 0.0082 | 0.94 |
| | 6 | 1.23 | 0.0122 | 1.40 |
| **3** | 0 | 0.00 | 0.0000 | 0.00 |
| | 2 | 0.69 | 0.0068 | 0.46 |
| | 4 | 1.40 | 0.0137 | 0.92 |
| | 6 | 2.11 | 0.0207 | 1.39 |
| **4** | 0 | 0.00 | 0.0000 | 0.00 |
| | 2 | 0.33 | 0.0033 | 0.94 |
| | 4 | 0.68 | 0.0067 | 1.93 |
| | 6 | 1.05 | 0.0104 | 2.98 |

**Table 5.4**

| Test: BR Stiff | | | | |
|---|---|---|---|---|
| LDP Position | Weight Applied (kg) | LDP Output (V) | Displacement (m) | Twist Angle (°) |
| 1 | 0 | 0.00 | 0.0000 | 0.00 |
| | 2 | 0.14 | 0.0013 | 0.30 |
| | 4 | 0.28 | 0.0027 | 0.61 |
| | 6 | 0.43 | 0.0041 | 0.94 |
| **2** | 0 | 0.00 | 0.0000 | 0.00 |
| | 2 | 0.26 | 0.0026 | 0.29 |
| | 4 | 0.55 | 0.0054 | 0.62 |
| | 6 | 0.81 | 0.0080 | 0.92 |
| **3** | 0 | 0.00 | 0.0000 | 0.00 |
| | 2 | 0.47 | 0.0046 | 0.31 |
| | 4 | 0.92 | 0.0090 | 0.61 |
| | 6 | 1.38 | 0.0135 | 0.91 |
| **4** | 0 | 0.00 | 0.0000 | 0.00 |
| | 2 | 0.24 | 0.0024 | 0.68 |
| | 4 | 0.47 | 0.0047 | 1.33 |
| | 6 | 0.69 | 0.0068 | 1.96 |

**Table 5.2 to Table 5.5 – Summary of LDP static tests. The linear relation shows that the deformation caused by releasing the free corner of the sled is equivalent to 2 kg being applied to the corner. Therefore the applied mass steps of *Sled*, 2 kg, 4 kg effectively becomes 2 kg, 4 kg, 6 kg.**

From these results a longitudinal and transverse twist angle can be calculated, (Fig 5.10), where:

$$\text{Longitudinal Twist Angle, } \boldsymbol{\alpha} = \sin^{-1}( \Delta LDP / y )$$

$$\text{Transverse Twist Angle, } \boldsymbol{\beta} = \sin^{-1}( \Delta LDP / x )$$

The values are also shown in Tables 5.2 to 5.5 and differ for the front and rear corners showing the rear of the sled has a greater twist as expected due to the torsional resistance

being limited from the saddle hinge, located towards the front of the sled. LDPs 1, 2, 3 are used to calculate α and LDP 4 for β. Only one twist angle is required to represent the twist of the frame. LDP 3 can be used to calculate both α and β and so can be used to add confidence to measured results by calculating both for comparison to LDPs on both the x and y axis.

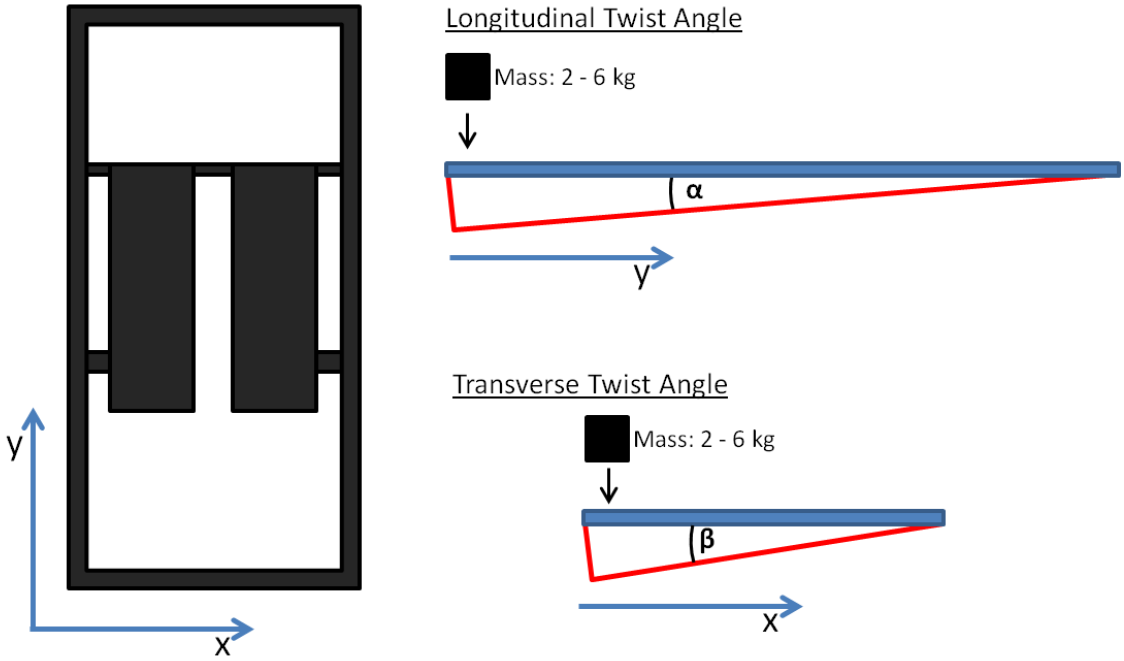


**Figure 5.10 – Diagram showing the longitudinal and transverse twist angles, α and β respectively.**

The data output from a test strain gauge is shown in Figure 5.11, here for the rear cross bar, gauge R1.1. The change in Voltage is identifiable with each additional mass applied. The output from the strain gauges between the fixed points of the frame showed negligible change in voltage indicating the predominant deformation measured was solely from the free corner. Tables 5.6 to 5.8 summarise the trends for each of the gauges. Symmetry of the frame results in similar voltage outputs for many gauges and so they are included in the summary tables labelled in brackets. Values less than 0.005 V are rounded down to 0 V to highlight the low level of voltage change recorded between the fixed points and values of this level are likely due to electrical noise and not indicative of any movement in those sections of the frame.

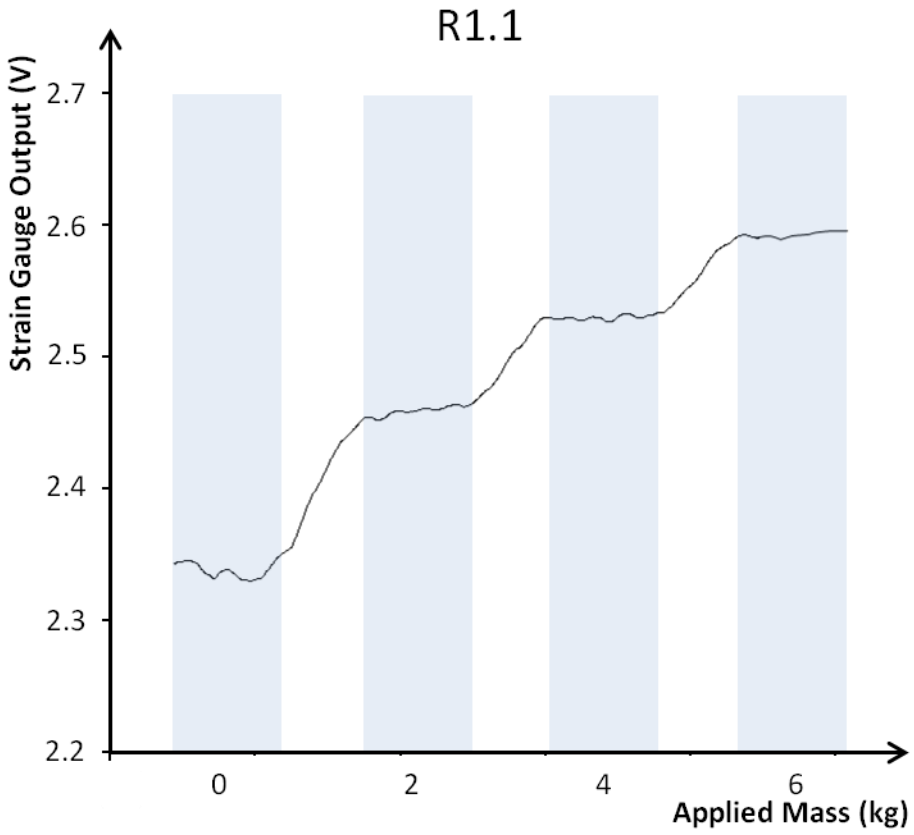


**Figure 5.11 – Strain Gauge output recorded during a static test. The gauge used was R1.1 and the test was BR *Loose.***

**Table 5.6**

| **Gauge:R1.3** *(R2.1)* | | | | |
|---|---|---|---|---|
| | Applied Mass (kg) | | | |
| Test | 0 | 2 | 4 | 6 |
| FR Stiff | 0 | 0 | 0 | 0 |
| FR Loose | 0 | 0 | 0 | 0 |
| FL Stiff | 0 | 0 | 0 | 0 |
| FL Loose | 0 | 0 | 0 | 0 |
| BR Stiff | 0 | 0.029 | 0.062 | 0.103 |
| BR Loose | 0 | 0.051 | 0.099 | 0.147 |
| BL Stiff | 0 | 0.069 | 0.144 | 0.206 |
| BL Loose | 0 | 0.102 | 0.201 | 0.295 |

**Table 5.7**

| **Gauge:4.2** *(5.2)* | | | | |
|---|---|---|---|---|
| | Applied Mass (kg) | | | |
| Test | 0 | 2 | 4 | 6 |
| FR Stiff | 0 | 0 | 0 | 0 |
| FR Loose | 0 | 0 | 0 | 0 |
| FL Stiff | 0 | -0.108 | -0.215 | -0.323 |
| FL Loose | 0 | -0.172 | -0.321 | -0.503 |
| BR Stiff | 0 | 0 | 0 | 0 |
| BR Loose | 0 | 0 | 0 | 0 |
| BL Stiff | 0 | -0.128 | -0.262 | -0.398 |
| BL Loose | 0 | -0.195 | -0.403 | -0.601 |
| **Gauge:4.1** *(4.3, 5.1, 5.3)* | | | | |
| FR Stiff | 0 | 0 | 0 | 0 |
| FR Loose | 0 | 0 | 0 | 0 |
| FL Stiff | 0 | -0.025 | -0.052 | -0.075 |
| FL Loose | 0 | -0.053 | -0.111 | -0.171 |
| BR Stiff | 0 | 0 | 0 | 0 |
| BR Loose | 0 | 0 | 0 | 0 |
| BL Stiff | 0 | -0.032 | -0.065 | -0.098 |
| BL Loose | 0 | -0.065 | -0.138 | -0.202 |

**Table 5.8**

| Gauge:3.1 | | | | |
|---|---|---|---|---|
| | Applied Mass (kg) | | | |
| Test | 0 | 2 | 4 | 6 |
| FR Stiff | 0 | -0.129 | -0.261 | -0.405 |
| FR Loose | 0 | -0.212 | -0.389 | -0.597 |
| FL Stiff | 0 | 0.130 | 0.261 | 0.403 |
| FL Loose | 0 | 0.207 | 0.411 | 0.601 |
| BR Stiff | 0 | 0 | 0 | 0 |
| BR Loose | 0 | 0 | 0 | 0 |
| BL Stiff | 0 | 0 | 0 | 0 |
| BL Loose | 0 | 0 | 0 | 0 |
| **Gauge:** | **3.2** | | | |
| FR Stiff | 0 | -0.047 | -0.084 | -0.126 |
| FR Loose | 0 | -0.063 | -0.142 | -0.207 |
| FL Stiff | 0 | 0.051 | 0.088 | 0.133 |
| FL Loose | 0 | 0.081 | 0.151 | 0.212 |
| BR Stiff | 0 | 0 | 0 | 0 |
| BR Loose | 0 | 0 | 0 | 0 |
| BL Stiff | 0 | 0 | 0 | 0 |
| BL Loose | 0 | 0 | 0 | 0 |

**Table 5.6 to Table 5.8 – Summary of Rosette static tests, change in gauge output is in V. Gauges that produce comparable results due to symmetry are indicated in brackets.**

Table 5.6 is for the back cross bar gauge R1.3 and shows the largest change in voltage for the BL tests. The values recorded show a rise in voltage as the mass is applied indicating compression in the strain gauge and a downward curvature of the bar as expected from the visual deformation. The BR tests also produce a rise in Voltage output but of lower magnitude, approximately 50% less, as the orientation of the strain gauge is angled across the plane of curvature. A similar trend is seen for R2.1 and the

contrary for R1.1 / R2.3. The offset to the placement of these gauges caused by the hole in the rear cross bar has proven beneficial as here we can see that all voltage changes are positive, therefore indicating compression, and the twist of the bar can be quantified using these gauges.

Table 5.7 shows that the angled gauges on the long bars, (R4.1, R4.3, R5.1, R5.3) produce a smaller output change than R4.2 and R5.2, approximately 75 % lower. They are all of comparable negative voltage change implying they are under tension. The long bars therefore do not significantly twist and the flex of the frame is mainly due to movement in the cross bars.

Table 5.8 highlights that gauge R3.1 produces a decrease in voltage for the FR tests and an increase in voltage for the FL tests. R3.1 is situated at the midpoint of the front cross bar and due to the angle these values are representative of the bar twisting putting the gauge under tension for the FR tests and compression for the FL tests. R3.2 is aligned in the direction of the bar and produces a similar trend but with 70% less magnitude as at this centre point of the bar the resultant twisting of the bar angles across the direction of gauge R3.2.

### *5.4.2 Dynamic Test Results*

The different locations of the Rosette gauges produce very different voltage outputs, as seen from the static tests. When also considering that the dynamic tests were carried out on different days, and so track conditions vary, requires them to be analysed accordingly. A total of 10 runs were recorded, 6 on the *stiff* frame and 4 on the *loose* frame setup. The overall descent times are shown in Figure 5.12.

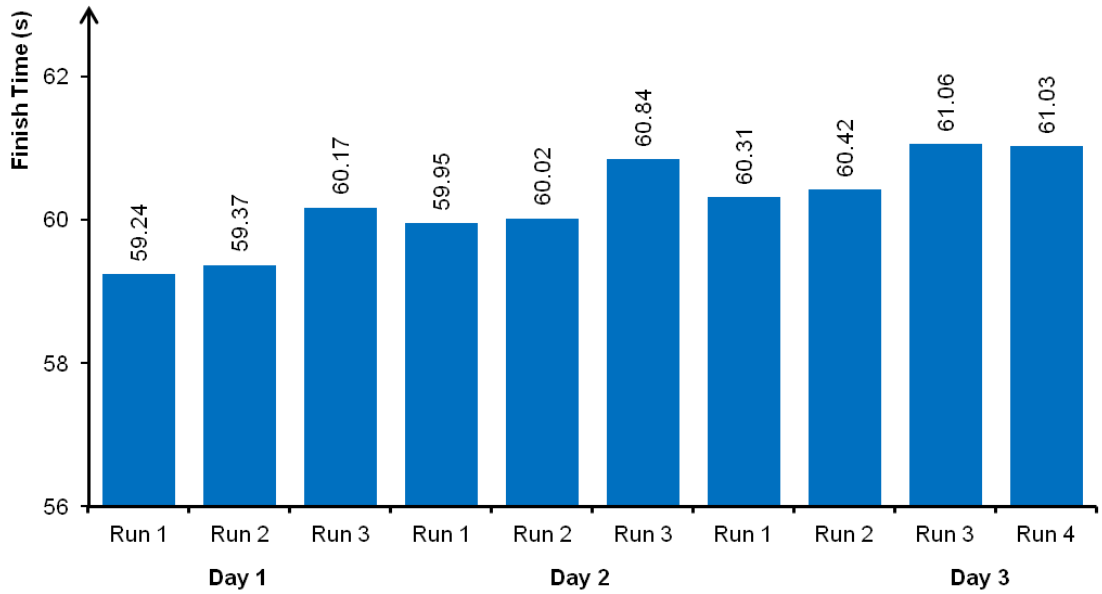


**Figure 5.12 – Summary of total descent times for all test runs.**

With the LDPs showing greatest response from the BR and BL tests suggests the rear bar to be an appropriate starting point. The LDP tests also show that the dominant twist of the frame comes from the cross bars and so I will consider the front cross bar after the rear cross bar and finally the long bars of the frame.

### *5.4.2.1 Rear Cross Bar Results*

The strain gauges placed on the rear cross bar produce the clearest results to determine bend locations. Figure 5.13 shows an example raw voltage output from the rear cross bar and the same data after a 10Hz low pass filter has been applied. Using the accelerometer trace in the forwards direction to timestamp where the run commences highlights an event in the strain gauge output where the loading phase of the push start occurs.

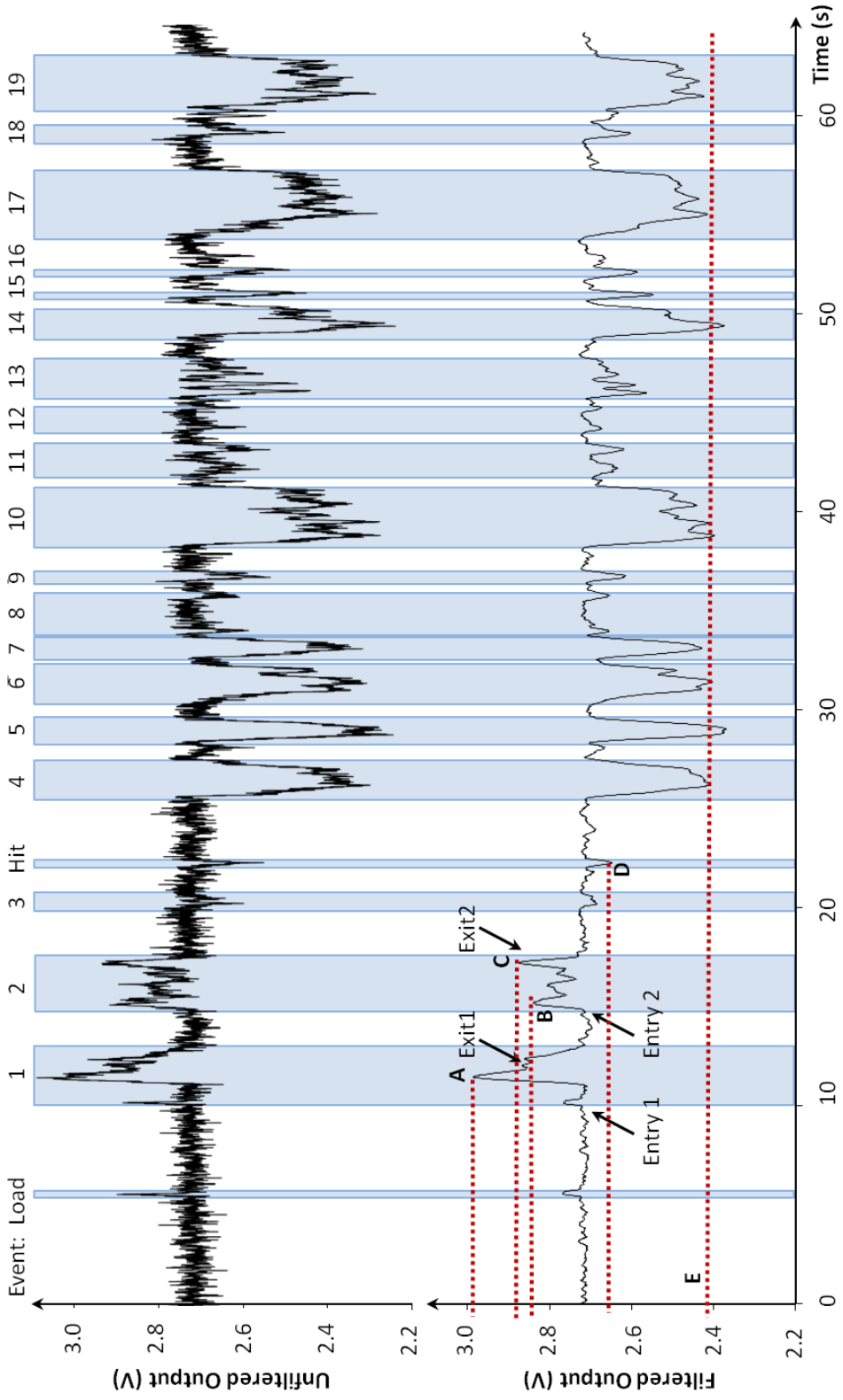


**Figure 5.13 – Example strain gauge data recorded during a full descent. The original raw data is shown, (top), and after a 10 Hz low pass filter is applied (bottom). Events can be identified including bend locations, athlete load in the push start and the impact with the wall on exiting curve 3. Exit curve 1, entry and exit curve 2 are used for later analysis and are labelled A, B, C respectively. The impact is marked at point D and a *High g Deformation* level with point E.**

Key points of interest are that at the lower velocities through curves 1 and 2 both the entries and exits can be identified. The impact with the wall on exit curve 3 is also visible. By curve 4 the sled has accumulated significant velocity and the 4, 5, 6, 7 section can clearly be seen, although now the entries and exits are not distinguishable for each curve. The voltage output now appears to be correlated to the centrifugal force as the sled travels through the curves. The remaining significant voltage changes verify this with also being curves of tighter radius and high g-forces, curves 10, 14, 17 and 19. These register as a drop in Voltage showing the deformation is now caused from the centrifugal force putting the strain gauge under tension. This does not mean that the sled is no longer under an asymmetric flex from athlete steering. The centrifugal force has caused the runners to splay outwards as the athlete is pushed on to the surface of the sled with greater force and this signal overpowers the twisting of the bar.

***Quantifying Voltage Output:*** The key region of interest being curves 1, 2, 3. The voltage output shows the entries and exits of the curves, (Fig 5.13). It is at these low velocities that the athlete movements can be correlated to the output with greatest confidence. The centrifugal force is low, the steering applied is specific and the duration of the steer is held for 1 to 2 s, in the case of exit 1, and so the output is more indicative of the flex of the frame. The peak voltage output is measured for the exit of curve 1 and both the entry and exit of curve 2, marked A, B, C on Figure 5.13, and translated to twist angle. Point D represents the peak voltage recorded at the impact on exit curve 3.

For the remainder of the track a peak magnitude appears to be achieved caused by the centrifugal force exerted on the sled frame and the sled construction reaching a point of maximum deformation allowed by the structural qualities of the frame. The transitions between the corners are short, particularly for curves 4 through 7 that are each separated by less than 3 m. The average peak value achieved in curves 4, 5, 6, 7, 10, 14, 17, 19 will therefore be used to quantify an average *High g Deformation*. This provides a

measure of how the frame is affected by the centrifugal forces experienced during a descent, point E on Figure 5.13.

***Variance with Frame Stiffness:*** Data was successfully recorded over a total of three descents. Two runs taken with the stiff frame and one run with the loose frame. Figures 5.14 and 5.15 show filtered strain gauge data for the two frame setups. The magnitudes recorded for curves 1 and 2 are shown in Figure 5.16.

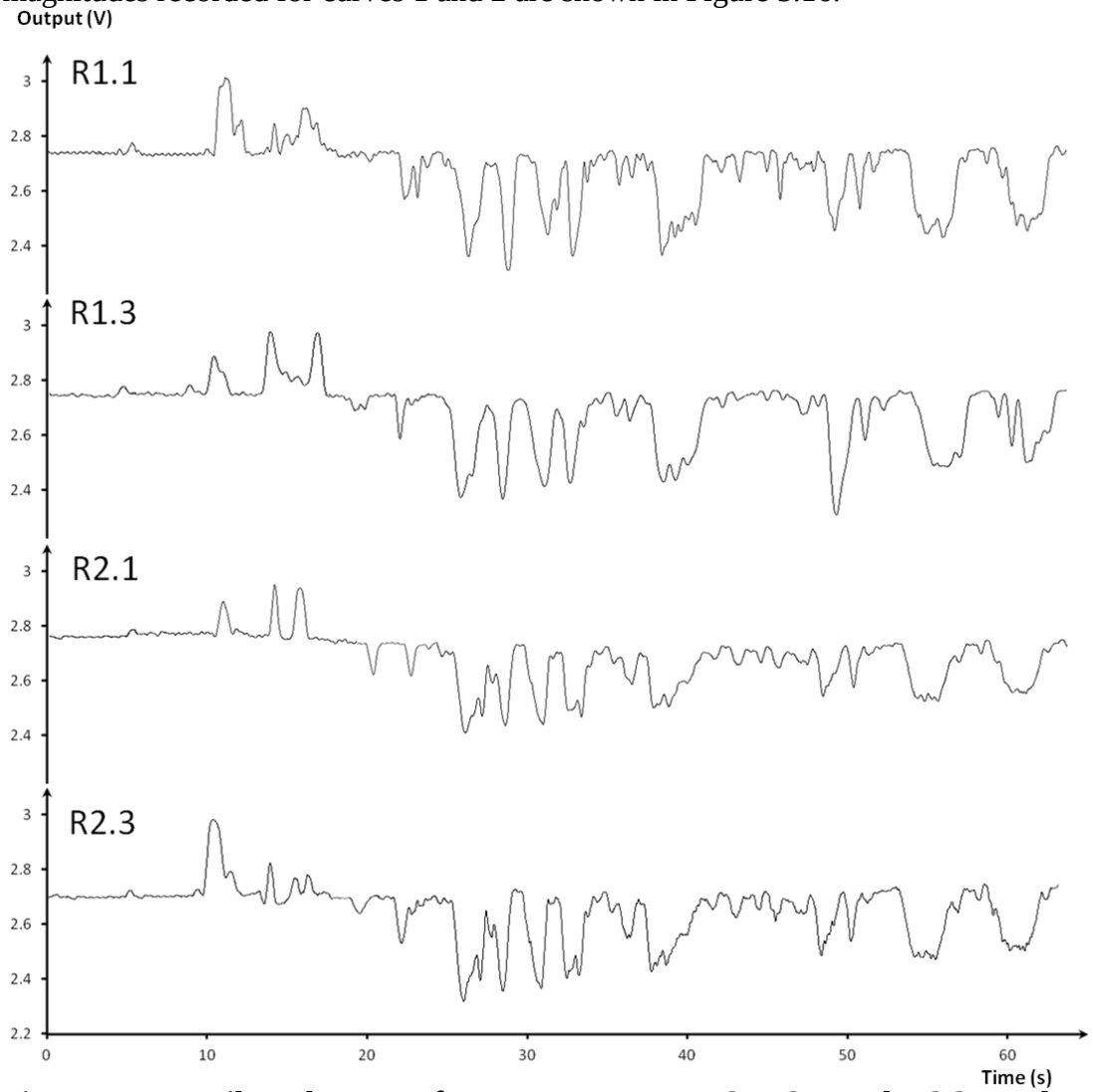


**Figure 5.14 – Filtered output for gauges R1.1, R1.3, R2.1 and R2.3 on the *stiff* frame.**

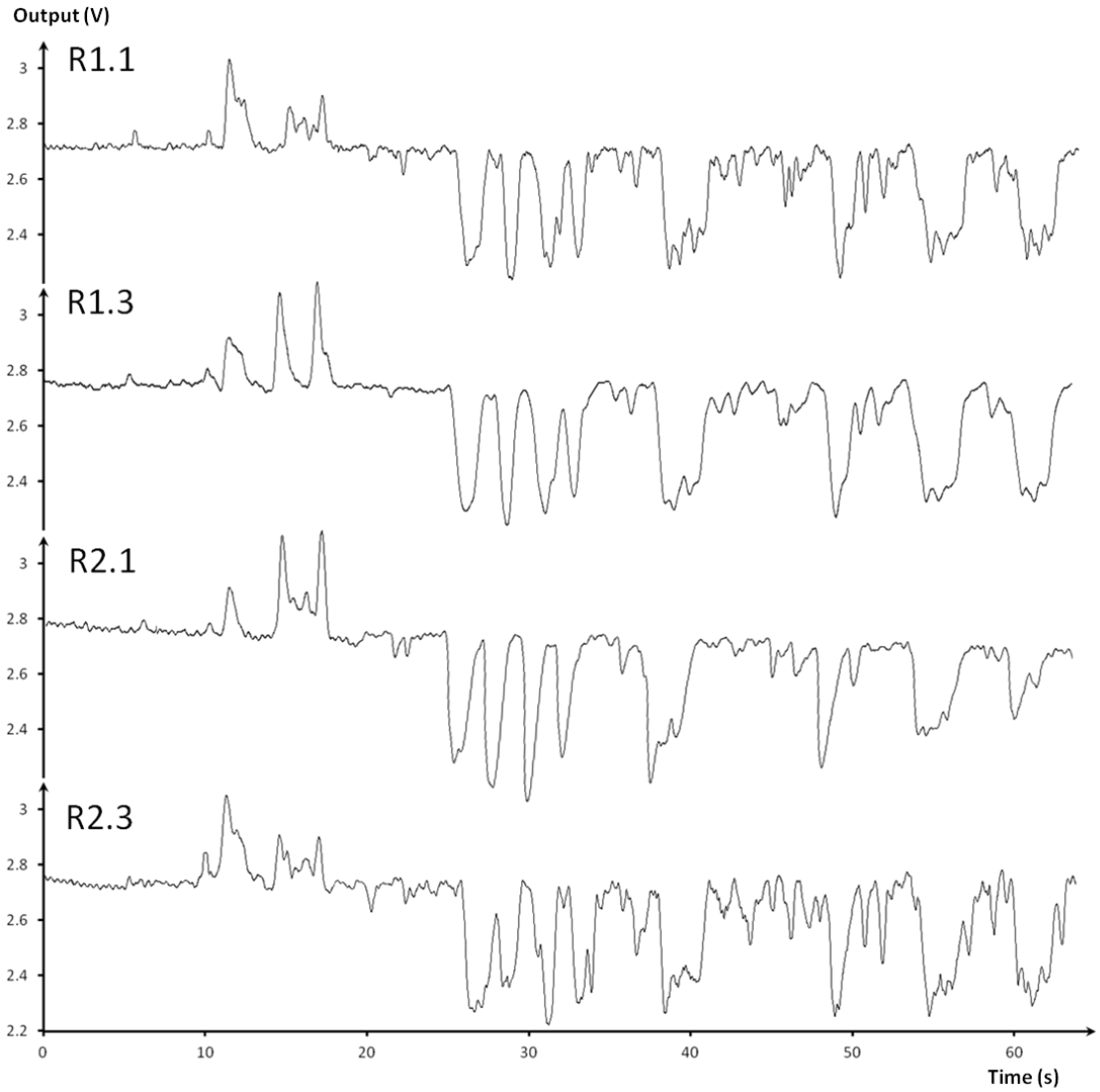


**Figure 5.15 – Filtered output for gauges R1.1, R1.3, R2.1 and R2.3 on the *loose* frame.**

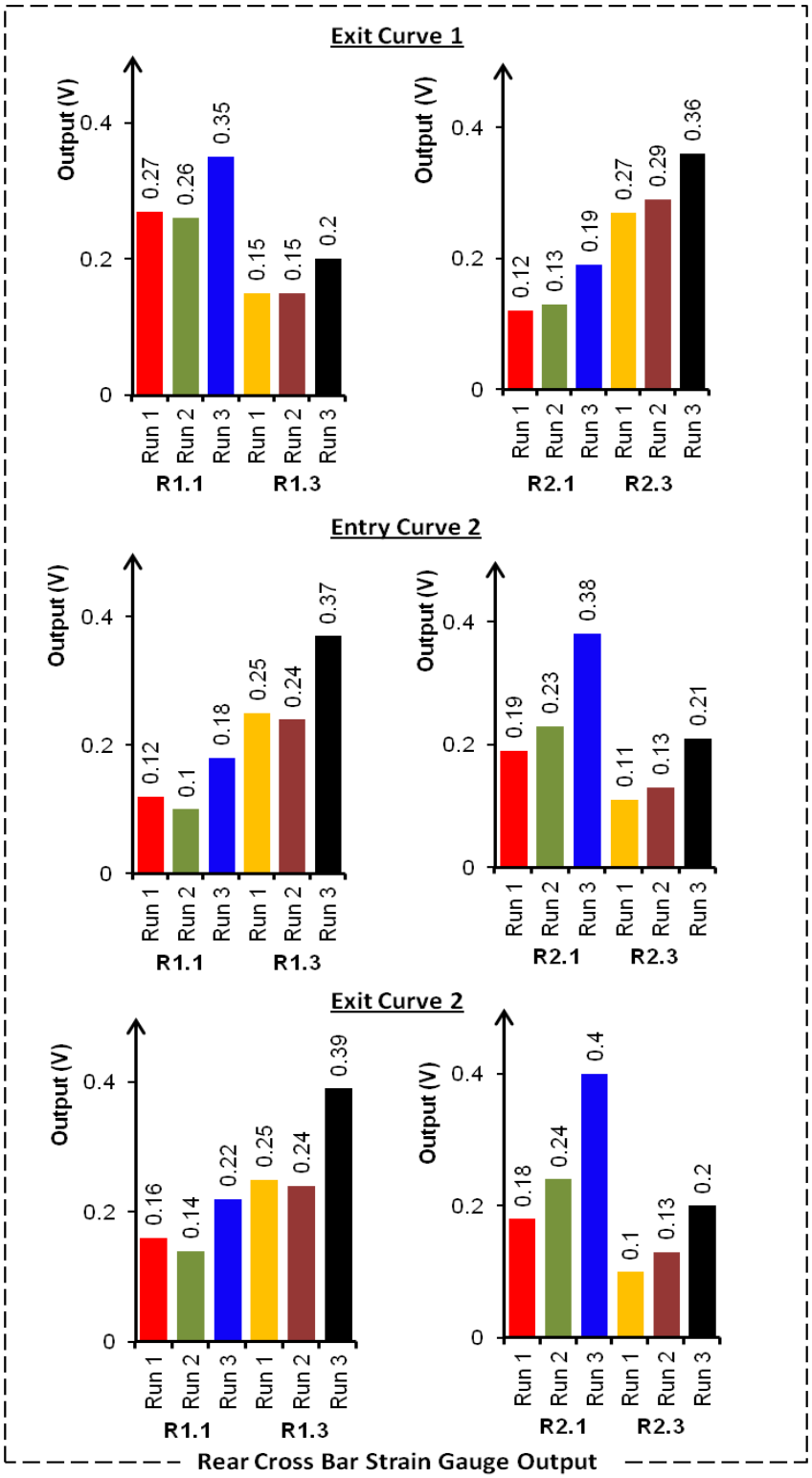


**Figure 5.16 – Summary of voltage magnitudes recorded for exit curve 1, entry and exit curve 2 from the rear cross bar rosettes.**

Curve 1 turns to the right and on the exit the Voltage recorded for R1.1 and R2.3 exceeds that from R1.3 and R2.1 indicating the downward force is applied to the back right corner. The reverse trend is observed in curve 2 as it turns to the left indicating a downward force applied to the back left corner. To compensate for unknowns of the specific trajectory on curve fillets a *controllable twist angle* is calculated using the average of the gauge outputs. The larger output from the gauge most orientated to bar flexure from knee pressure (R1.3, R2.1 for curve 1 and R1.1, R2.3 for curve 2) is used to calculate an average and then the twist angle extrapolated from the data tables. To verify the result the same method is applied to the smaller outputs and their corresponding data tables. For comparison the stiff frame, (Run 1 and Run 2) has a *controllable rear twist angle* of 1.07° and the loose frame (Run 3) 1.77°.

The magnitude of impact on exit curve 3 is of similar value for all the rear gauges with an average value of 0.16 V for the stiff frame and 0.07 V for the loose frame. Similarly the High g Deformation average for a stiff frame is 0.30 V and 0.47 V for the loose frame.

#### *5.4.2.2 Front Cross Bar Results*

Three runs were also taken recording the front cross bar strain gauges, two for the stiff frame and one for the loose frame. The output successfully recorded for the transverse gauge in line with the cross bar, R3.2, and the 45° gauge R3.1. The filtered voltage output is plotted in Figure 5.17. For the front cross bar the rosette of strain gauges was attached to the midpoint of the bar. The gauge in the transverse direction, R3.2, exhibits a signal indicative of the higher g-force curves. The 45° gauge, R3.1, has both positive and negative voltage traces as at the midpoint of the bar it measures the twist of the bar. The voltage for curve 1, curve 2 can again be measured (Fig 5.18) as can the impact on exit 3 and the *High g Deformation* band.

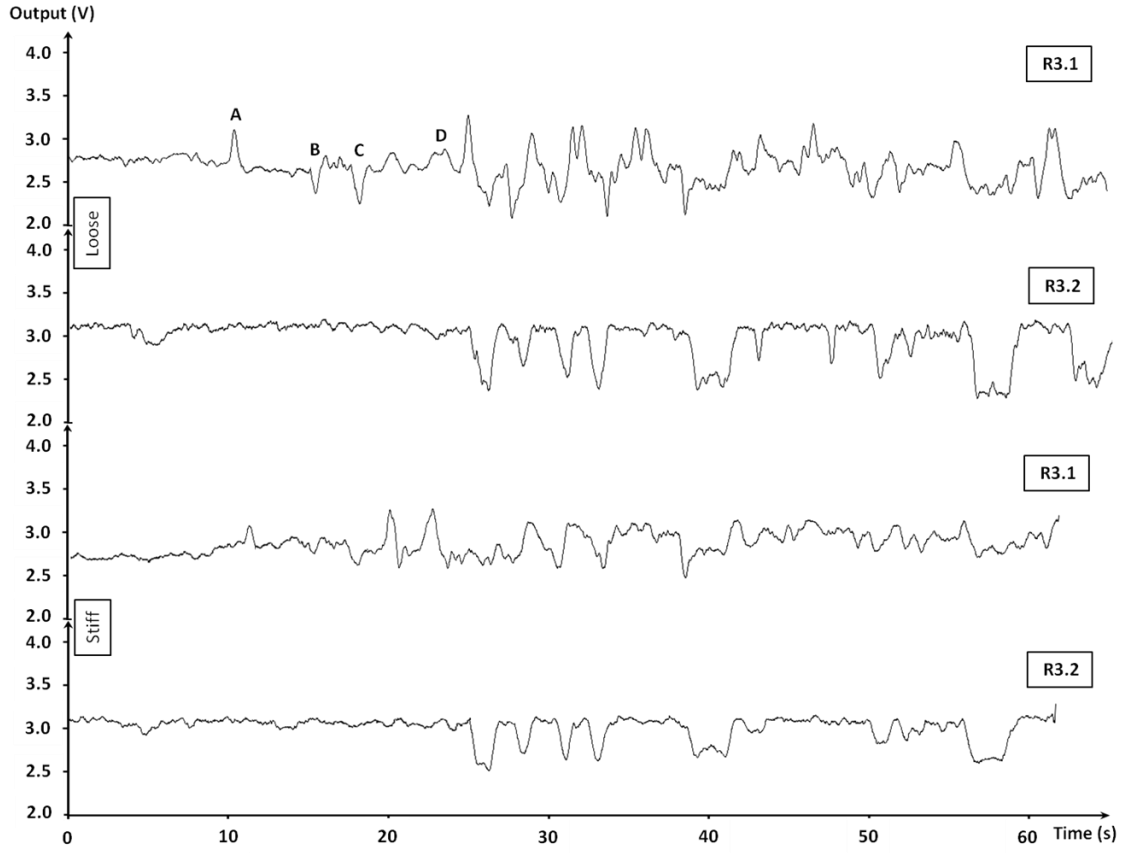


**Figure 5.17 – Filtered output for the front cross bar gauges R3.1 and R3.2 for both the stiff and loose frame setups. Exit curve 1 and the entry and exit of curve 2 are marked A, B, C respectively and the impact on exit curve 3 is indicated at D.**

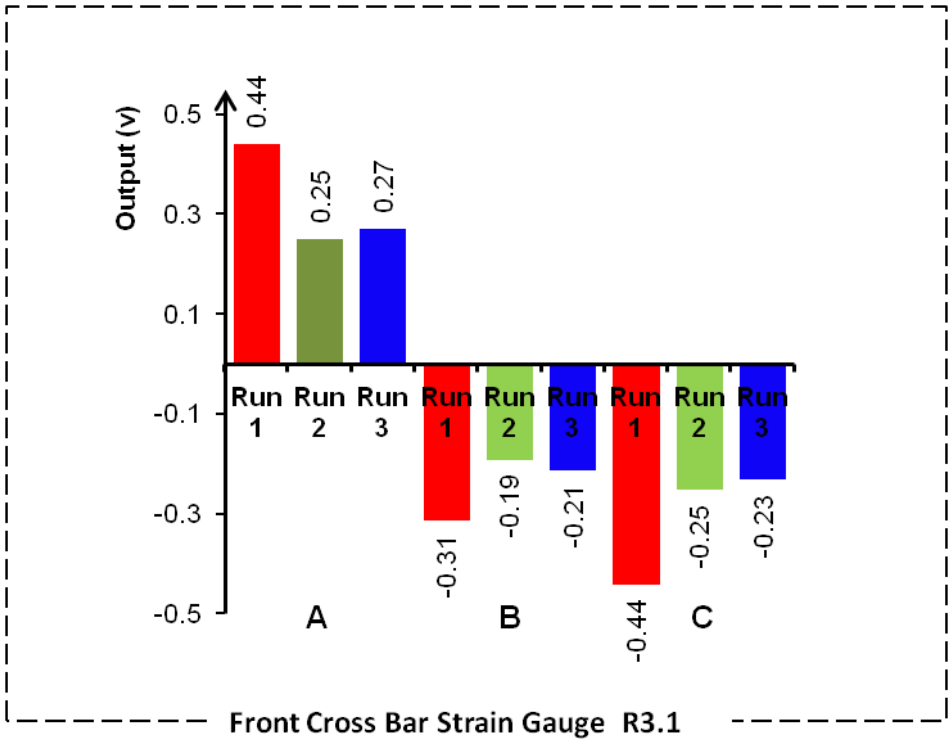


**Figure 5.18 – Peak values recorded by R3.1 at exit curve 1, entry and exit curve 2 indicated by A,B and C respectively.**

These result can be quantified in the same way as the rear cross bar results giving a *controllable front twist angle* of 0.35° for the stiff frame and 0.59° for the loose frame, These values are smaller than those found at the rear of the frame as expected due to the front hinge of the saddle plate limiting movement of the front cross bar.

The magnitude of impact on exit curve 3 from R3.2 is 0.40 V for the stiff frame and 0.25 V for the loose frame. The high g deformation band for the stiff frame is 0.51 V and 0.72V for the loose frame which is consistent with the trends found for the rear cross bar.

#### *5.4.2.3 Long Bar Results*

The static LDP results show that minimal twist is experienced in the long bars. This is confirmed in the dynamic data as gauge R4.2 shows the dominant voltage output while R4.1 and R4.3 have similar signal shapes but of a magnitude approximately 25% that of R4.2, similarly for the R5 gauges.

A total of 4 runs were recorded for both these rosettes. R4.2 failed partway through the first run but showed a similar signal to R5.2 prior to the failure, as expected due to symmetry. A comparison of the stiff and loose frame raw data results are plotted in Figure 5.19 for all four descents from R5.2. Run 1 and Run 2 were on the *stiff* setup whilst Run 3 and Run 4 on the *loose* setup. The point of the athlete loading onto the sled can clearly be identified. It can also be seen that the signal from the stiff setup shows sharper peaks in the raw data, whilst the loose setup has larger magnitudes in the high g deformation band. Figure 5.20 shows the filtered output for these four runs recorded on R5.2, the magnitude of the voltage output is typically 25% greater for the loose frame, measured from the high g deformation band.

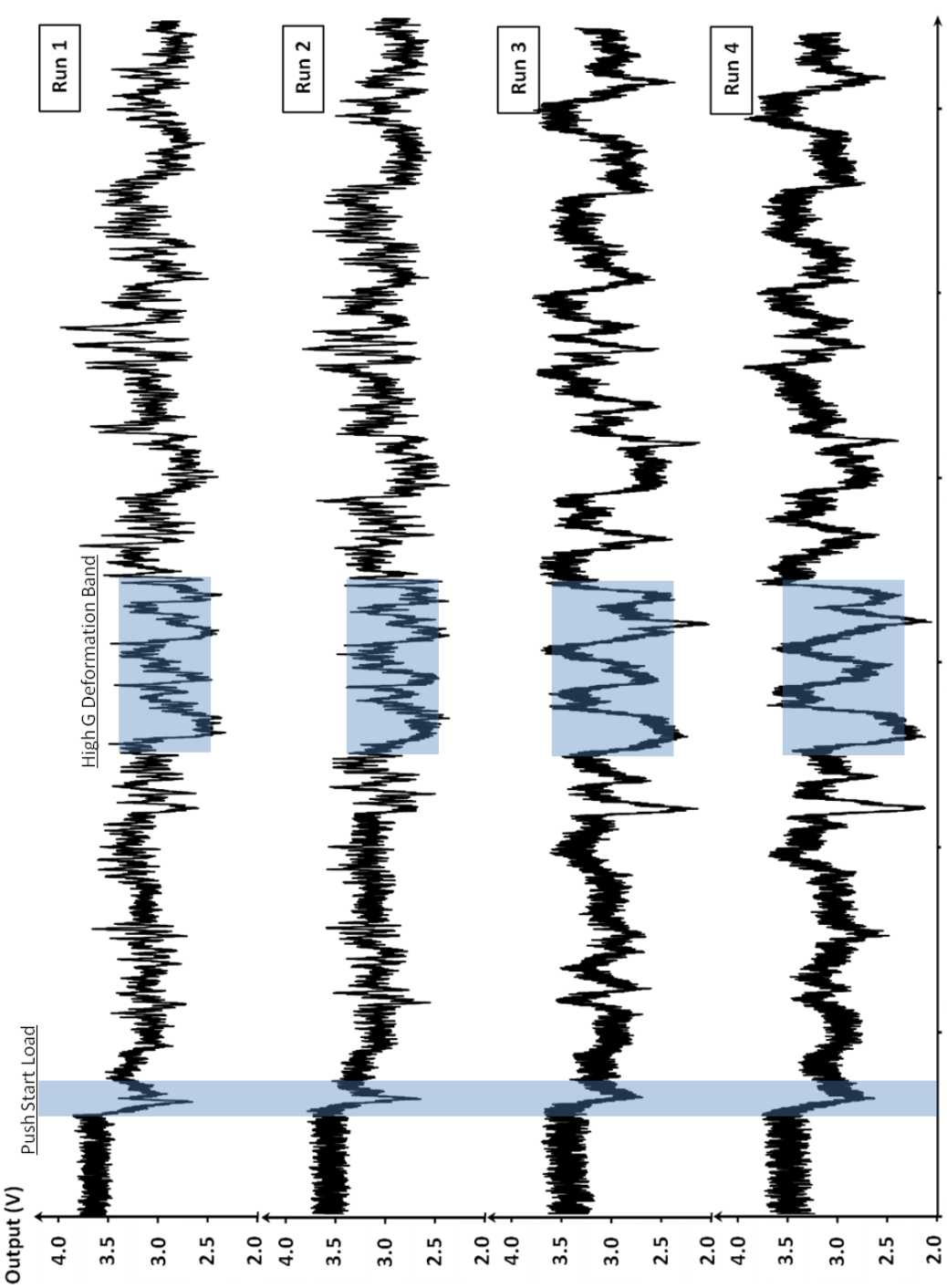


**Figure 5.19 – Raw output from R5.2 for Runs 1, 2, 3 and 4. The point of athlete loading onto the sled can be seen and the high g deformation band is indicated.**

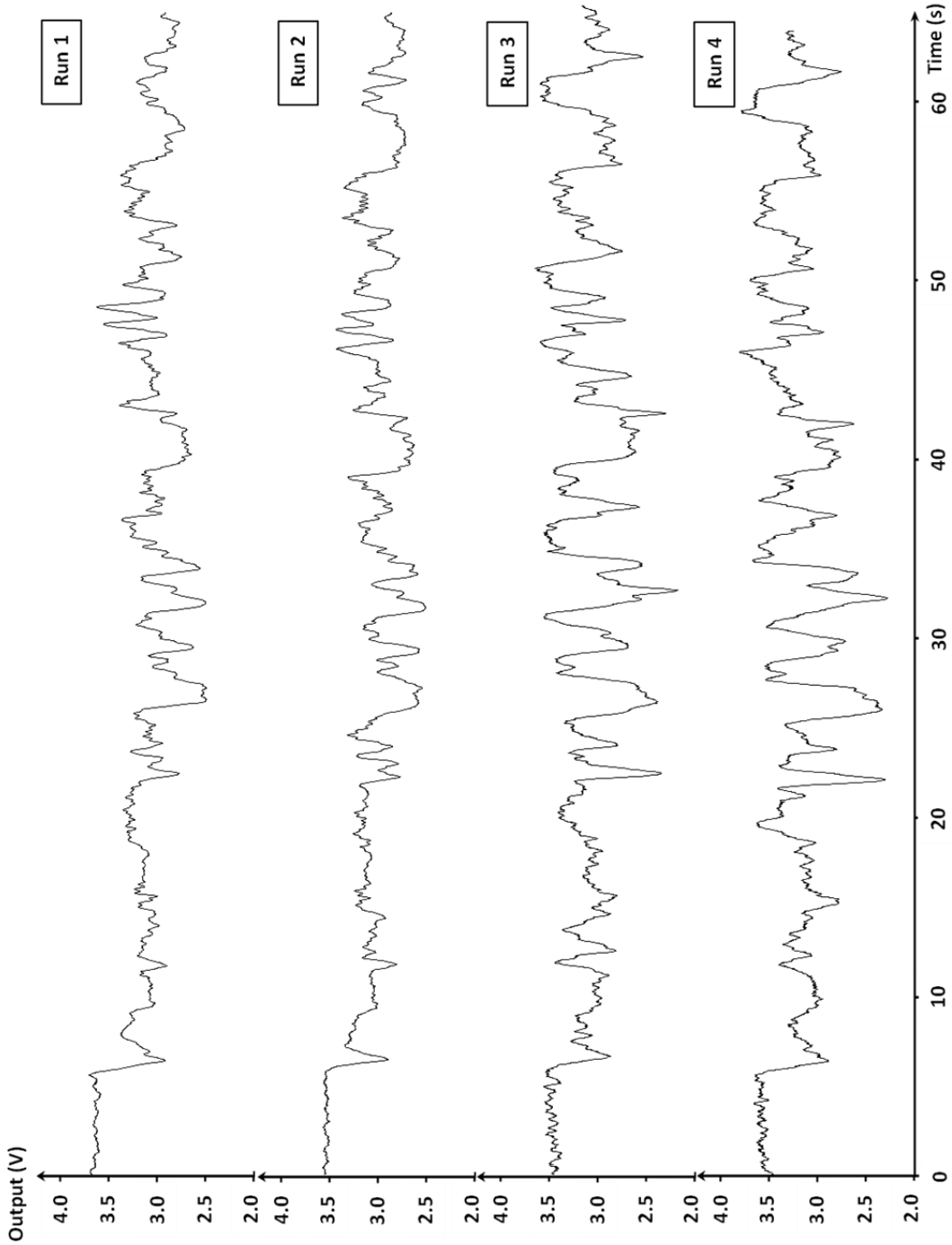


**Figure 5.20 – R5.2 data for all four runs after being processed with a 10Hz low pass filter.**

### 5.5 Discussion

For both the front and rear cross bars the loose frame showed a greater controllable twist angle could be achieved through curves 1 and 2. My ability to position the loose frame setup was more accurate and resulted in a gentle touch with the wall between curves 3 and 4 whereas the stiff sled setup had more severe of an impact followed by skidding towards curve 4. Although only 6 runs of data from the strain gauges was recorded here I found over multiple visits to the Lake Placid Sliding centre that the loose frame set up was easier to position and avoid heavy impacts on exit curve 3. The maximum deformation band recorded on the front and back cross bars was largest on the loose frame. With the signals correlated to the centrifugal force suggests the vertical force through the sled frame causes it to distort such that the runners are pushed outwards.

The data recorded from the long bar rosettes showed a sharper signal on the stiff frame. From a performance perspective the stiff frame produced a bumpier ride suggesting the sharp peaks are a result of my body interaction on the sled surface unable to dissipate vibrations that occur as the sled travels over the ice. The loose frame felt smoother to slide on, the maximum deformation band also has a larger trace showing the overall movement is greater.

### 5.6 Conclusion

In skeleton the goal is to achieve optimum trajectories for faster descent times and so presents motivation for understanding the deformation of the frame and effectiveness of sled control. This is of particular interest at the slower velocities near the start of the track in order to generate velocity and minimise driving error as typically the sleds are more difficult to control at these points.

A dual stiffness test sled was used. Applying strain gauges to the long bars, front and rear cross bars enabled the deformation of the sled to be quantified. Static tests showed that the predominant twist was due to movement in the cross bars. With the cross section of these cross bars being smaller with 3mm x 30mm and the thicker long bars being 8mm x 40mm (at widest point) this can be observed as the load is applied. The main deformation occurs in the crossbars bending and twisting helically whilst the long bars bend in a single plane, with more similarity to a cantilever than a twisting helix.

During the static tests the applied load at the corner points was related to a twist angle of the frame. This provided the calibration values for the output of the strain gauges under both stiff and loose frame setups. Using these calibration values the magnitude of the frame deformation during a descent can be quantified. This deformation in turn is related to the asymmetry created at the contact between the runners and the ice and so has a correlation to the overall control of the sled.

Dynamic tests targeted points in the track where athlete movements can best be applied to replicate the type of deformation measured in the static tests. At the slower velocities the twist angle of the sled on the entries and the exists of curves 1, 2 and 3 can be calculated. The loose frame had a rear twist angle of 1.77°, front twist angle of 0.59° and a smoother ride experienced by the athlete than the stiff frame with a rear twist angle of 1.07° and front twist angle of 0.35°. The larger twist angle of the loose frame is expected and did enable the athlete to position the sled more accurately resulting in smooth flowing lines from one curve to the next. The method for loosening the frame by allowing the rear of the saddle plates movement also enabled the long bars to act more like a leaf spring. This created the smoother ride experienced by the athlete as less rigidity in the vertical plane reduced the harshness of the sleds motion during the descent.

However the maximum deformation in the high g-force curves for the loose frame was also greater which would result in a larger alteration to the contact patch between the runners and the ice. Although the greater twist angle enabled the sled to be positioned more accurately the overall descent times were slower. This indicates that the smooth ride and improved response came at the sacrifice of excessive ice interaction under the high g-forces experienced reducing the overall acceleration of the sled.

During the course of this investigation I also was able to test Sled A, which became my race sled for 3 seasons. I was therefore unable to attach strain gauges to it as the FIBT forbids electrical instrumentation in races. Sled A produced a similar twist angle to the loose frame setup of sled C and also felt smooth during a descent. The resultant times were faster than the both the stiff and loose frame set up on Sled C. This is attributed to the thinner long bars and thicker cross bars of Sled A (discussed in Chapter 2) resulting in a more complex deformation of the frame than flexing entirely from the crossbars. The thinner long bars also twisting helically when under load on Sled A suggests that although the twist angle may be comparable between Sled A and Sled C, the dynamic movement of the contact patch between the runners and ice will differ. This presents motivation for further work to modify frame geometry so that twist angle could be optimised for a responsive sled without sacrificing velocity.

# 6 CONCLUSIONS

In skeleton races the medal position are separated by hundredths of a second. An increased understanding of the trajectory and equipment response enables the athlete to target areas of their training to improve their overall performance.

The push start study in Chapter 3 showed the benefit of installing a single axis accelerometer inside the sled, capturing detailed information about the initial drive off the starting block, ability to further accelerate to top speed and load smoothly onto the sled. The initial drive can be quantified with a peak acceleration. The loading phase has a number of key measurements to quantify the athlete performance with a maximum and minimum acceleration level, load duration and change in velocity. This information provides indicators on the success of the athlete's performance. Subtleties in acceleration throughout the push phase are identified, braking steps and deceleration during the load onto the sled, that are more difficult to determine through traditional coaching methods and video capture and so is of benefit to improve athlete training. The sensitivity of the accelerometer used to collect this data required careful calibration and accurate measurements of track geometry in order to compensate for the change in orientation.

The push start alone does not determine the medal positions. Chapter 4 used a tri-axial accelerometer to investigate the trajectory during a full descent of the Koenigssee track in Germany. The forwards acceleration provides a timestamp for the beginning of the descent whilst the vertical axis measures the g-force within the curves. Of main interest was the transverse acceleration as this provided information on the sled's trajectory as the sled and athlete travels through the curves. Without detailed track geometry and the curve profiles changing from variable ice thickness means the output cannot be

calibrated as accurately as for the push start study. However, the rise and fall time in the *S-Bends* can be quantified and the relative magnitudes indicate the location of the high point achieved within the curve. When considered as a sequence of curves this provides information on the overall success of the trajectory and aids the athlete to optimise their steers for improved performance. Comparison of data recorded in the *Bendaway* shows whether the athlete successfully *threaded the needle* and more importantly the magnitude and timing of wall impacts, from which the athlete can alter their approach for subsequent descents to be improved. With additional information available at the *Kreisle* from entry velocity, video capture and measured track geometry enables the accelerometer to be more accurately calibrated. The data can be used to identify smoothness of entry and a measure of athlete ability to control the oscillations. Key traces in the data show subtleties on the entry that are often unable to view due to shades protecting the track from the sun. Failing to achieve a smooth entry can result in oscillations that require more extreme steers by the athlete to achieve a good exit and maximise velocity for the lower section of the track.

The addition of strain gauges to the frame of the sled enables the deformation of the frame to be quantified, Chapter 5. Using a dual stiffness test sled, Sled C, at the Lake Placid Track in the USA shows the difference between a stiff frame and a loose frame. Combined with athlete perception, the data showed the stiff frame to have less response than the loose frame and a harsher ride. However, it was the stiff frame that resulted in the fastest descents indicating the smoothness of the ride and ability to position the sled more accurately was excessive and sacrificed acceleration. Additionally, Sled A was used and achieved even faster descents. With comparable twist angle to the stiff setting of Sled C, Sled A was more responsive and smoother to ride. This is due to Sled A having thinner long bars and thicker cross bars than Sled C resulting in a more complex deformation of the frame. This in turn presents motivation for further investigation into

frame geometry; the relationship between twist angle and frame response and potentially modal analysis and smoothness of ride to minimise the harshness of the interaction between the runners and the ice.

The experimental methods and analysis techniques presented here, from data collected 2006 – 2008, formed a foundation to aid my pursuit of the Winter Olympics 2010. During my qualification through the international racing circuits I was able to generate some of the highest top speeds in the world. With limited track time and resources compared to the larger nations in the sport, I hope this shows how targeting key aspects of training can have significant results. I am continuing to research the equipment to help athletes that are currently racing. The materials and dimensions outlined in this thesis should be considered an overview of sled construction that I hope highlights the importance of accounting for both materials and subtleties in geometry when manufacturing sleds. If there are any questions about my work, please do contact me. I hope I can aid in keeping the sport of skeleton safe and fair and help future athletes to fulfil their potential and achieve their dreams.

## REFERENCES

Akkok M, Ettles C M, Calabrese S J. Parameters Affecting the Kinetic Friction of Ice. Journal of Tribology. 1987; 109: 552-561

BBSKA. Athletic Standards for Talent Identification Days. 2007; http://www.bobskeleton.org.uk/talent_identification_athletic_standards_for_talent_id_days-123.html

BCS. Physical Tests for Development and World Cup Athletes. 2007; http://www.bobsleigh.ca/Content/Recruitment/Camp%20Schedules%20and%20Results.asp

Bejan A. The Fundamentals of Sliding Contact Melting and Friction. Journal of Heat Transfer. 1989; 111: 13-20

Bowden F P, Hughes T P. The Mechanism of Sliding on Ice and Snow. Proceedings of the Royal Society of London. Series A, Mathematical and Physical Sciences. 1939; 172: 280-298

Braghin F, Cheli F, Donzelli M, Melzi S, Sabbioni E. Mutli-Body Model of a Bobsleigh: Comparison with Experimental Data. Multibody System Dynamics. 2011; 25(2): 185-201

Brennan S M, Kollár L P, Springer G S. Modelling the Mechanical Characteristics and On-Snow Performance of Snowboards. Sports Engineering. 2003; 6(4): 193-206

Bromley K, Factors Affecting the Performance of Skeleton Bobsleds. University of Nottingham. 1999, PhD

Brüggemann GP, Morlock M, Zatsiorsky V M. Analysis of the Bobsled and Men's Luge Events at the XVII Olympic Winter Games in Lillehammer. Journal of Applied Biomechanics. 1997; 13: 98-108

Bullock N, Martin D T, Ross A, Rosemond D, Holland T, Marino F E. Characteristics of the Start in Women's World Cup Skeleton. Sports Biomechanics. 2008; 7(3): 351-360

Bullock N, Gulbin J P, Martin D T, Ross A, Holland T, Marino F. Talent Identification and Deliberate Programming in Skeleton: Ice Novice to Winter Olympian in 14 Months. Journal of Sports Sciences. 2009a; 27(4): 397-404

Bullock N, Martin D T, Ross A, Rosemond D, Jordan M J, Marino F E. An Acute Bout of Whole-Body Vibration on Skeleton Start and 30 m Sprint Performance. European Journal of Sports Science. 2009b; 9(1): 35-39

Bullock N, Hopkins W, Martin D, Marino F. Characteristics of Performance in Skeleton World Cup Races. Journal of Sports Sciences. 2009c; 27(4): 367-372

Bullock N, Hopkins W G. Methods for Tracking Athletes' Competitive Performance in Skeleton. Journal of Sport Sciences. 2009d; 27(9): 937-940

Champoux Y, Richard S, Drouet J M. Bicycle Structural Dynamics. Sound and Vibration. 2007; Materials Reference Issue: 16-22

Cochrane D, Stannard S. Acute Whole Body Vibration Training Increases Vertical Jump and Flexibility Performance in Elite Female Field Hockey Players. British Journal of Sports Medicine. 2005; 39: 860-865

Colbeck S C, Najarian L, Smith H B. Sliding Temperatures of Ice Skates. American Journal of Physics. 1997; 65(6): 488-492

Cormie P, Deane R, Triplett N, McBride J. Acute Effects of Whole-Body Vibration on Muscle Activity, Strength and Power. Journal of Strength and Conditioning Research. 2006; 20: 257-261

Dabnichki P, Motallebi F, Avital E. Advanced Bobsleigh Design. Part 1: Body Protection, Injury Prevention and Performance Improvement. Proceedings of the Institution of Mechanical Engineers Part L – Journal of Materials Design and Applications. 2004; 218(L2): 129-137

De Koning J J, Groot G, Schenau G J I. Ice Friction During Speed Skating. J. Biomechanics. 1992; 25(6): 565-571

De Koning J J, Houdijk H, Groot G, Bobbert M F. From Biomechanical Theory to Application in Top Sports: the Klapskate Story. Journal of Biomechanics. 2000; 33: 1225-1229

Evans D C B, Nye J F, Cheeseman K J. The Kinetic Friction of Ice. Proceedings of the Royal Society of London. Series A, Mathematical and Physical Sciences. 1975; 347: 493-512

Fauve M, Rhyner H U, Mottet A. Analysis and Optimisation of the Sliding Properties of Steel Luge Runners on Ice. The Engineering of Sport 7. 2008; 579-586

Foster R, Lanningham-Foster L, Levine J. Optimization of Accelerometers for Measuring Walking. Proceedings of the Institution of Mechanical Engineers, Part P: Journal of Sports Engineering and Technology. 2008; 222: 53-60

Gasbarro L, Beghi A, Frezza R, Nori F, Spagnol C. Motorcycle Trajectory Reconstruction by Integration of Vision and MEMS Accelerometers. Decision and Control, IEEE. 2004; 1: 779-783

Hainzlmaier C, Mack C, Wolf S, Wintermantel E. Computational Mechanics in Bobsleigh: FE Model of Runner and Ice. The Engineering of Sport 5. 2004; 256-262

Hainzlmaier C. A Tribologically Optimized Bobsleigh Runner. Zentralinstitut für Medizintechnik, 2005

Hastings R. The Use of Computational Fluid Dynamics to Investigate and Improve the Aerodynamics of Bob Skeleton Racing. The University of Edinburgh. 2008 MEng.

Hokkirigawa K. Tribology in Bobsleigh and Skeleton - Toward Salt Lake from Nagano, Journal of Japanese Society of Tribologists. 2002; 47(2): 69-74

Horowitz P, Hill W. The Art of Electronics. Cambridge University Press. 1989; 2nd Edition

Houdijk H, Wijker A J, De Koning J J, Bobbert M F, De Groot G. Ice Friction in Speed Skating: Can Klapskates Reduce Ice Frictional Loss? Medicine and Science in Sports and Exercise. 2001; 33 (3): 499-504

Hubbard M, Kallay M, Rowhani P. Three-Dimensional Bobsled Turning Dynamics. International Journal of Sport Biomechanics. 1989; 5: 222-237.

Huyghe B, Doutreloigne J, Vanfleteren J. 3D Orientation Tracking Based on Unscented Kalman Filtering of Accelerometer and Magnetometer Data. IEEE Sensors Applications Symposium. 2009; Feb: 148-152

James D A, Davey N, Rice T. An Accelerometer Based Sensor Platform for Insitu Elite Athlete Performance Analysis. Sensors, Proceedings of IEEE. 2004; 3: 1373-1376

Larman R, Turnock S, Hart J. Mechanics of the Bob Skeleton and Analysis of the Variation in Performance at the St Moritz World Championship of 2007. The Engineering of Sport 7. 2008; 2:117-126

Lembert S, Schanchner O, Raschner C. Development of a Measurement and Feedback Training Tool for the Arm Strokes of High-Performance Luge Athletes. Journal of Sports Sciences. 2011; 29: 1593-1601

Lewis O. Aerodynamics Analysis of a 2-Man Bobsleigh. Delft University of Technology. 2006 Master of Science.

Maeno N, Arakawa M. Adhesion Shear Theory of Ice Friction at Low Sliding Velocities, Combined with Ice Sintering. Journal of Applied Physics. 2003; 95: 134

Marmo B A, Blackford J R, Jeffree C E. Ice Friction, Wear Features and their Dependence on Sliding Velocity and Temperature. Journal of Glaciology. 2005; 51: 391-398

Marmo B A, Farrow I S, Buckingham MP, Blackford J R. Frictional Heat Generated by Sweeping in Curling and its Effect on Ice Friction. Journal of Materials: Design and Applications. 2006; 220(4): 189-197

Mössner M, Hasler M, Schindelwig K, Kaps P, Nachbauer W. An Approximate Simulation Model for Initial Luge Track Design. Journal of Biomechanics. 2011; 44: 892-896

Motallibe F, Dabnichki P. Advanced Bobsleigh Design 2: Aerodynamic Modifications to a Two-Man Bobsleigh. Proceedings of the Institution of Mechanical Engineers Part L – Journal of Materials Design and Applications. 2004; 218(L2): 139-144

Morlock M, Zatsiorsky V M. Factors Influencing Performance in Bobsledding: 1: Influences of the Bobsled Crew and the Environment. International Journal of Sport Biomechanics. 1989; 5: 208-221

Nordt A A, Springer G S, Kollár L P. Simulation of a Turn on Alpine Skis. Sports Engineering. 1999; 2(3): 181-199

Nordt A A, Springer G S, Kollár L P. Computing the Mechanical Properties of Alpine Skis. Sports Engineering. 1999; 2(2): 65-84

Oghi Y. Microcomputer-based Acceleration Sensor Device for Sports Biomechanics – Stroke Evaluation by using Swimmer's Wrist Acceleration. Sensors, Proceedings of IEEE. 2002; 1: 699-704

Oksanen P, Keinonen J. The Mechanism of Friction of Ice. Journal of Wear. 1982; 78: 315-324

Penner, R A. The Physics of Sliding Cylinders and Curling Rocks. American Journal of Physics. 2001; 69(3): 332-339

Platzer H, Raschner C, Patterson C. Performance-Determining Physiological Factors in the Luge Start. Journal of Sports Sciences. 2009; 27: 221-226

Poirier L, Lozowski E P, Thompson R I. Ice Hardness in Winter Sports. Cold Regions Science and Technology. 2011; 67: 129-134

Roche J, Turnock S, Wright S. An Analysis of the Interaction Between Slider Physique and Descent Time for the Bob Skeleton. The Engineering of Sport 7. 2008; 2: 101-109

Sahashi T, Ichino S. Carving-Turn and Edging Angle of Skis. Sports Engineering. 2001; 4(3): 135-145

Sands W A, Smith S L, Kivi D M R, McNeal J R, Dorman J C, Stone M H, Cormie P. Anthropometric and Physical Abilities Profiles: US National Skeleton Team. Sports Biomechanics. 2005; 4(2): 197 – 214

Sata K, Smith S L, Sands W A. Validation of an Accelerometer for Measuring Sport Performance. Journal of Strength and Conditioning Research. 2009; 23(1): 341-347

Schulson E M. The Structure and Mechanical Behaviour of Ice. JOM-Journal of the Minerals Metals and Materials Society. 1999; 51(2): 21-27

Seifert K, Camacho O. Implementing Positioning Algorithms Using Accelerometers. Sensors, Freescale Semiconductors. 2007; 1-13

Slawson S E, Justham L M, West A A, Conway P P, Caine M P, Harrison R. Accelerometer Profile Recognition of Swimming Stokes (P17). The Engineering of Sport 7. 2008; 1: 81-87

Stiffler A K. Friction and Wear with a Fully Melting Surface. Transactions of the ASME, Journal of Tribology. 1984; 106: 416-419

Strausky H, Krenn J R, Leitner A, Aussenegg F R. Sliding Plastics on Ice: Fluorescence Spectroscopic Studies on Interfacial Water Layers in the μm Thickness Regime. Applied Physics B Lasers and Optics. 1998; 66(5): 599-602

Tada N, Hirano Y. Simulation of a Turning Ski Using Ice Cutting Data. Sports Engineering. 1999; 2(1): 55-64

Waegli A, Schorderet A, Prongué C, Skaloud J. Accurate Trajectory and Orientation of a Motorcycle derived from low-cost Satellite and Inertial Measurement Systems (P42). The Engineering of Sport 7. 2008; 1: 223-230

Zanoletti C, La Torre A, Merati G, Rampinini E, Impellizzeri F. Relationship Between Push Phase and Final Race Time in Skeleton Performance. Journal of Strength and Conditioning Research. 2006; 20(3): 579-583